POLITECNICO
MILANO 1863

DIPARTIMENTO DI MECCANICA

Wind interaction of super long span bridges and new experimental technologies for wind tunnel - ocean basin hybrid testing

A. Zasso, G. Diana, D. Rocchi, T. Argentini

Politecnico di Milano, Dept. of Mechanical Engineering, Milano, ITALY
alberto.zasso@polimi.it

Coastal Highway Route E39 Project

- Very wide crossings → Long span Bridges
- Relevant aerodynamic issues

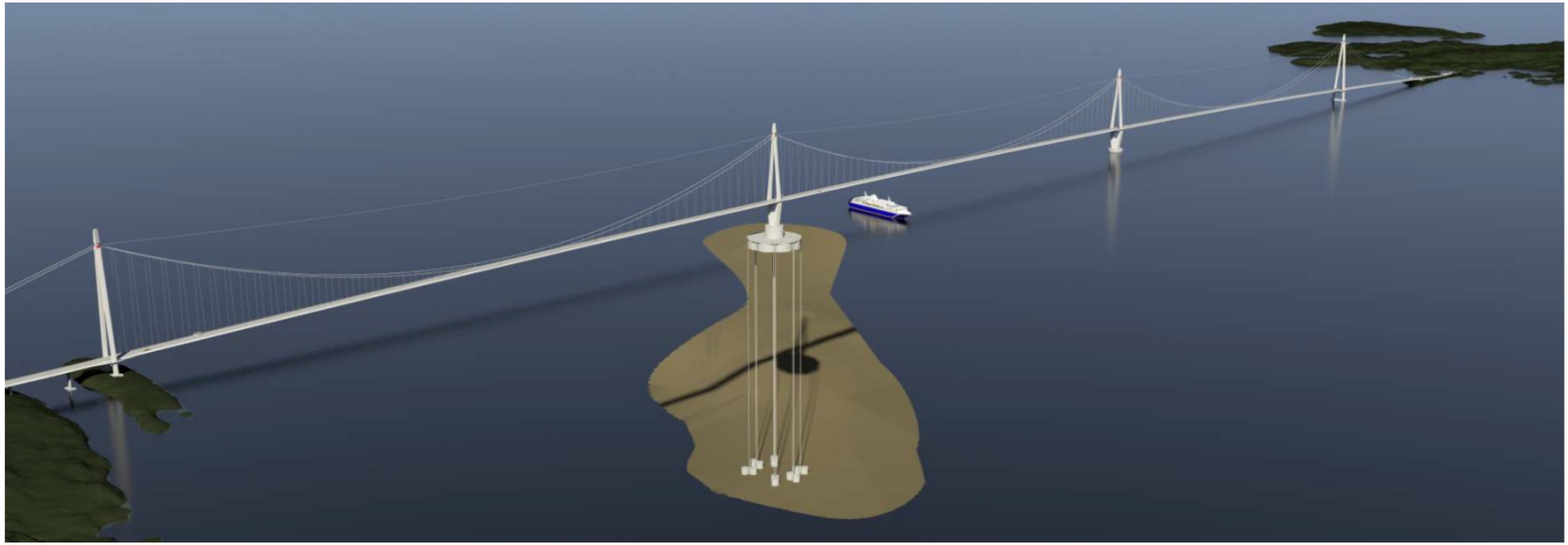

Source: Norwegian Public Roads Administration

Record span Messina Bridge Project

- Very wide crossing → 3300m single span solution
- **Key role played by aerodynamics to make it feasible**

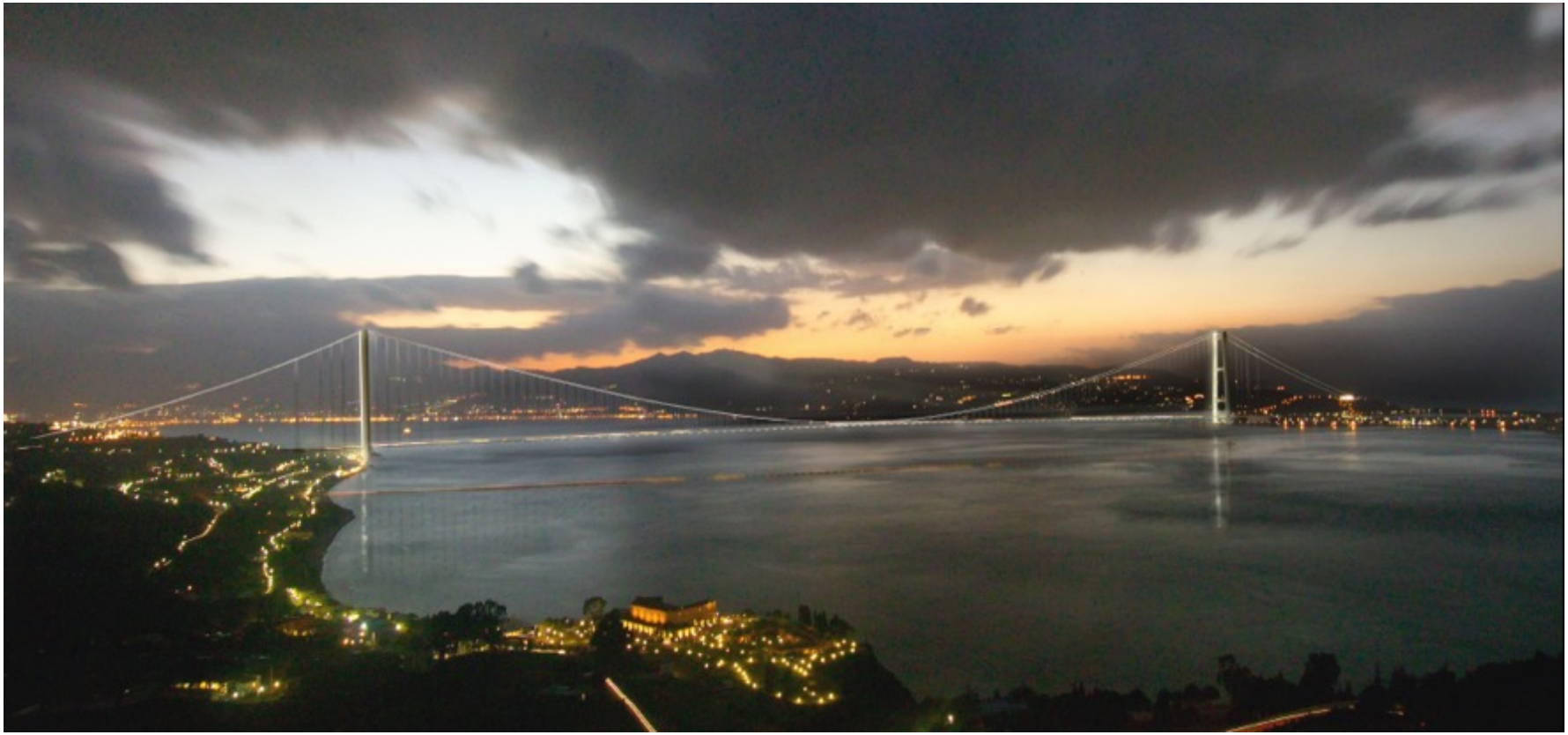

General arrangement of the suspension bridge

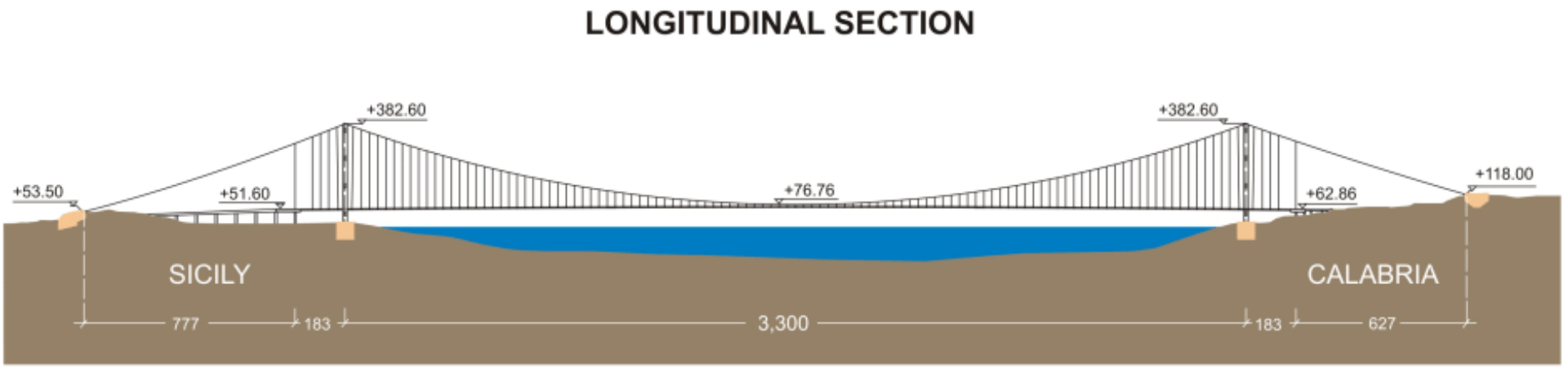

Central span:	3,300 m
Suspended side spans:	183 m
Overall suspended length:	3,666 m
Distance between anchorages:	5,070 m

Deck section

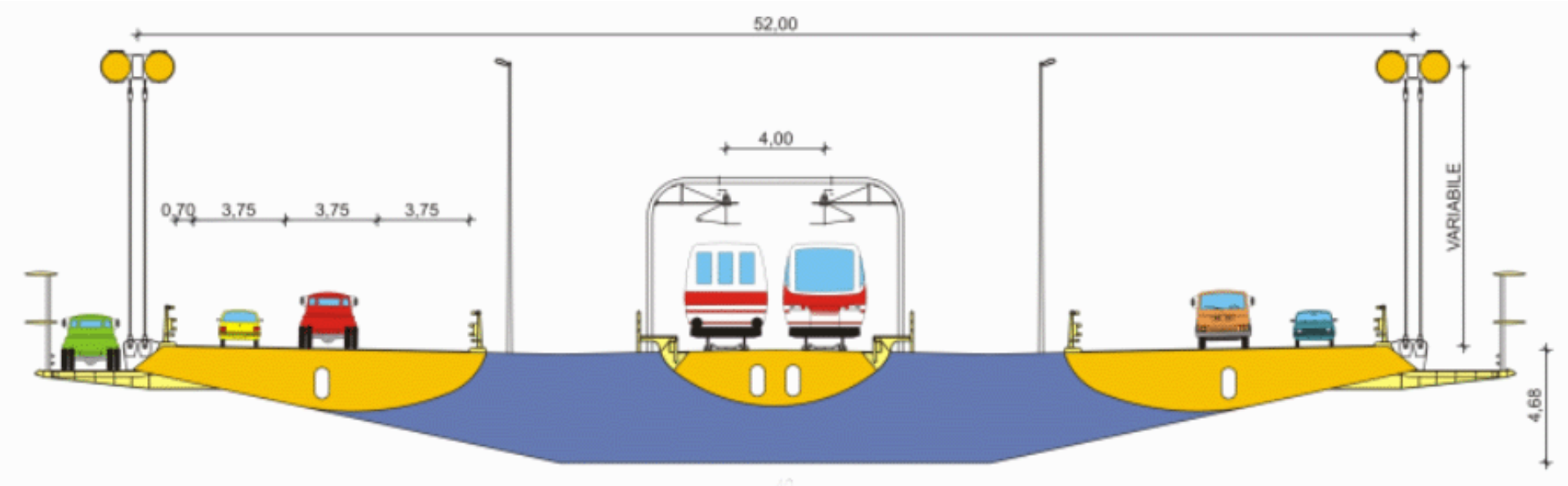

Deck width:	60m
Highway lanes:	2 x 2 lanes + emergency
Railway tracks:	2
Traffic capacity:	6,000 vehicles / hr 200 trains / day

Deck detail

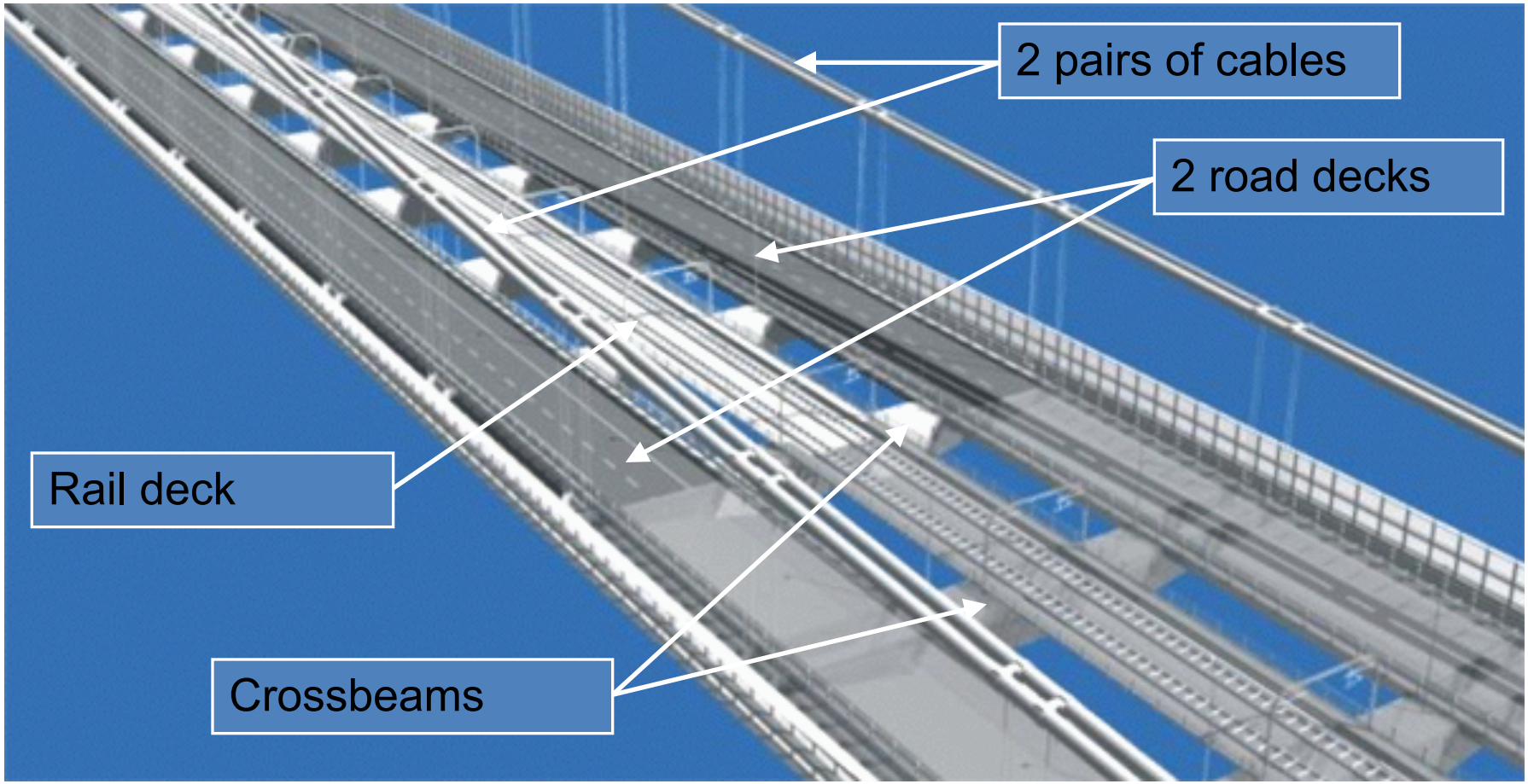

Towers and navigation channel

Tower height: 399 m

Navigation clearance 65 x 600 m

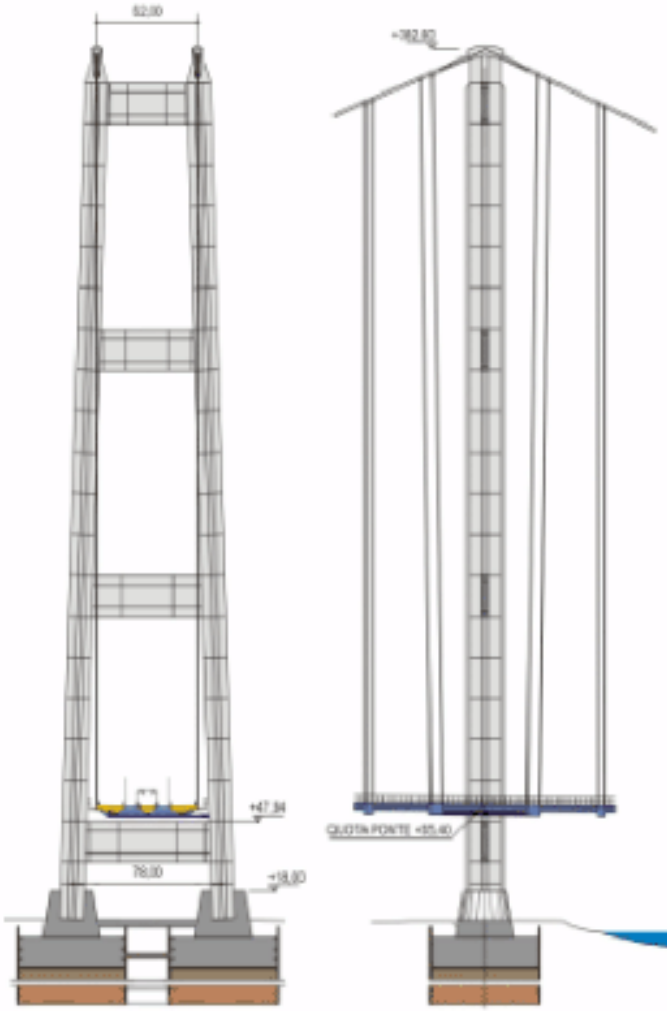

Wind actions

- Problems and solutions related to wind effects:

1. **Static loads**
2. One degree of freedom instability
3. Flutter instability
4. Buffeting
5. Vortex shedding

Static loads

Deck aerodynamic contribution is predominant

- On towers
- On main cables and hangers
- On deck

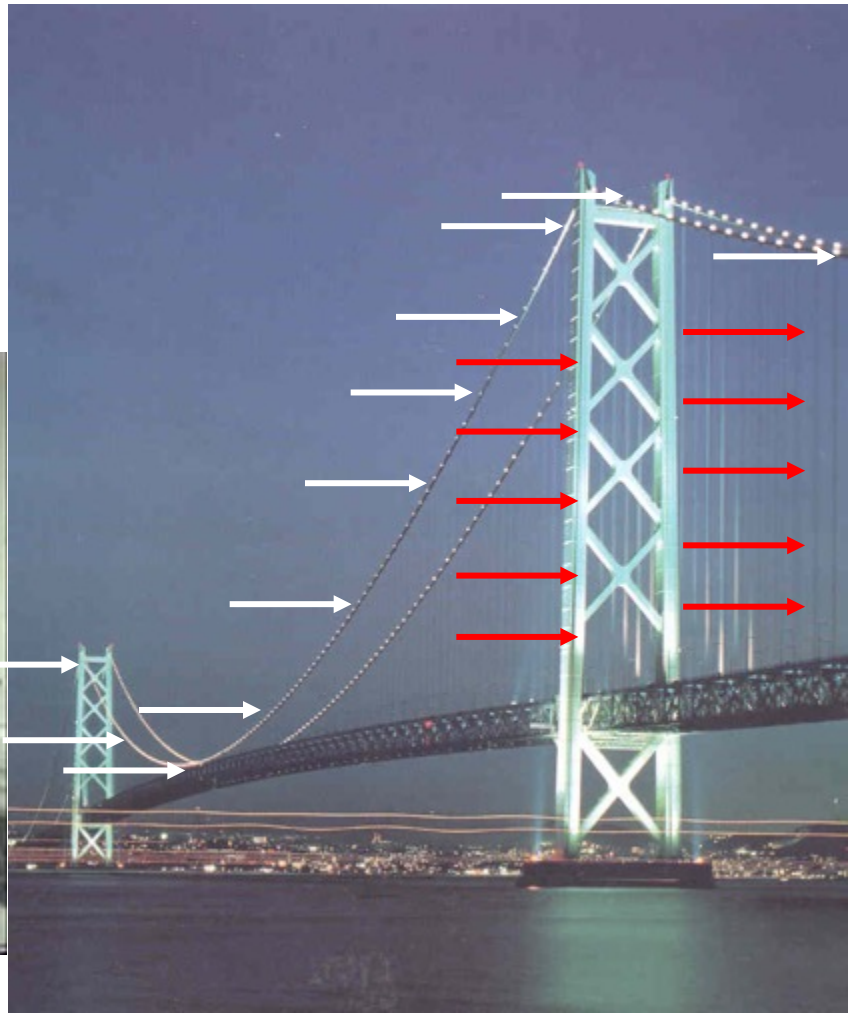

Static loads

The deck produce the most important static load
that is transferred through the hangers to the main cable
and from the main cable to the top of the towers
producing a high bending moment
that affects in large amount
the design of the bridge

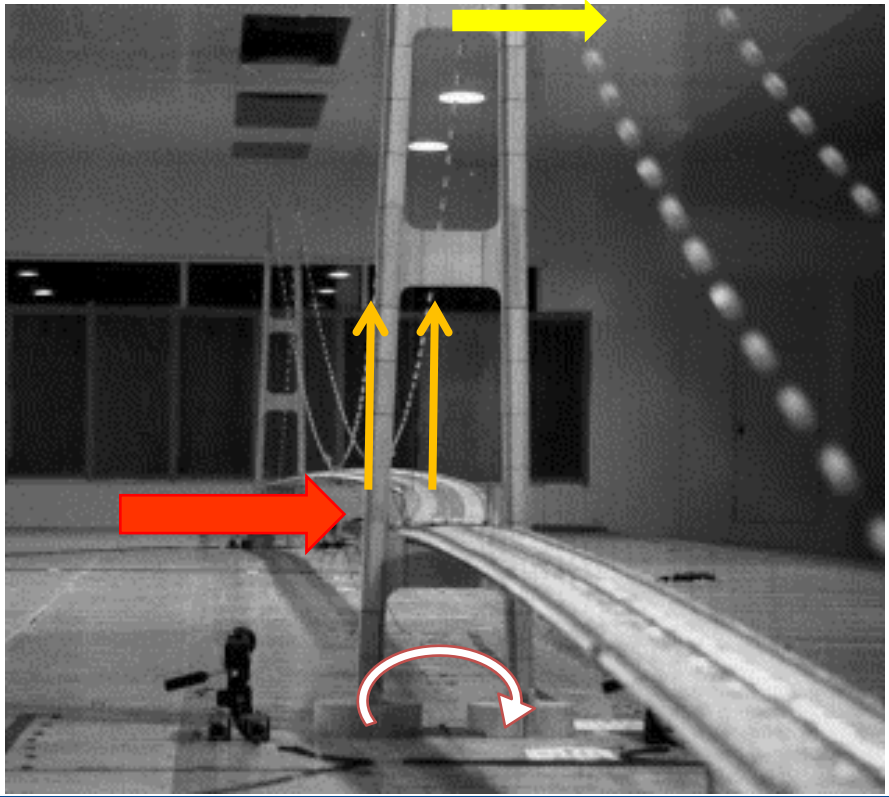

The drag of the deck

must be as low as

possible

Drag force as low as possible

Low value of the Drag coeffcient C_D → wing profile

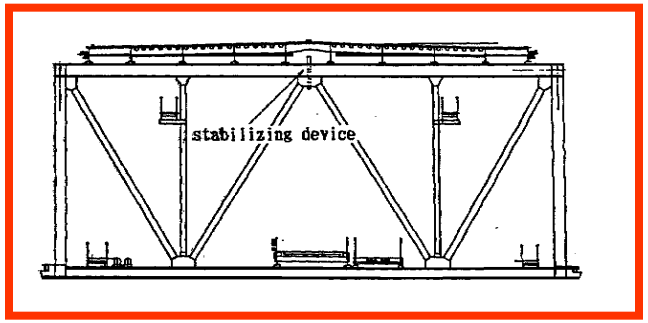

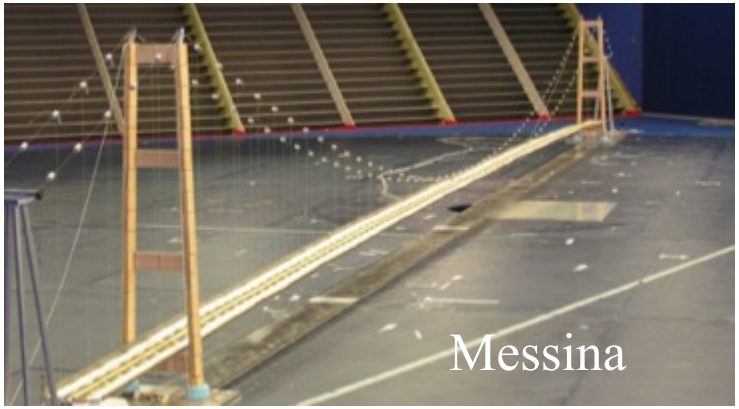

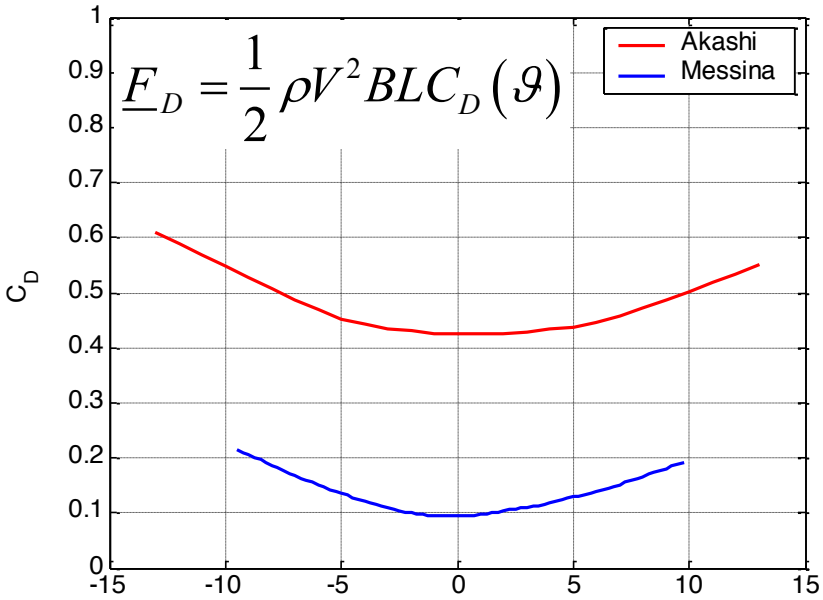

Static aerodynamic loads

Static deflection under maximum design wind speed measured in wind tunnel on full aeroelastic models

Akashi: 60 m/s - 25 m

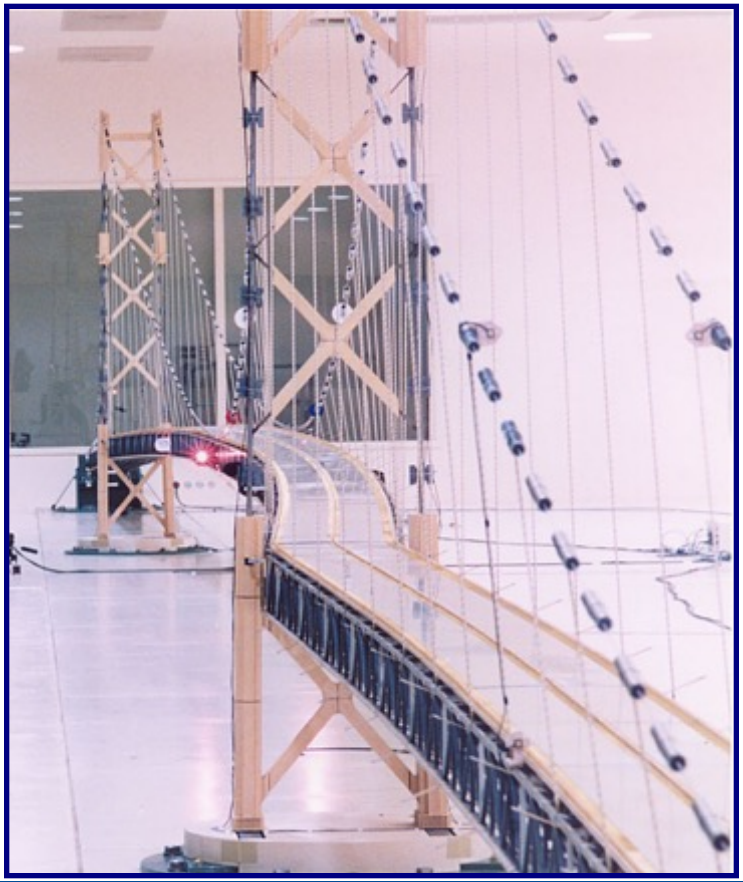

Messina: 62 m/s - 10 m

Deck shape

In order to have low drag
an airfoil section must be used

Messina Bridge (3300 m)

Tsing Ma Bridge (1377 m)

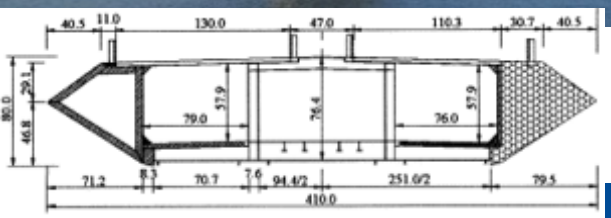

Humber Bridge (1410 m)

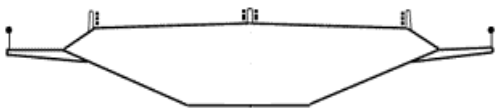

Storebaelt Bridge (1624 m)

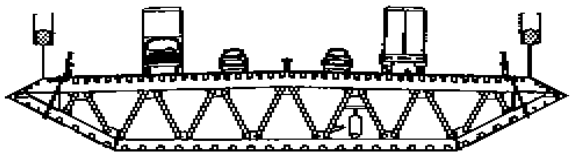

Static Aerodynamic Coefficients: Relevant Sections

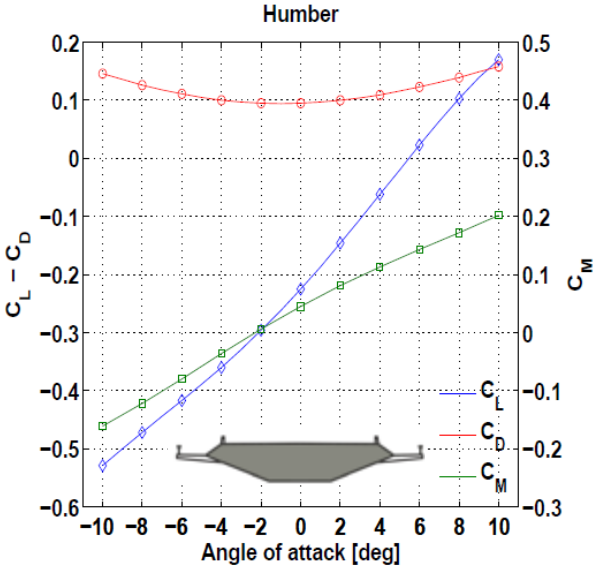

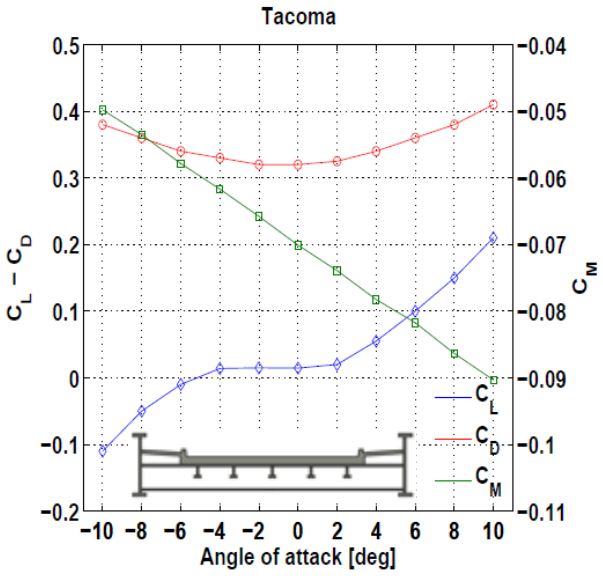

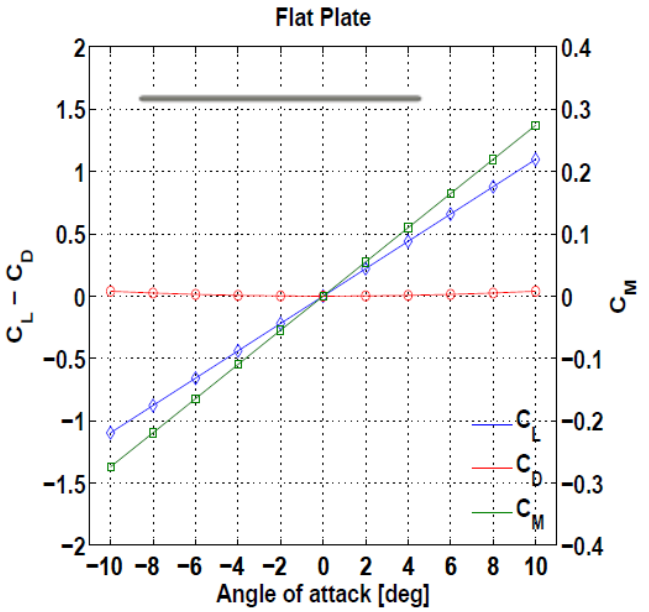

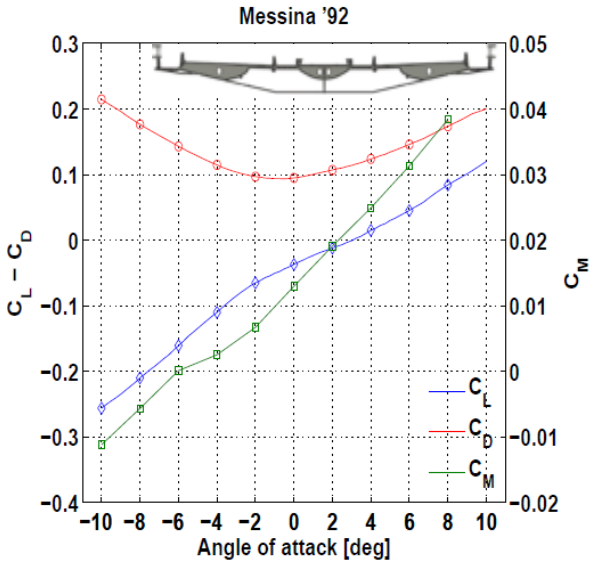

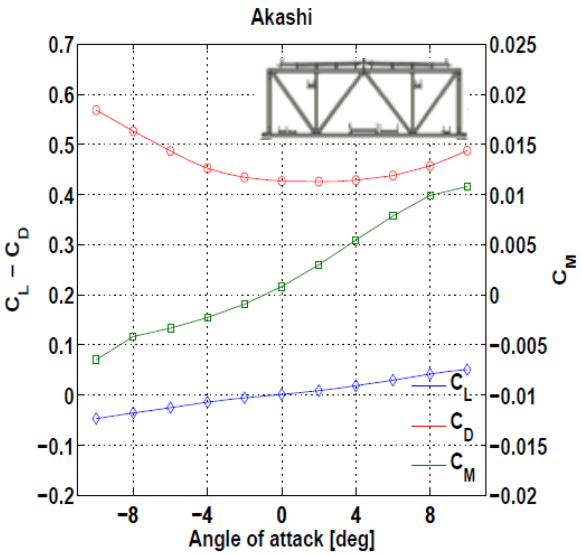

Wind actions

- Problems and solutions related to wind effects:

1. Static loads
2. **One degree of freedom instability**
3. **Flutter instability**
4. Buffeting
5. Vortex shedding

Motion-induced forces

Linearized Quasi-steady corrected theory, in matrix form:

$$\underline{F}_{aero} = -\frac{1}{2}\rho U^2 B \begin{bmatrix} 0 & 0 & -K_{D0} \\ 0 & 0 & -K_{L0} \\ 0 & 0 & -BK_{M0} \end{bmatrix} \begin{bmatrix} y \\ z \\ \theta \end{bmatrix} - \frac{1}{2}\rho UB \begin{bmatrix} 2C_{D0} & (K_{D0}-C_{L0}) & (K_{D0}-C_{L0})B_{1y} \\ 2C_{L0} & (K_{L0}+C_{D0}) & (K_{L0}+C_{D0})B_{1z} \\ B2C_{M0} & BK_{M0} & B(K_{M0})B_{1\theta} \end{bmatrix} \begin{bmatrix} \dot{y} \\ \dot{z} \\ \dot{\theta} \end{bmatrix}$$

Stiffness matrix

Damping matrix

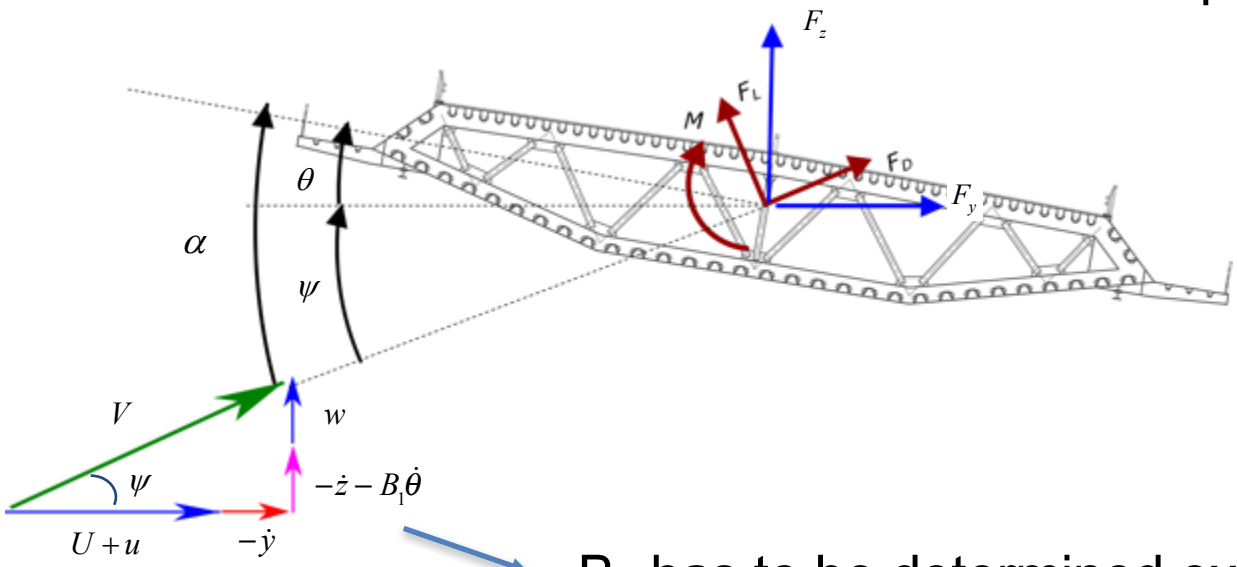

B_1 has to be determined experimentally

Motion-induced forces

Linearized Quasi-steady corrected theory, in matrix form:

$$\underline{F}_{se} = +\frac{1}{2}\rho U^2 B \begin{bmatrix} 0 & 0 & K_{D0} \\ 0 & 0 & K_{L0} \\ 0 & 0 & BK_{M0} \end{bmatrix} \begin{bmatrix} y \\ z \\ \theta \end{bmatrix} - \frac{1}{2}\rho UB \begin{bmatrix} 2C_{D0} & \left(K_{D0} - C_{L0}\right) & \left(K_{D0} - C_{L0}\right)B_{1y} \\ 2C_{L0} & \left(K_{L0} + C_{D0}\right) & \left(K_{L0} + C_{D0}\right)B_{1z} \\ B2C_{M0} & BK_{M0} & B\left(K_{M0}\right)B_{1\theta} \end{bmatrix} \begin{bmatrix} \dot{y} \\ \dot{z} \\ \dot{\theta} \end{bmatrix}$$

Dependence on V*: Flutter derivatives (defined over a range of V*)

$$\underline{F}_{se} = +\frac{1}{2}\rho U^2 B \begin{bmatrix} p_6^* \frac{\pi}{2V_\omega^{*2}} \frac{1}{B} & p_4^* \frac{\pi}{2V_\omega^{*2}} \frac{1}{B} & p_3^* \\ h_6^* \frac{\pi}{2V_\omega^{*2}} \frac{1}{B} & h_4^* \frac{\pi}{2V_\omega^{*2}} \frac{1}{B} & h_3^* \\ a_6^* \frac{\pi}{2V_\omega^{*2}} \frac{1}{B} B & a_4^* \frac{\pi}{2V_\omega^{*2}} \frac{1}{B} B & a_3^* B \end{bmatrix} \begin{bmatrix} y \\ z \\ \theta \end{bmatrix} - \frac{1}{2}\rho UB \begin{bmatrix} p_5^* U & p_1^* & p_2^* B \\ h_5^* \frac{1}{U} & h_1^* & h_2^* B \\ a_5^* B & a_1^* B & a_2^* B \end{bmatrix} \begin{bmatrix} \dot{y} \\ \dot{z} \\ \dot{\theta} \end{bmatrix}$$

Stiffness matrix

Damping matrix

Wing like deck shape

This type of section do not suffer of one degree of freedom instability like old Tacoma Narrow Bridge

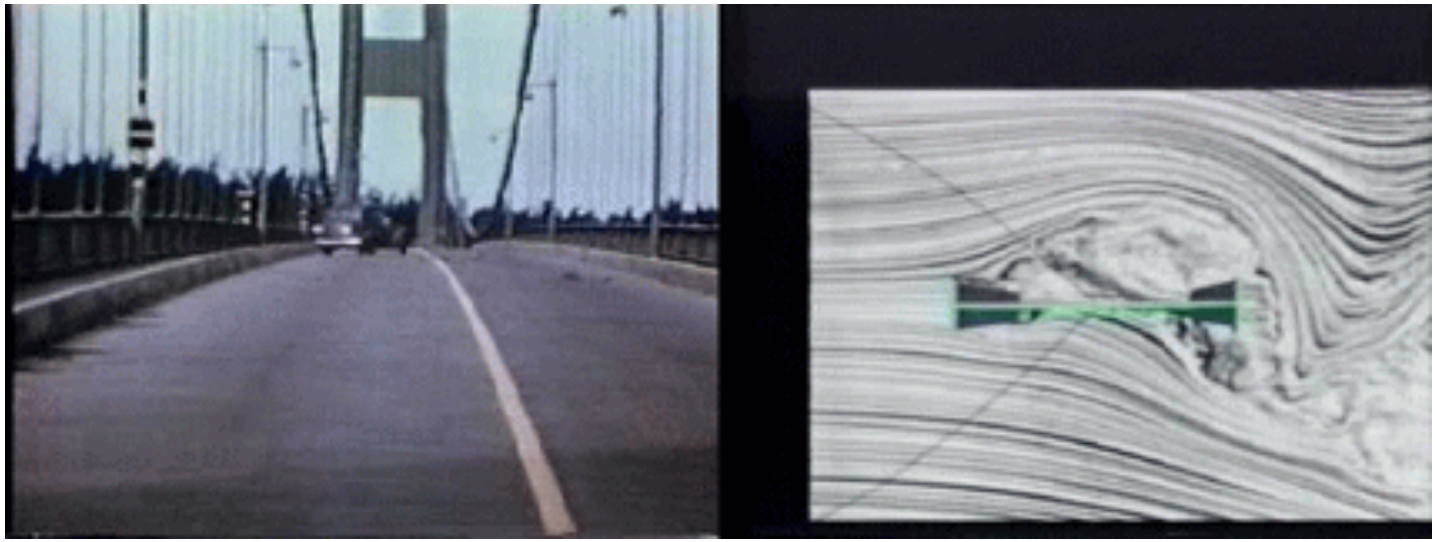

But it suffer of two degrees of freedom instability of the flutter type

I will try to explain in a simple way the mechanism

Instability problems or aeroelasticity

If, for any reason, for a generic wind V, the deck rotates of α an elastic moment, proportional to the structural stiffness K_t^{str} , is produced

Due to wind action, an aerodynamic moment arises, with the same sign of the rotation α, producing a negative torsional aerodynamic stiffness K_t^{aer}

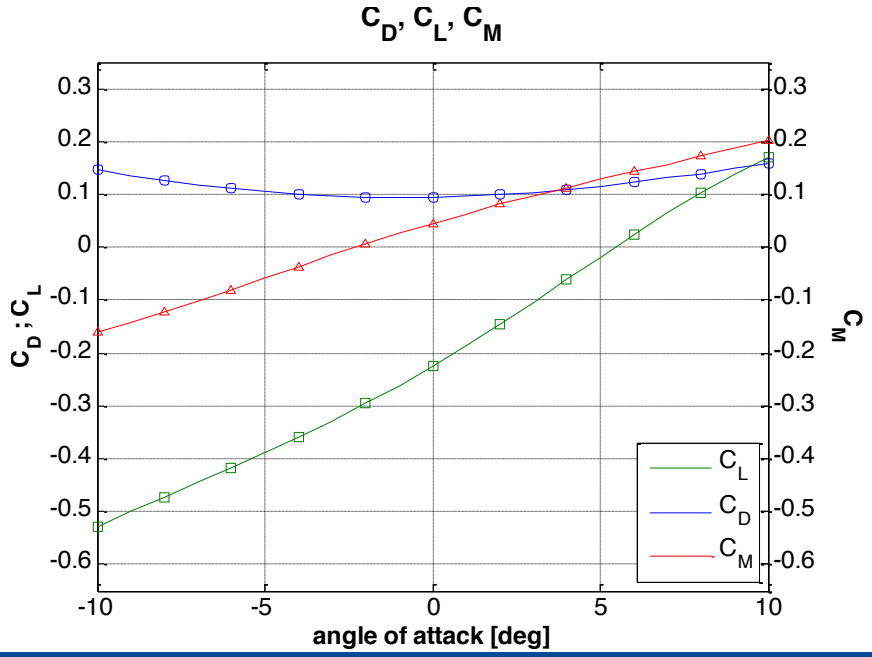

Humber Bridge

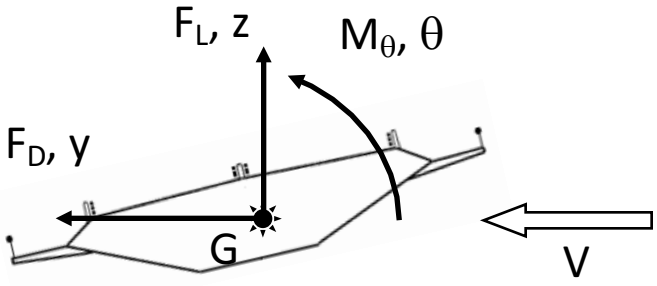

Linearization of the aeroelastic terms

In first approximation:

$$K_t^{aer} = -\frac{1}{2}\rho V^2 B^2 L \frac{\partial C_M}{\partial \psi}$$

Where $\frac{\partial C_M}{\partial \psi}$ is the slope of the moment coefficient

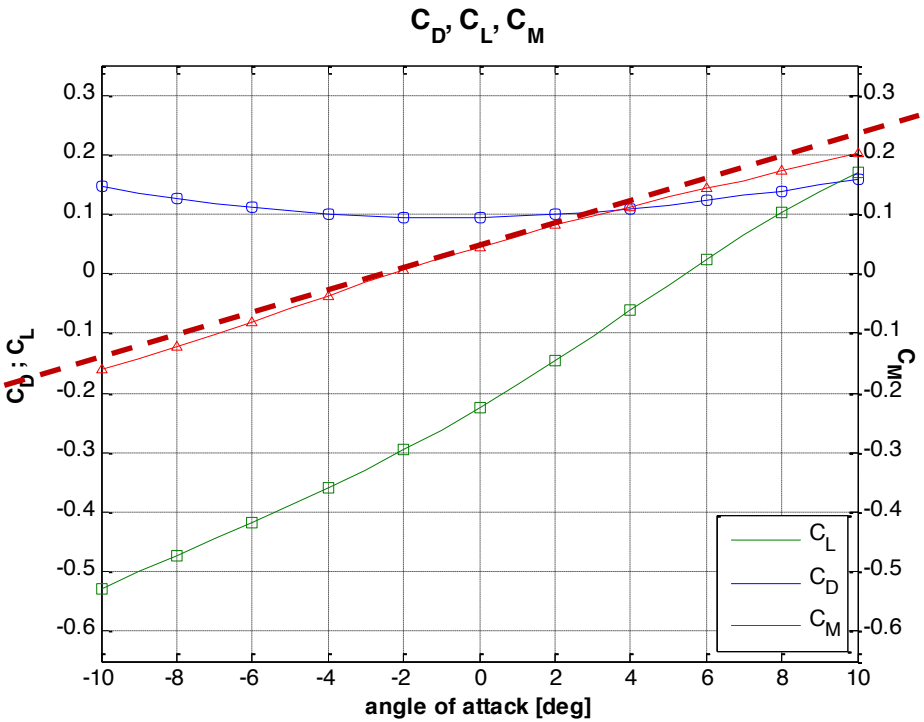

Humber Bridge

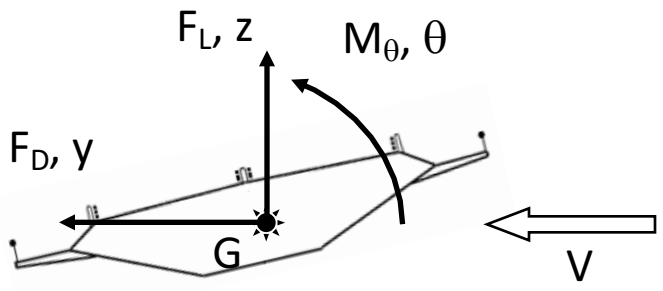

Linearization of the aeroelastic terms

The total torsional stiffness is: $K_t^{tot} = K_t^{str} + K_t^{aer}$

Being K_t^{aer} negative and proportional to V^2

Increasing the wind speed K_t^{tot} decreases and as a consequence the torsional frequencies are decreasing

First vertical mode

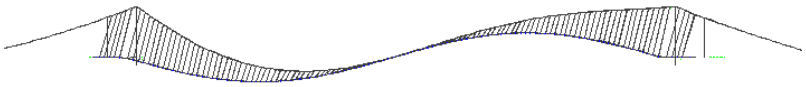

First torsional mode

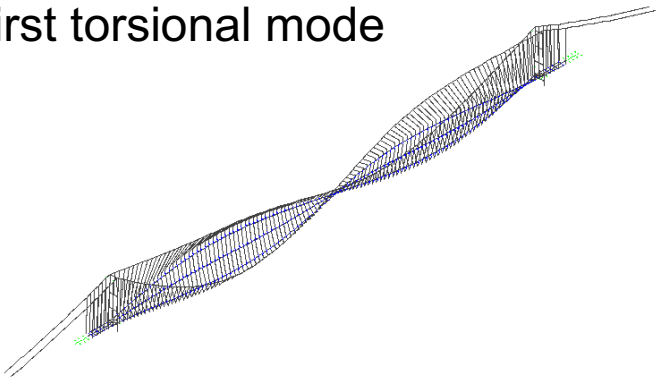

Their coupling gives rise to flutter instability

2 d.o.f. instability (flutter): natural frequencies

$$K_t^{tot} = K_t^{str} + K_t^{aer}$$

$$K_t^{aer} = \frac{1}{2}\rho V^2 B^2 L \frac{\partial C_M}{\partial \psi}$$

$$\omega = \sqrt{\frac{\mathbf{k_{tot}}}{\mathbf{J}}}$$

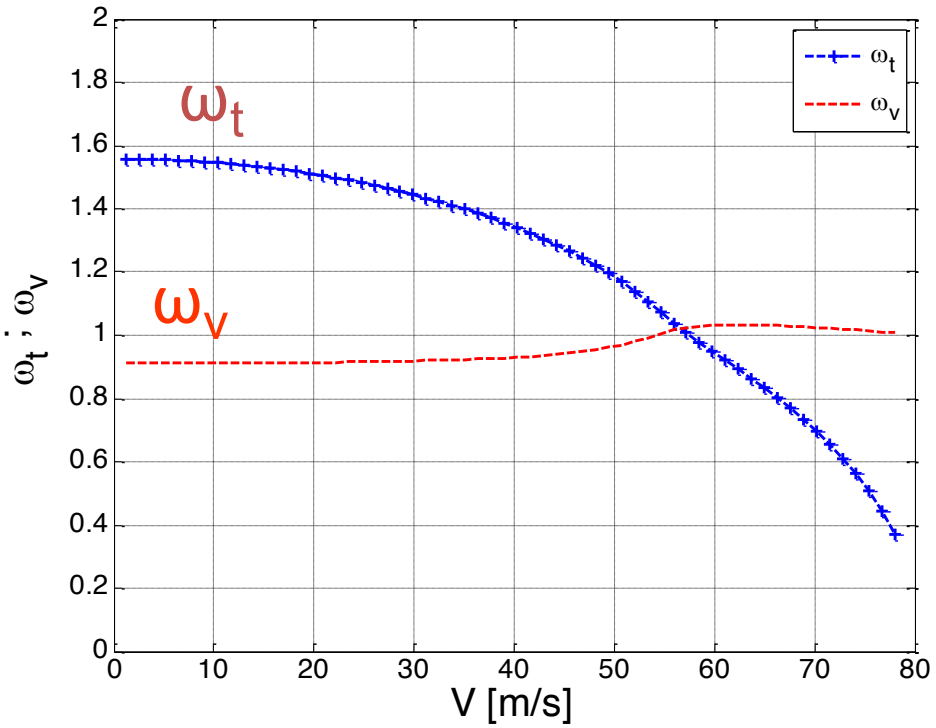

2 d.o.f. instability (flutter)

When this two frequencies become equal a two degree of freedom flutter is produced:

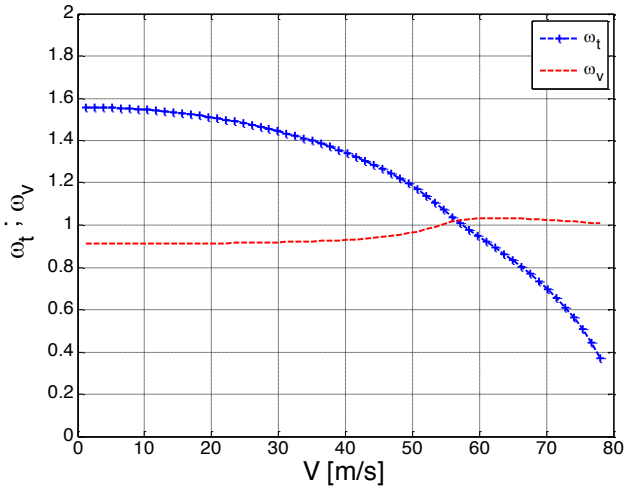

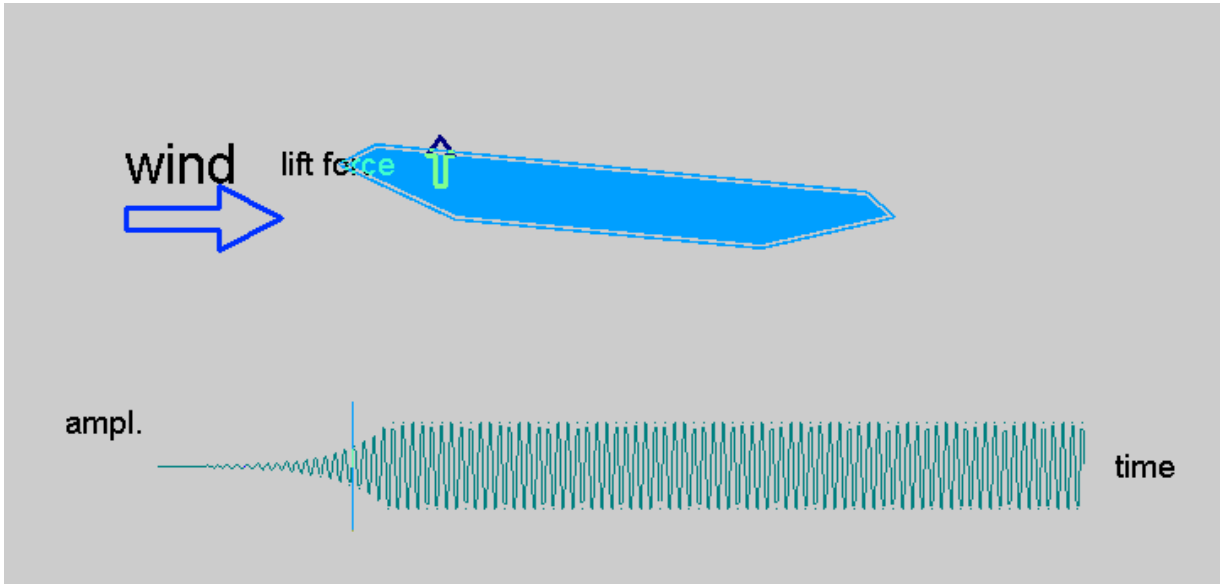

Why this is a problem increasing the span length?

$\omega_t - \omega_v$

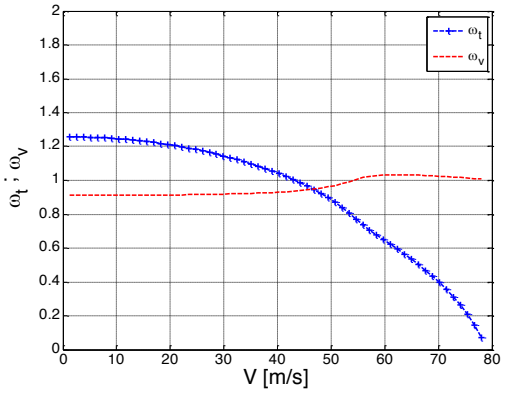

$\omega_t - \omega_v$

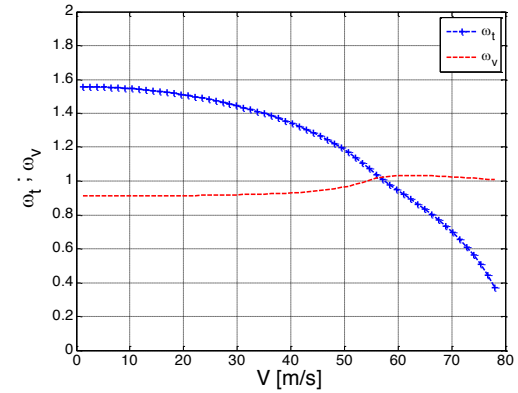

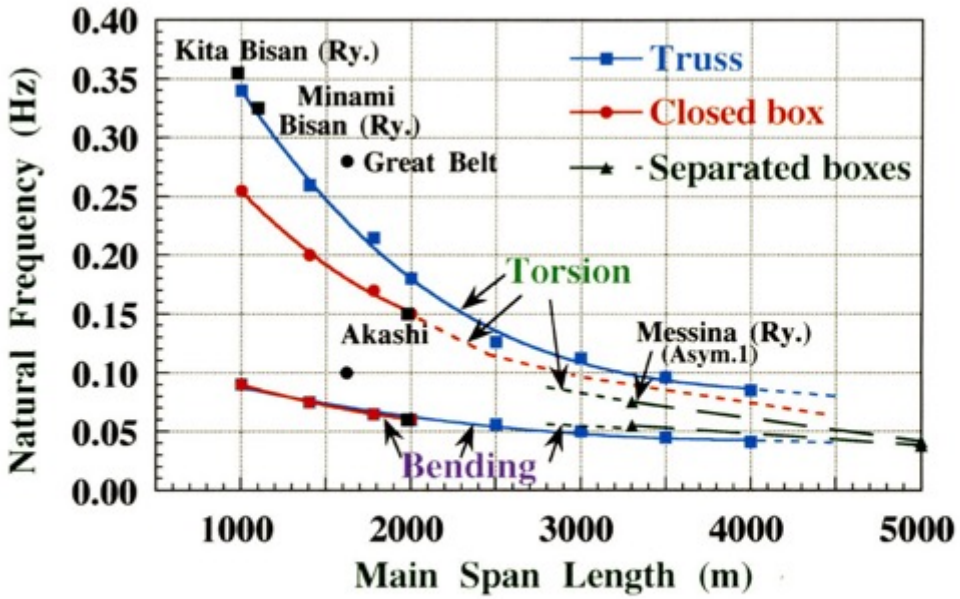

Reduction of Natural Frequency with Span Length in Suspension Bridge

Aerodinamic optimization

If the Humber or Storebealt deck section aerodynamics were applied to the the Messina structural properties then Messina flutter wind speed would be:

$$V_{flutter} = 40 \text{ m/s}$$

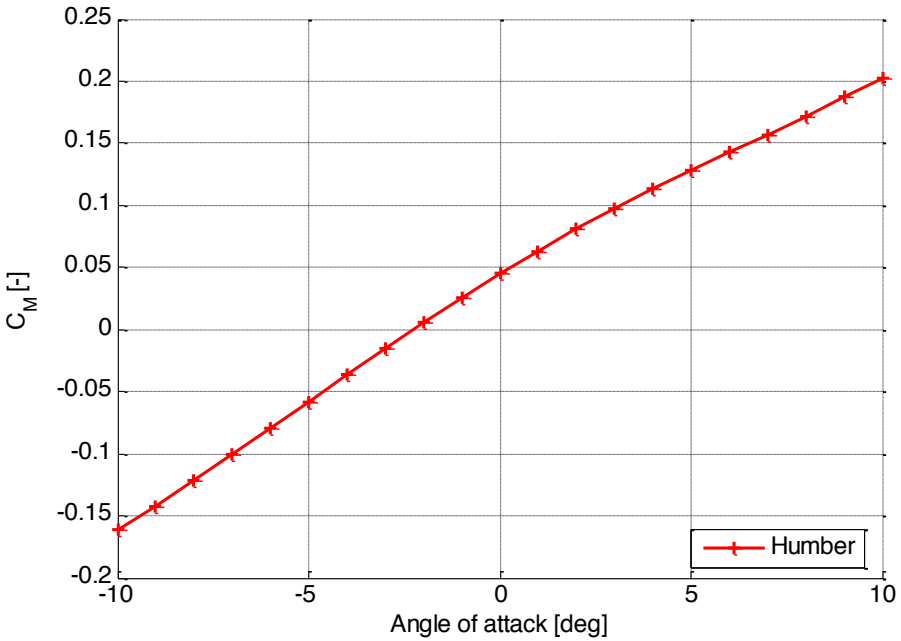

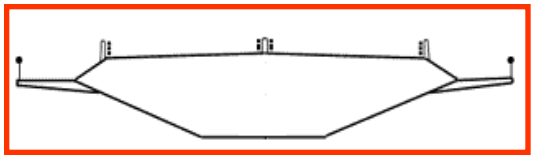

How to come out from this problem? 2 ways:

1) Structural solution:

by increasing the structural torsional stiffness of the deck (like Akashi)

Drawbacks:

- High drag
- Not feasible increasing the span length since the cable contribution to the torsional stifness becomes larger and larger and the effect of deck stiffness becomes negligible

How to come out from this problem? 2 ways:

2) Aerodynamic solution:

by decreasing the aerodynamic torsional stiffness

$$K_t^{aer} = \frac{1}{2}\rho V^2 B^2 L \frac{\partial C_M}{\partial \psi}$$

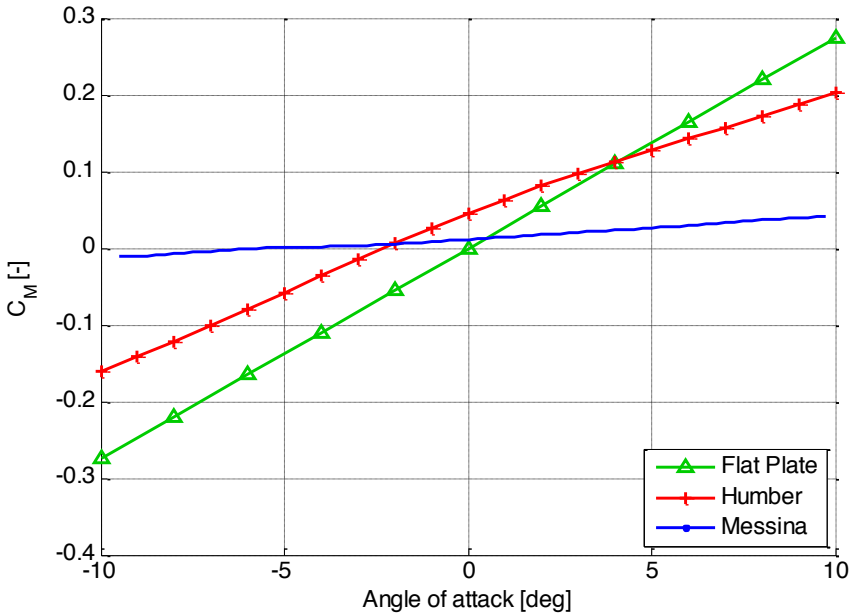

Using Humber bridge aerodynamics : $V_{flutter}$ = 40 m/s

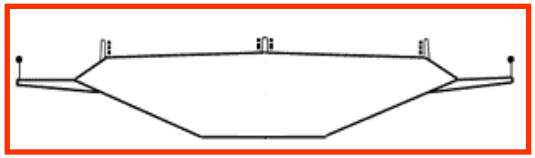

Using Messina bridge aerodynamics : $V_{flutter}$ = 90 m/s

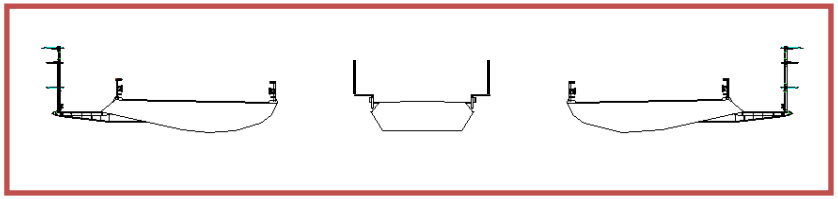

Messina bridge solution:

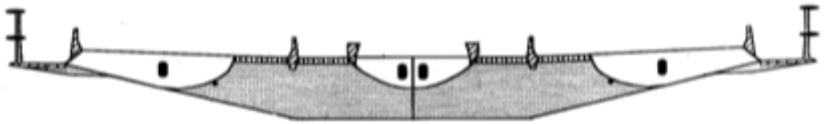

The secret of Messina bridge is the multi box deck section with:

- very low (BUT POSITIVE !) lift and moment DERIVATIVES

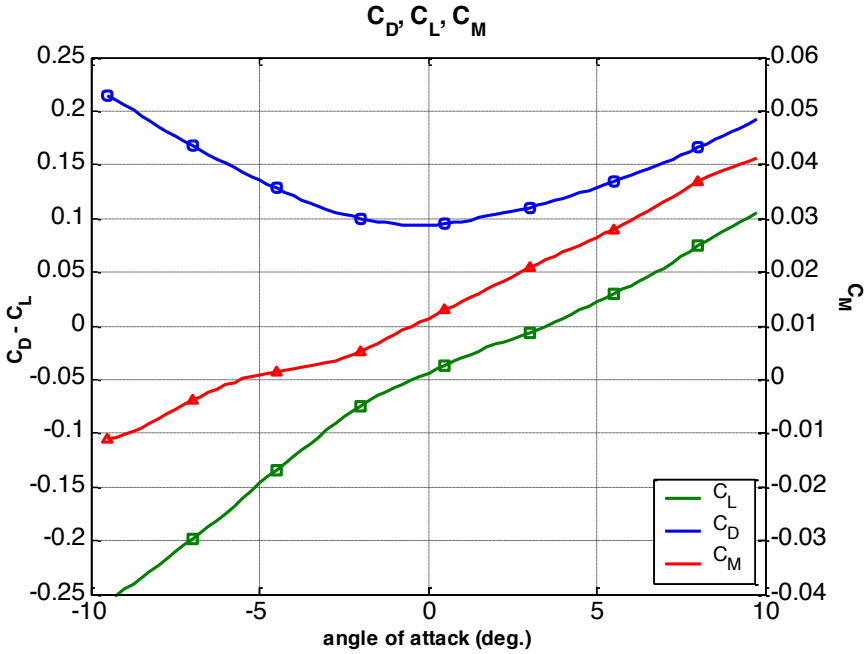

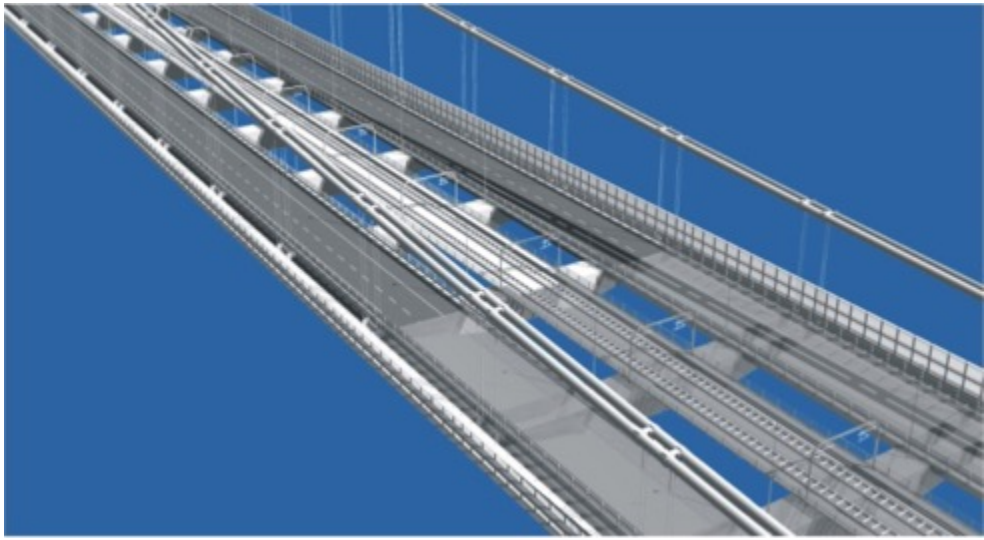

Messina bridge solution:

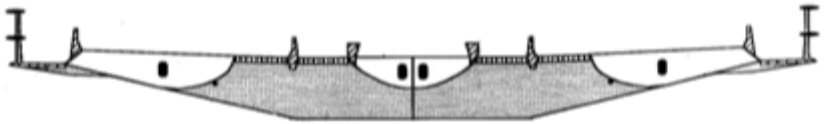

The secret of Messina bridge is the multi box deck section with:

- very low (BUT POSITIVE !) lift and moment DERIVATIVES
- transparent wind screen with aerodynamic damping devices

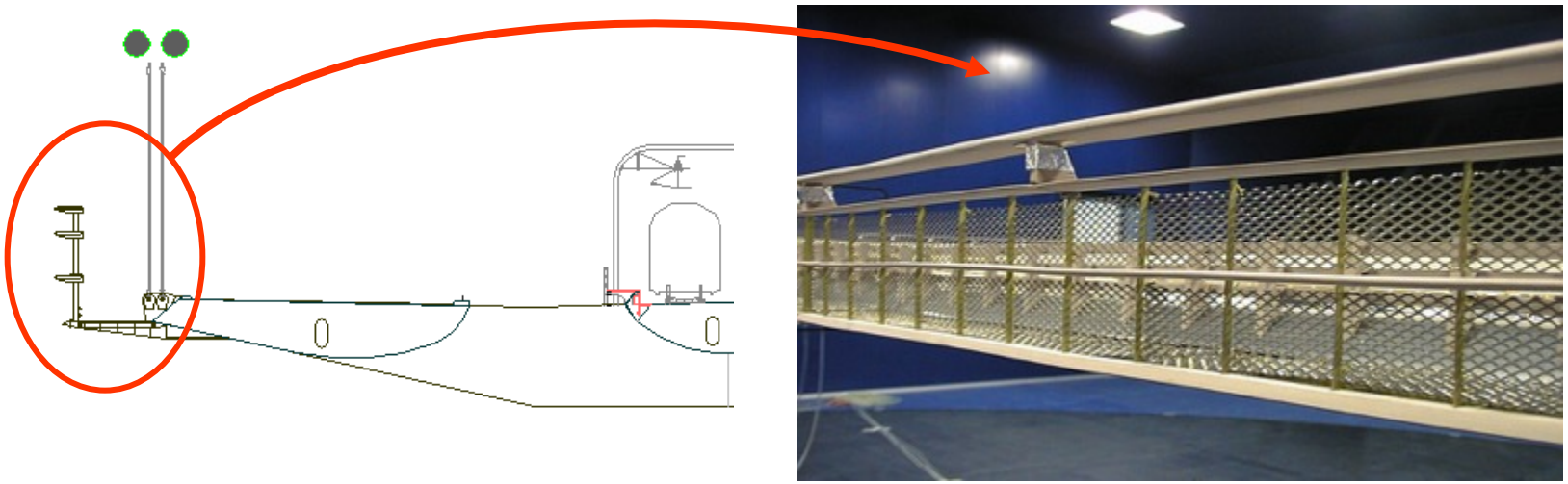

Total damping requirements

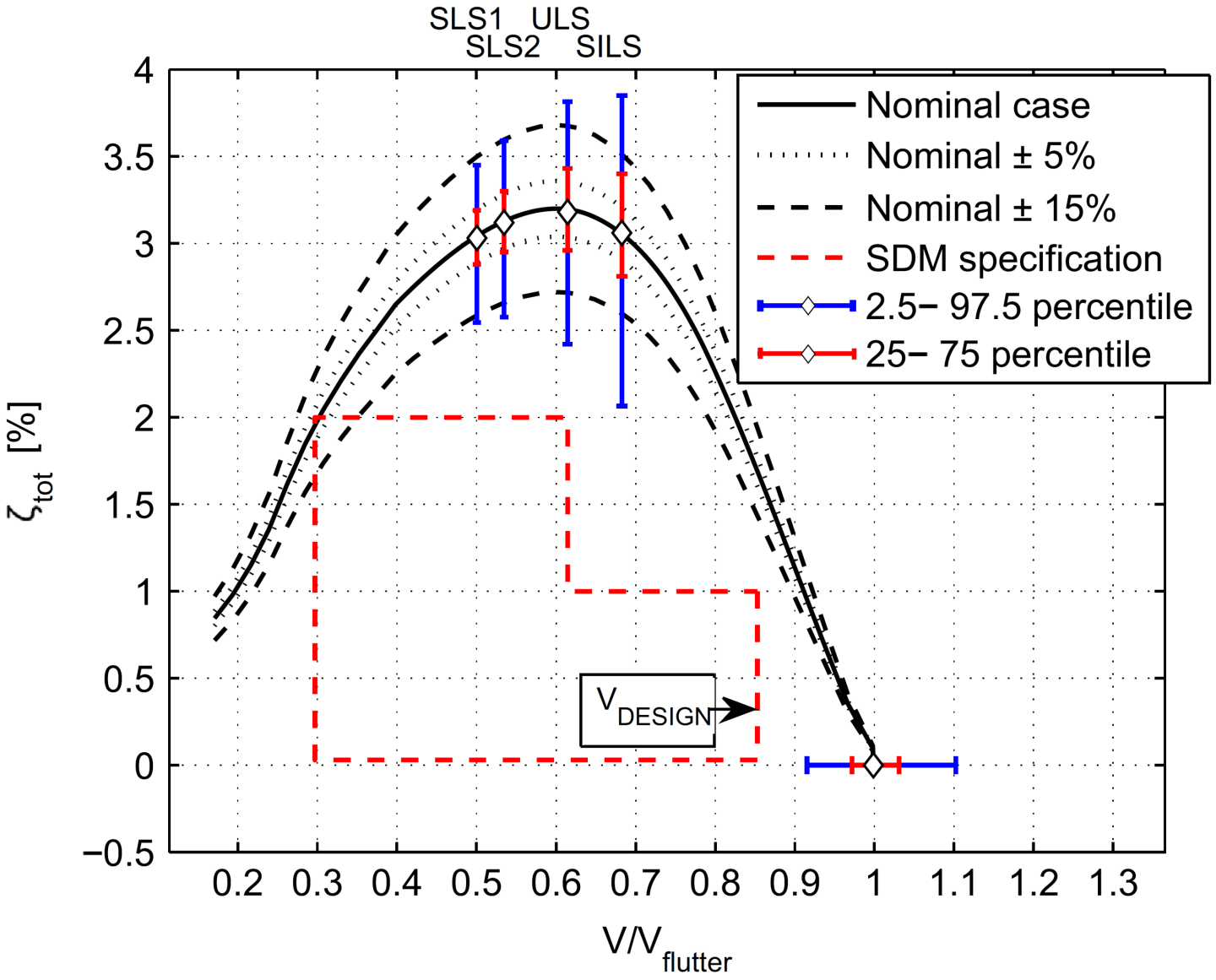

Wind actions

- Problems and solutions related to wind effects:

1. Static loads
2. One degree of freedom instability
3. Flutter instability
4. **Buffeting**
5. Vortex shedding

Bridge buffeting response simulation

Aerodynamic Force Model (2D)

$$F = F(x, \dot{x}, u, w)$$

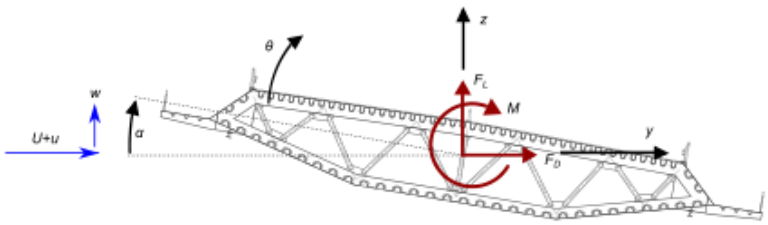

- Linear models
- Nonlinear models

Cross PSD of turbulent wind field

FEM Analysis of fhe bridge

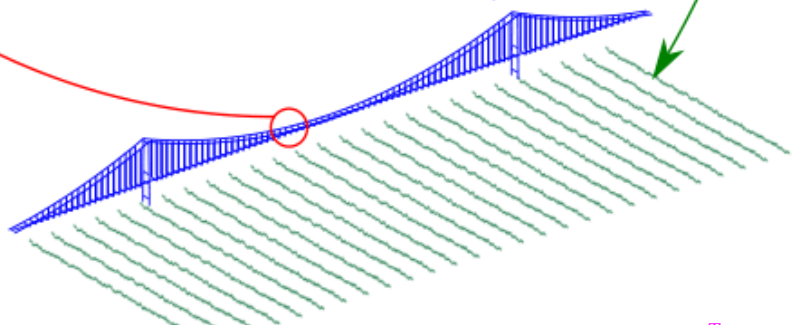

$$\left[M_s^*\right]\ddot{\underline{q}} + \left[C_s^*\right]\dot{\underline{q}} + \left[K_s^*\right]\underline{q} = \left[\Phi\right]^T \underline{F}_{aero}$$

Multi-modal sectional approach

Buffeting Response

Time / Frequency

Buffeting response validation

- Full aeroelastic model

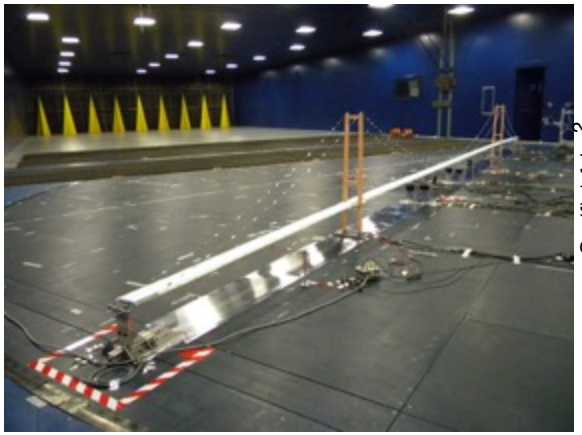

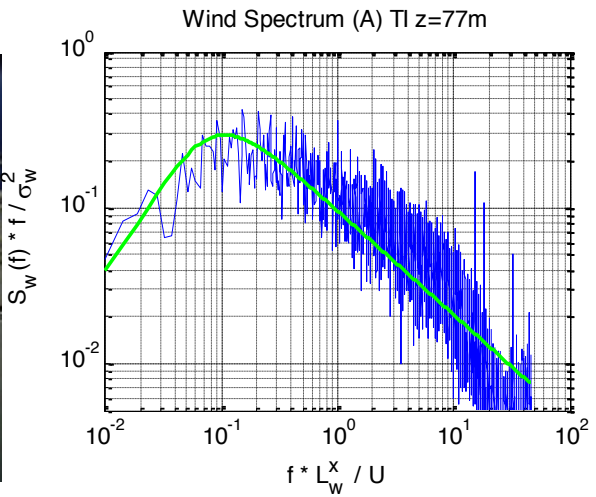

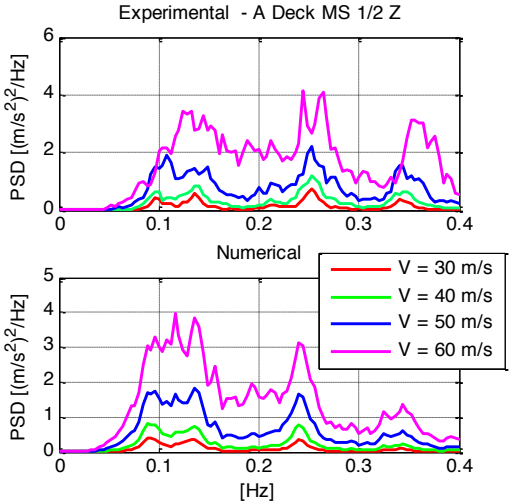

- Suspended sectional model

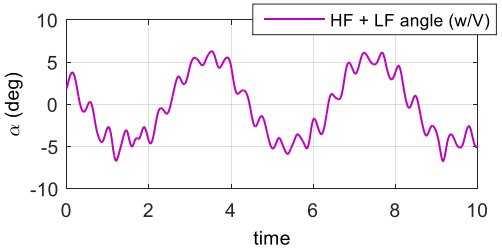

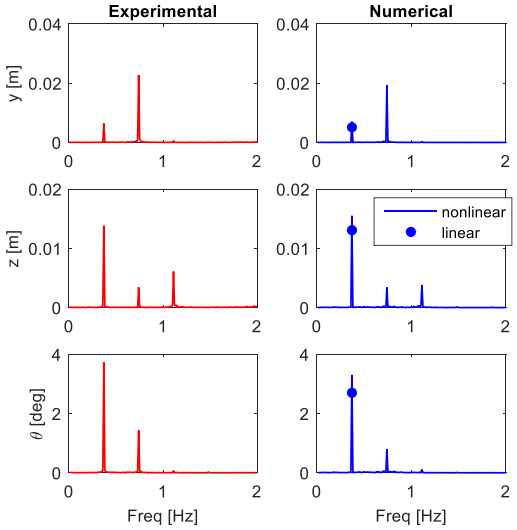

Pros and cons

- Full Aeroelastic Model

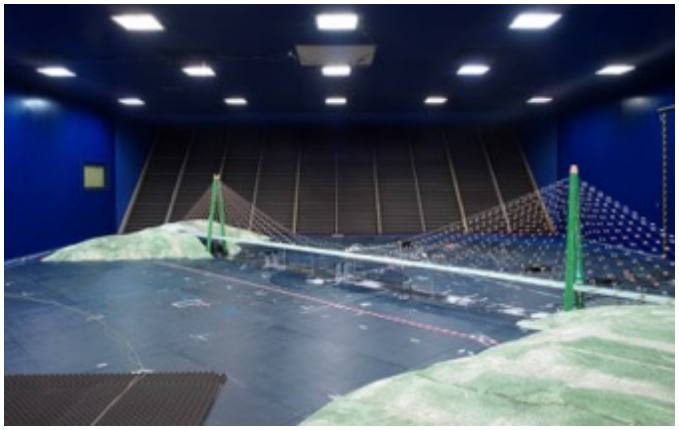

ADVANTAGES

- Multimodal excitation
- Modal shape effect
- Coupling effects
- Useful for complex stability analysis
- Different wind directions and orography

DISADVANTAGES

- Small geometrical scale
- Difficulty in controlling damping
- Difficult to measure turbulence along the deck at many locations

- Suspended sectional model

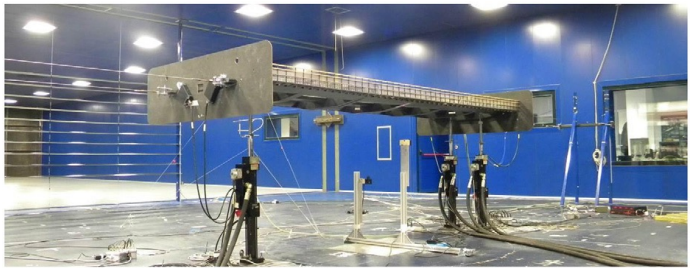

ADVANTAGES

- Large scale
- Accuracy of geometrical details
- Measurement of pressure distribution / global forces
- Low damping
- VIV
- Active turbulence generator

DISADVANTAGES

- All the sections are characterized by the same aerodynamic behavior
- Multimodal excitation can not be considered
- Low wind speed test, for low reduced velocities V*

Active turbulence generator

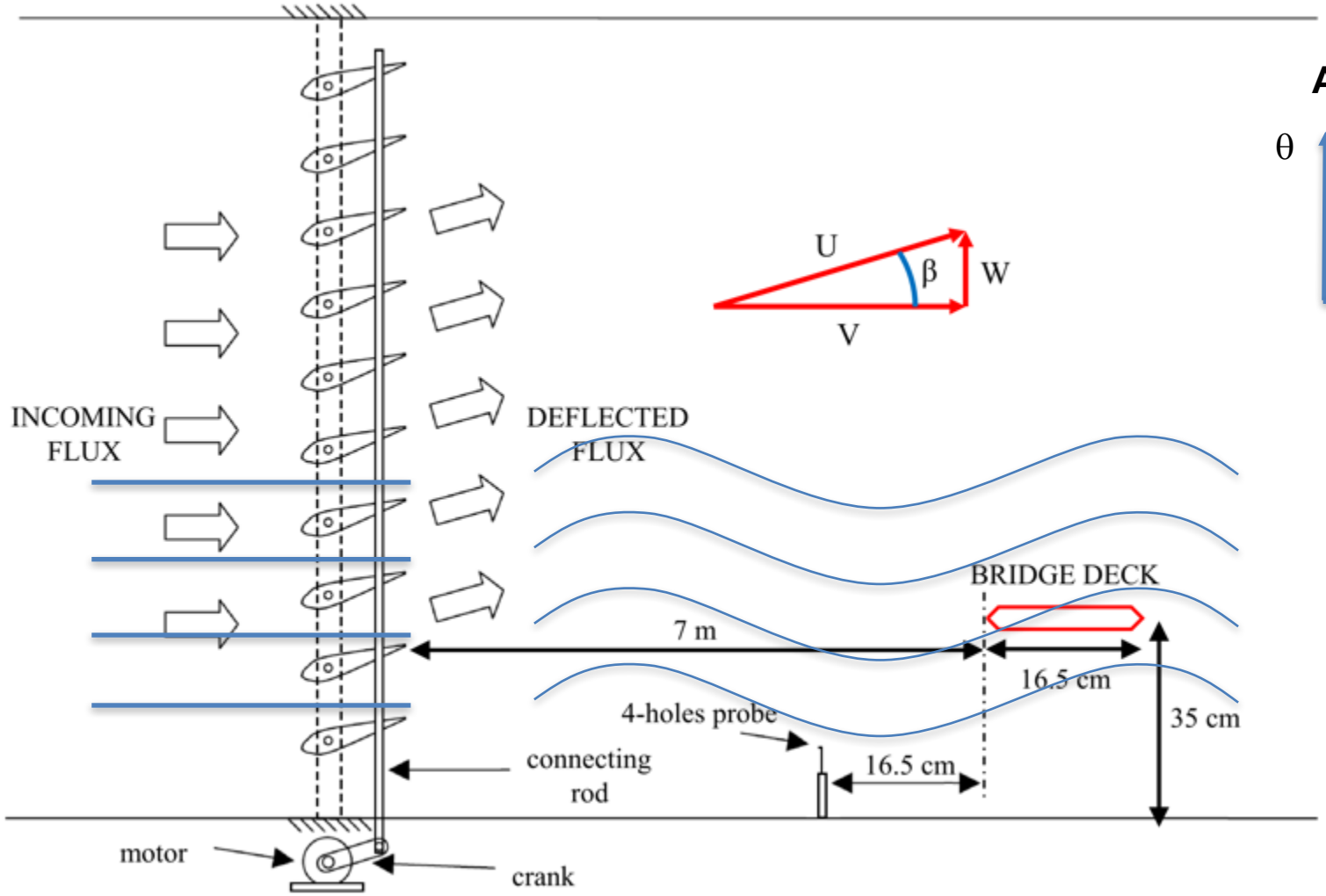

Airfoil motion:

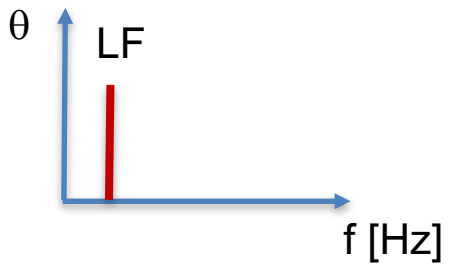

Active turbulence generator

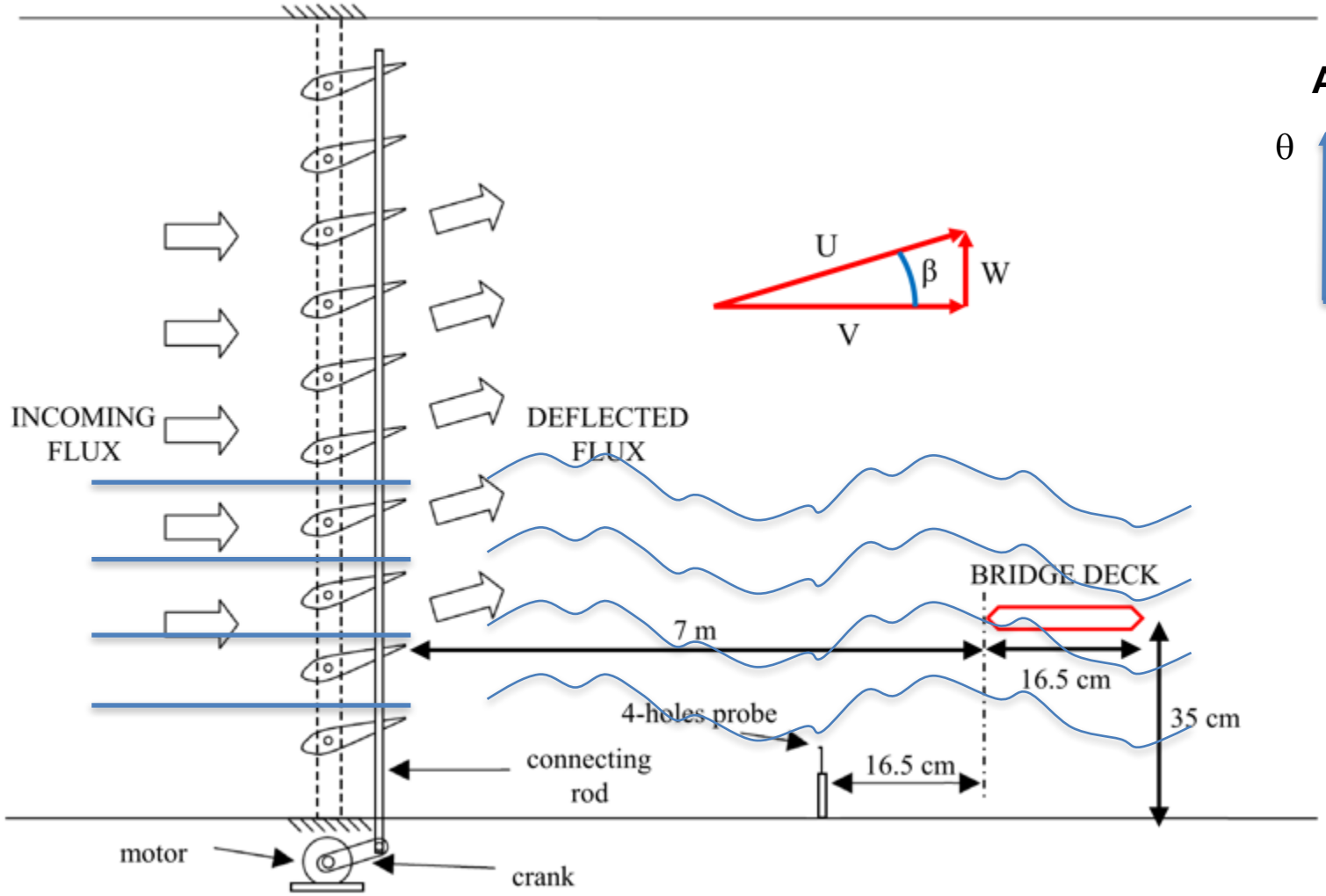

Airfoil motion:

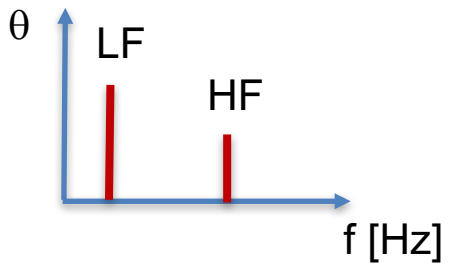

Experimental results

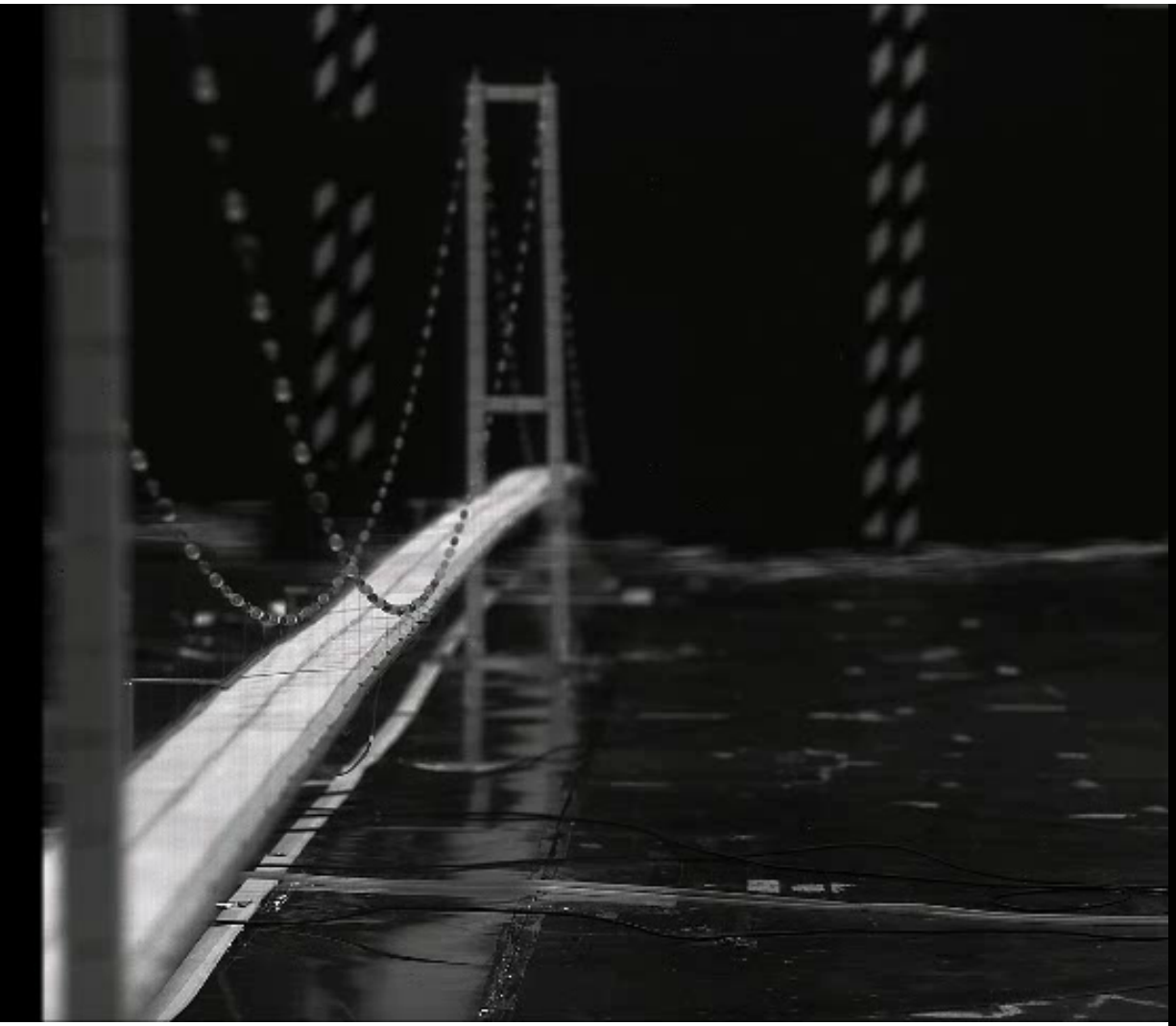

- Mean wind speed
  U = 5 m/s
- Low frequency 0.1 Hz,
  w/U = 2 deg
- High frequency 2.6 Hz,
  w/U = 1 deg
- Large aeroelastic coupling
  (flutter at 5.6 m/s)
- Forcing near resonance

Experimental results

- Low frequency + high frequency (LF = 0.1 Hz, HF = 2.57 Hz)

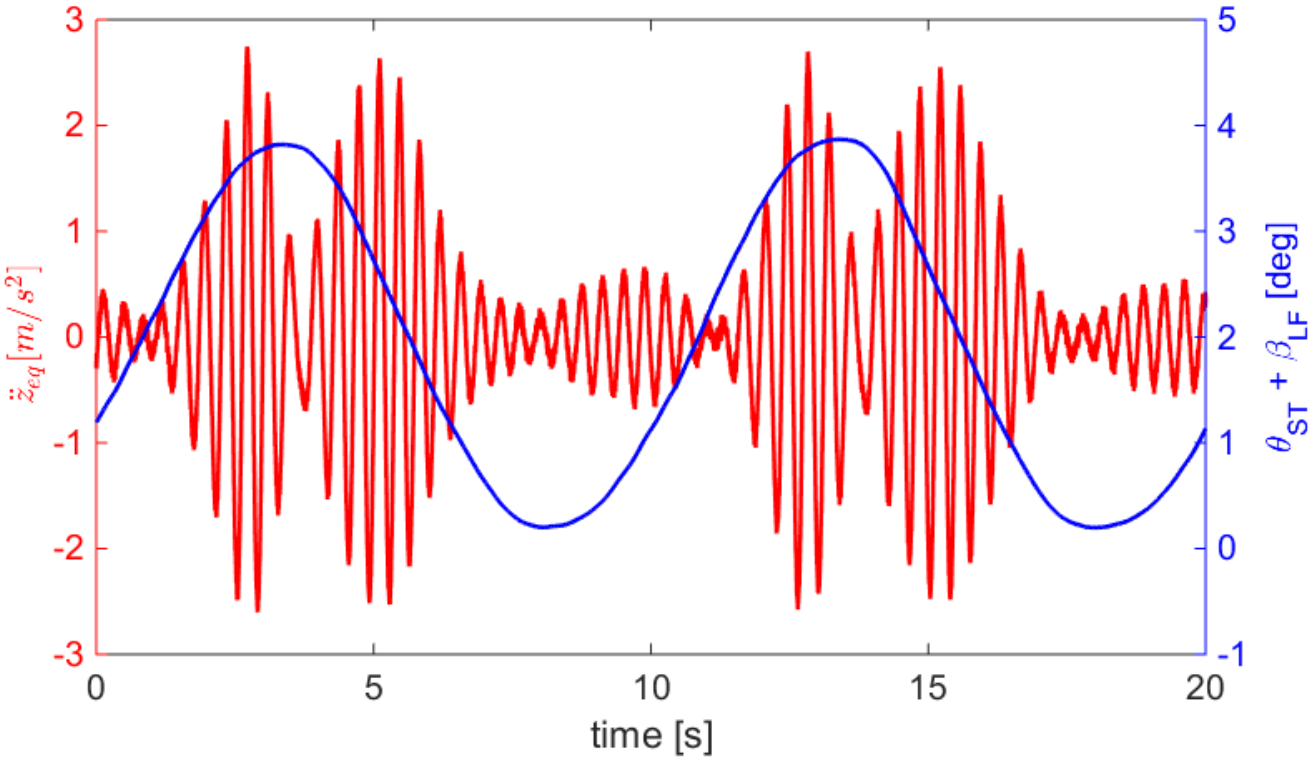

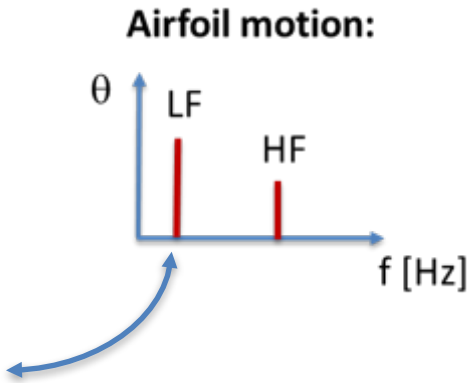

There is a correlation between the LF angle of attack and the HF response of the bridge

Experimental results

- Only high frequency (HF = 2.57 Hz)

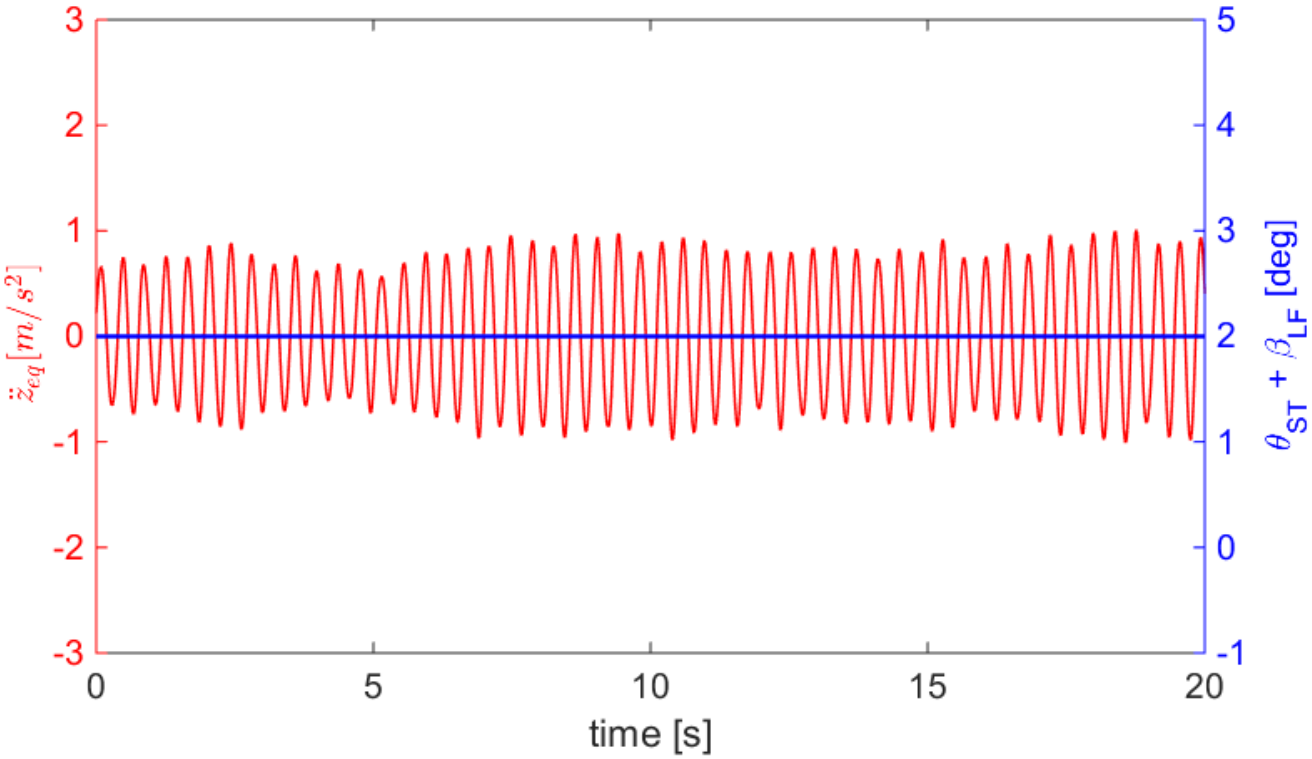

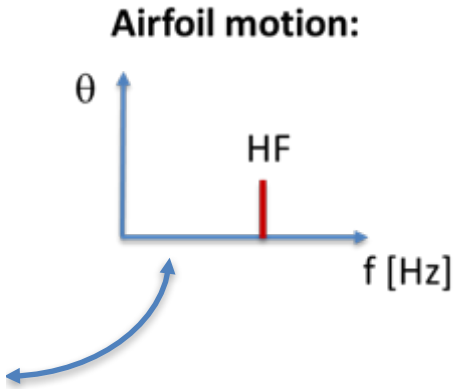

Adequate Wind Tunnel: still a key point !

POLIMI Wind Tunnel: Boundary Layer / Smooth Flow / Open Jet

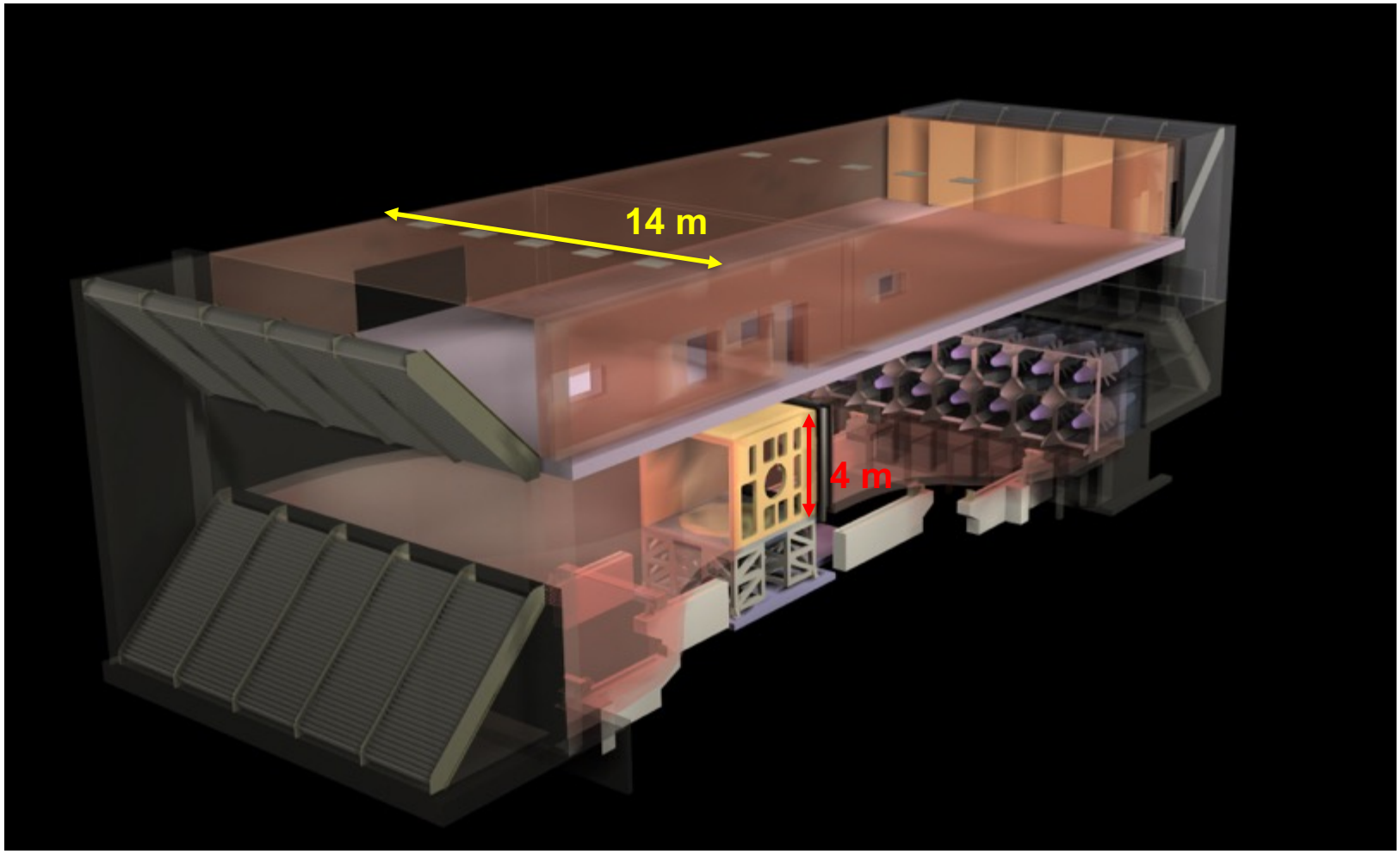

Deck WT tests

Messina - ELK

FORCE Technology (Denmark):

- Model scale: 1: 80 (Deck chord = 0.75 m)
- Maximum wind speed: up to 24 m/s (Re = 1.2 10^6)
- Investigated: Stability – Vortex shedding

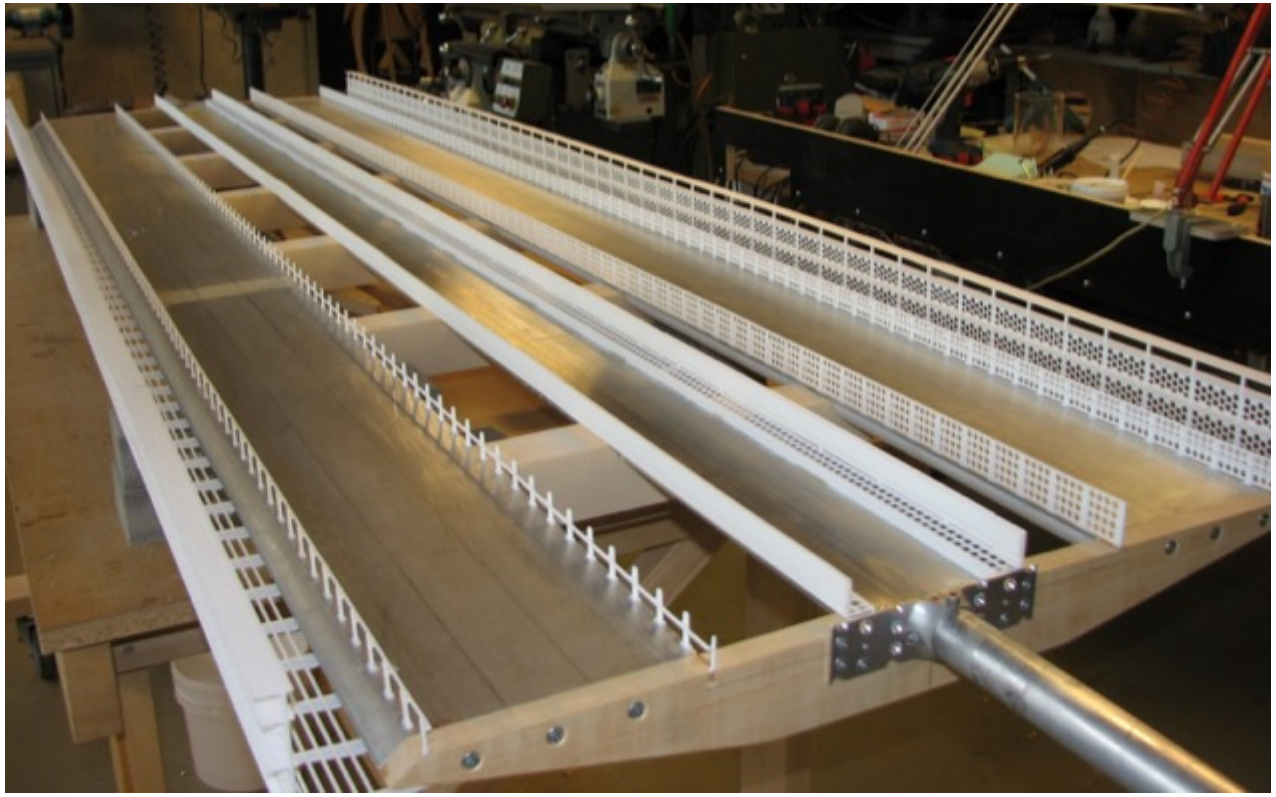

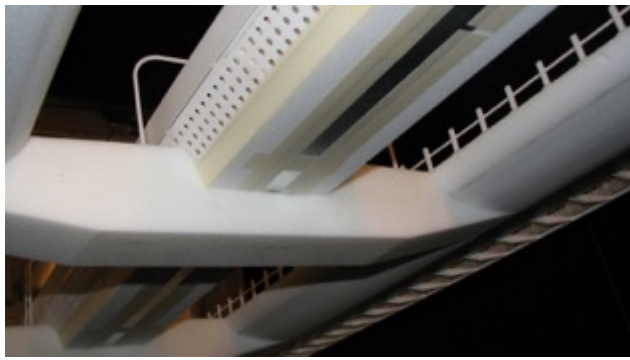

Deck WT tests

Messina - ELK

Alan G. Davenport WE group (Canada):

Alan G. Davenport Wind Engineering Group

- Model scale: 1: 80 (Deck chord = 0.75 m)
- Maximum wind speed: up to 24 m/s (Re = 1.0 10^6)
- Investigated: Stability – Vortex shedding

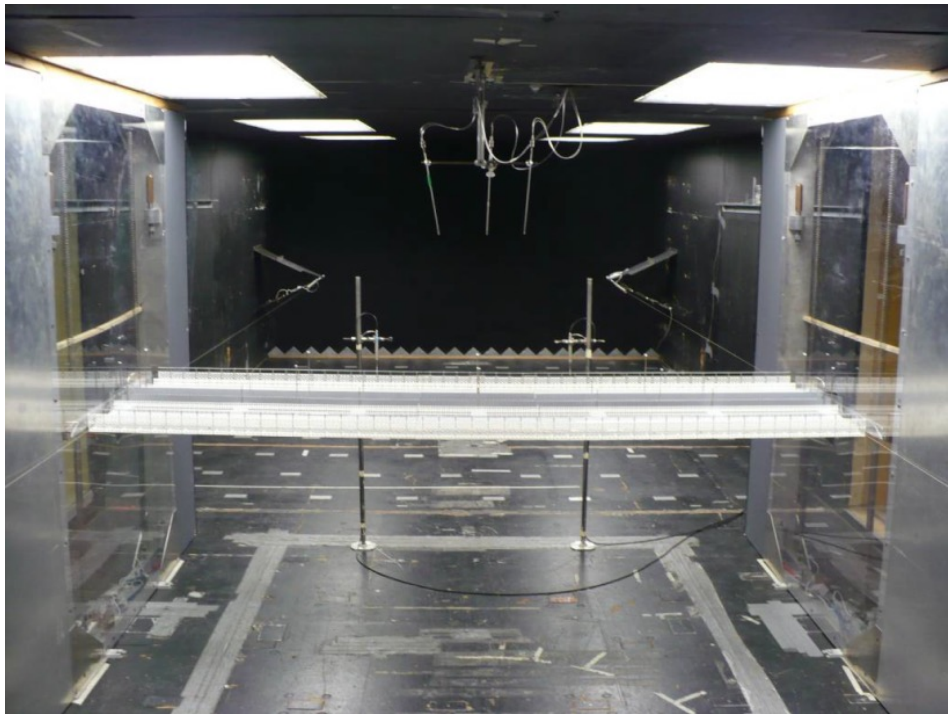

Deck WT tests

Messina - ELK

NRC (Ottawa Canada):

National Research Council Canada

- Model scale: 1: 30 (Deck chord = 2.0 m)
- Maximum wind speed: up to 55 m/s (Re = 7.3 10^6)
- Investigated: Stability – Vortex shedding

Deck WT tests @POLIMI Messina - PMC

POLIMI (Milan Italy):

- Model scale: 1: 45 (Deck chord = 1.33 m)
- Maximum wind speed: up to 50 m/s (Re = 4.4 10^6)
- Investigated: Stability – Vortex shedding

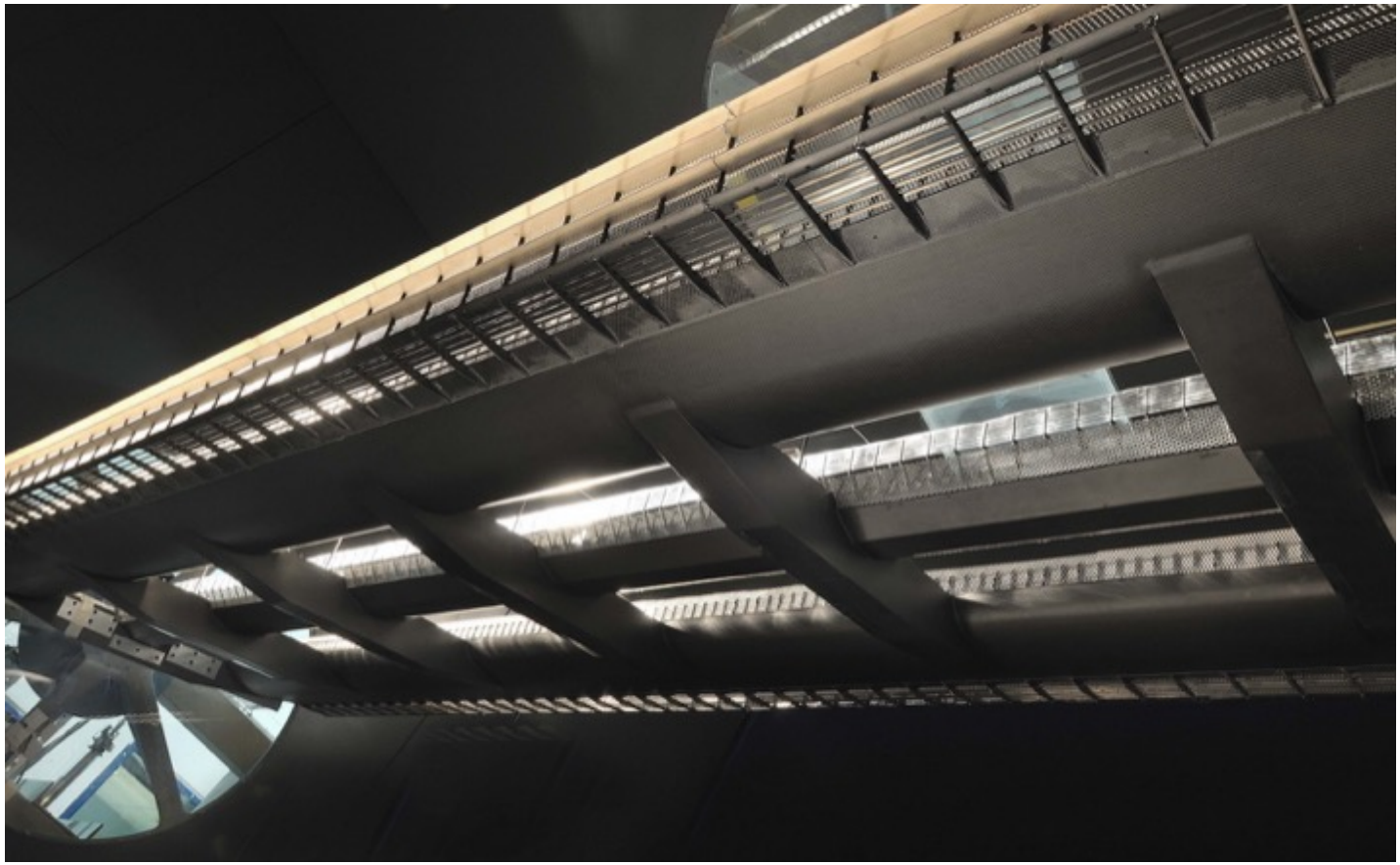

Deck WT tests @POLIMI Messina - PMC

POLIMI (Milan Italy):

- Model scale: 1: 45 (Deck chord = 1.33 m)
- Maximum wind speed: up to 50 m/s (Re = 4.4 10^6)
- Investigated: **Stability** – Vortex shedding

Full Aeroelastic Bridge @POLIMI BB3

- Combined effects of exposure angle and upwind roughness considered
- e.g.: incoming turbulent wind Exposure 45° → 347° NW

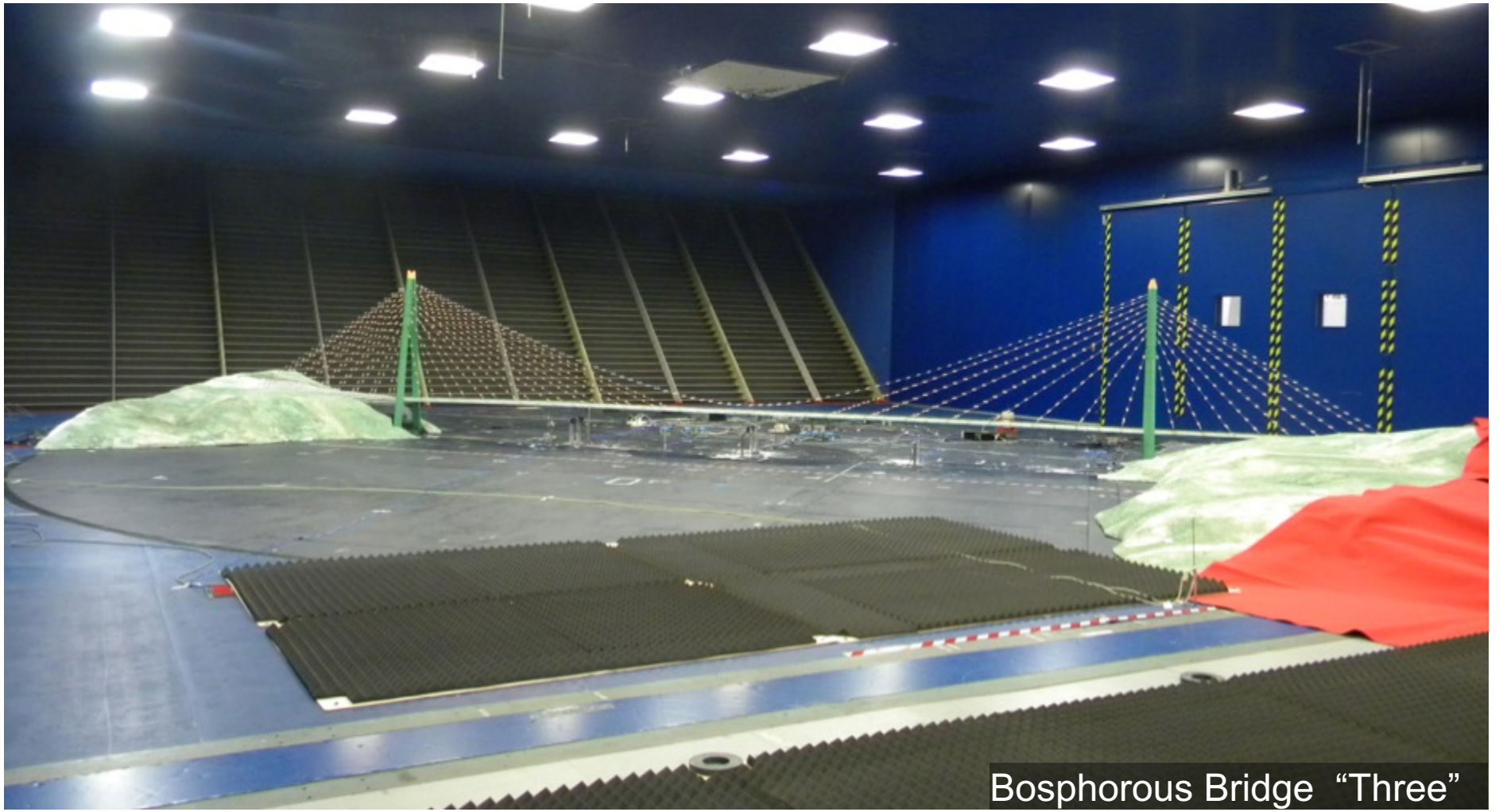

Full Aeroelastic Bridge @POLIMI Messina

- Length scale 1:300 / Total length 13.8m / All suspended spans present
- The whole model is positioned on a turning table

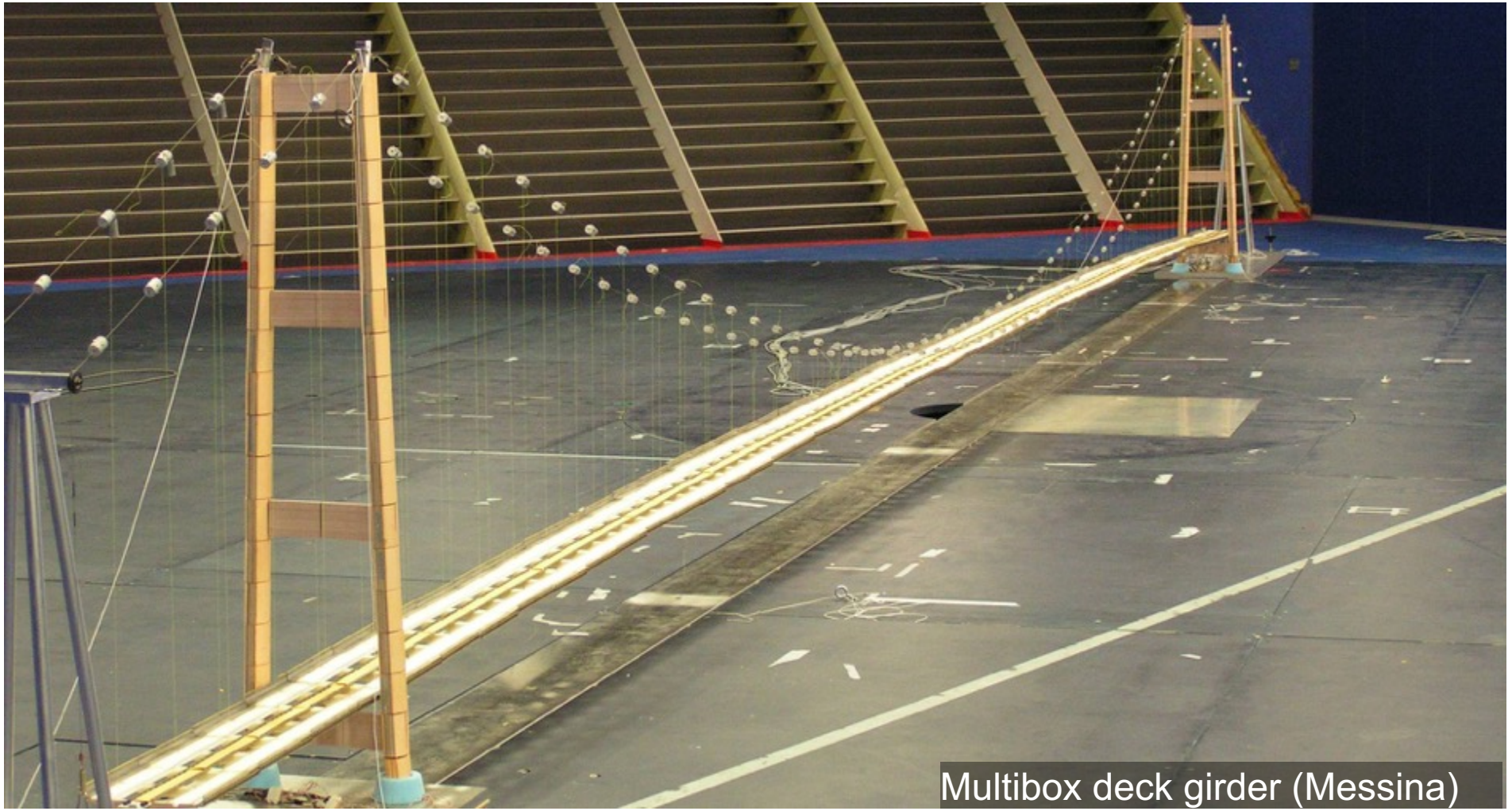

Multibox deck girder (Messina)

Full Aeroelastic Bridge @POLIMI Izmit Bay Bdg

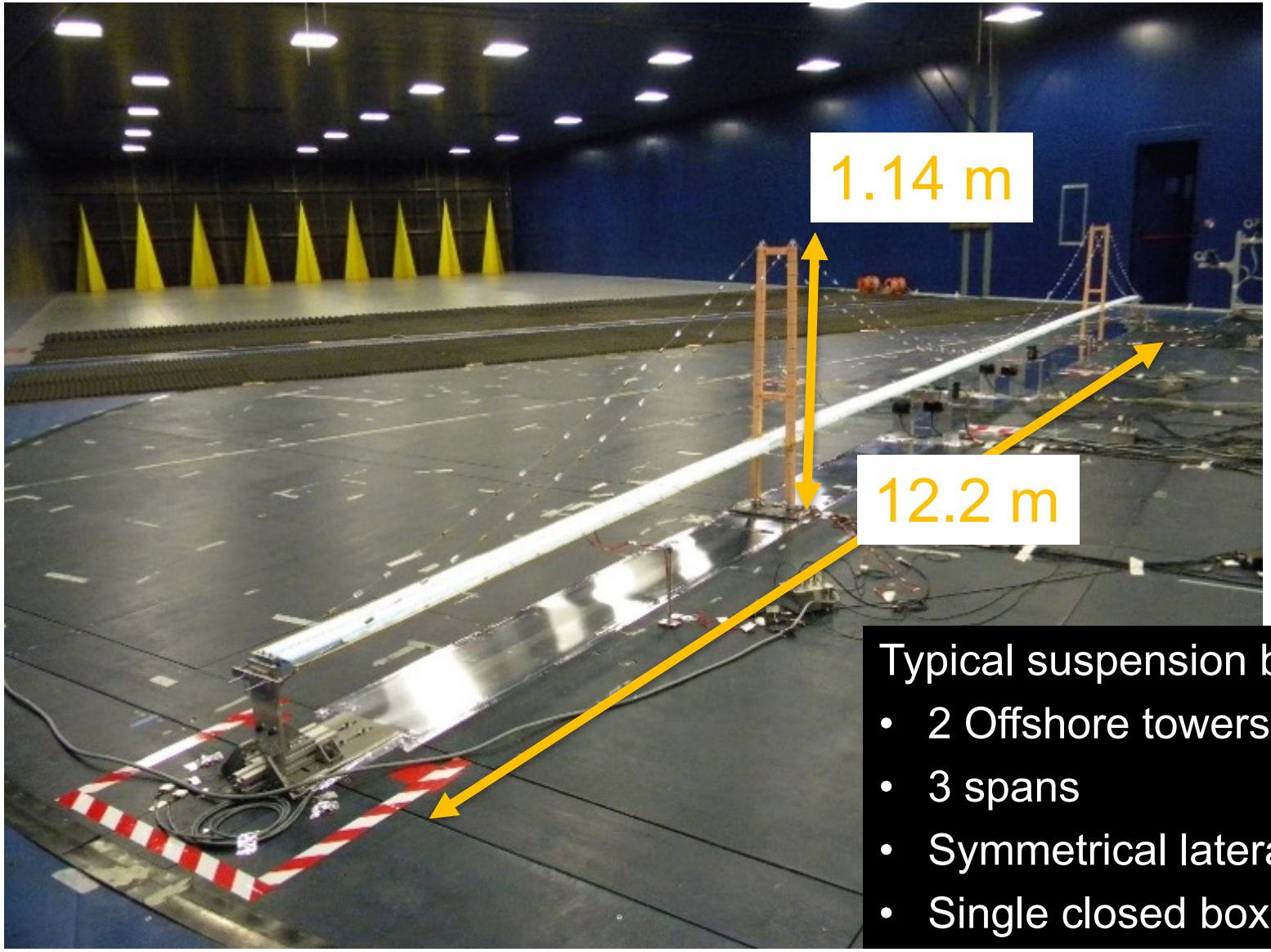

Typical suspension bridge:

- 2 Offshore towers
- 3 spans
- Symmetrical lateral spans
- Single closed box deck

Wind actions: Vortex Induced Vibrations (VIV)

- Problems and solutions related to wind effects:

1. Static loads
2. One degree of freedom instability
3. Flutter instability
4. Buffeting
5. **Vortex shedding**

VIV: Deck Shape Optimization (scale 1:45)

TWO SECTIONAL MODELS

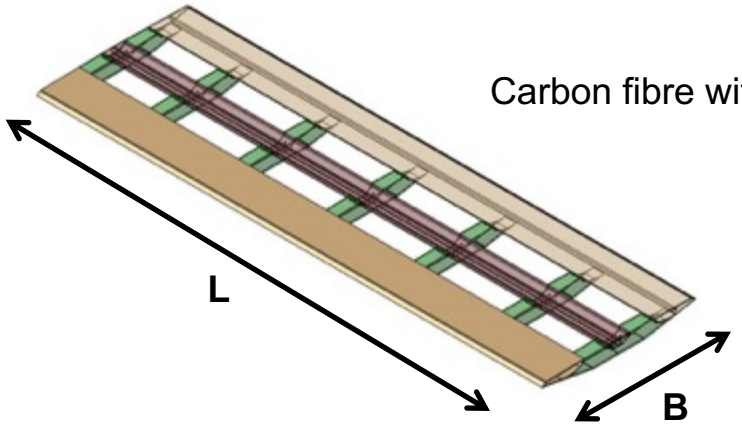

Carbon fibre with fittings glued on

lenght L [m]	*4*
width B [m]	*1.33*
Aspect ratio L/B	*3*

- The models differ for the shape of the railway girder

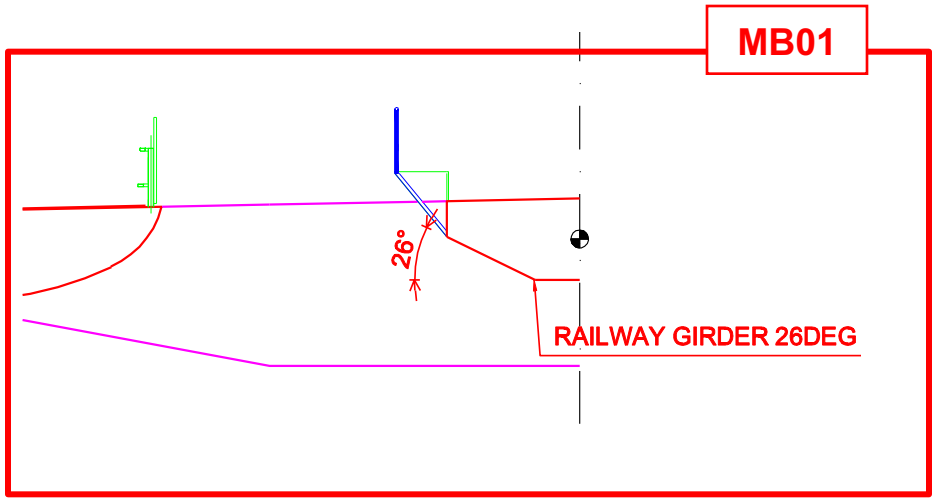

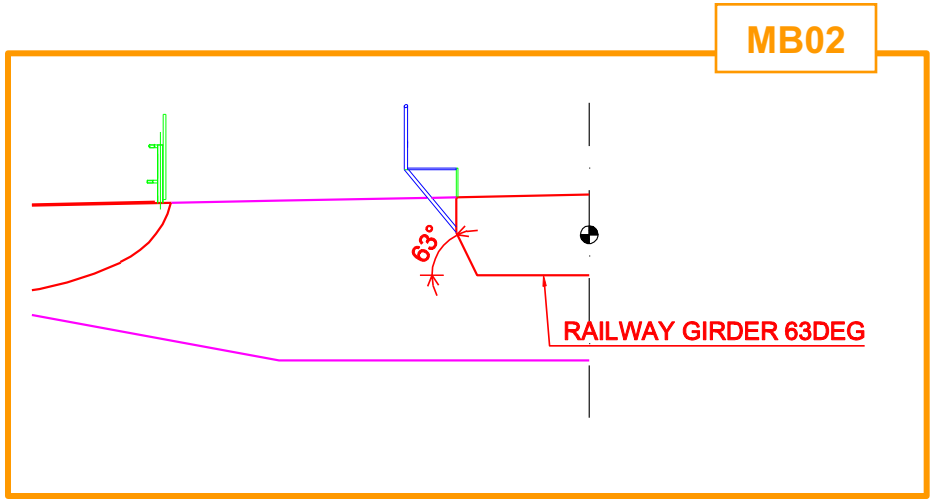

VIV: Deck Shape Optimization (scale 1:45)

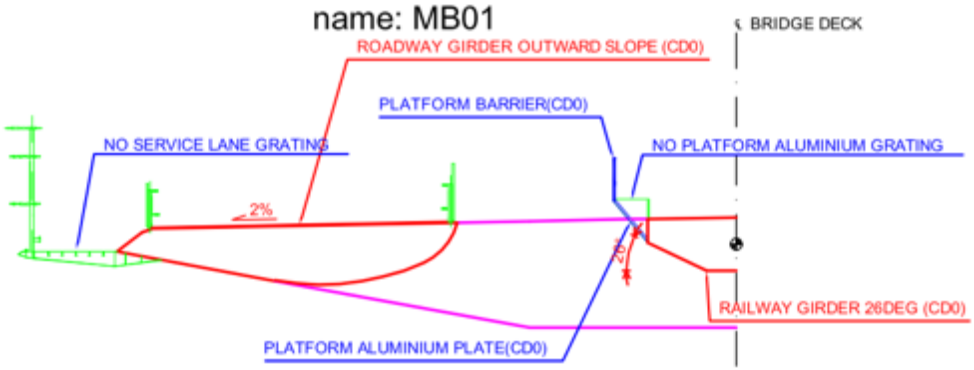

Figure 4.31 Configuration name:MB01

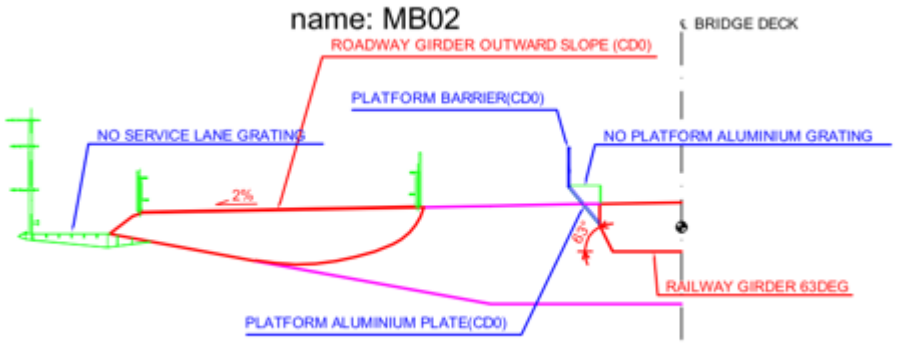

Figure 4.32 Configuration name:MB02

VIV: (almost) rigid model set-up (scale 1:45)

- External force balance set-up + Pressure Taps

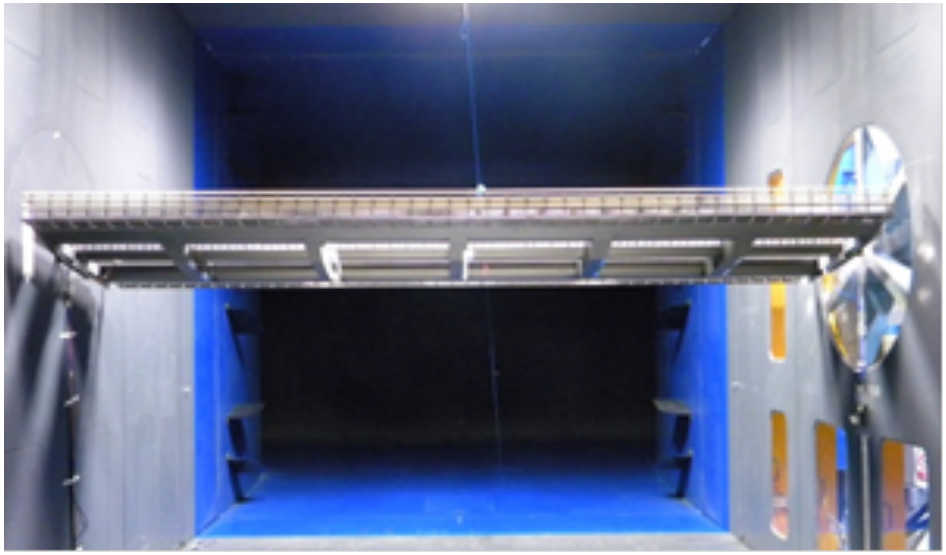

High velocity test section:

- Maximum velocity: 55 m/s
- Turbulence level: < 0.1 %

The model was placed in the middle of the test section and it spanned all the test section width

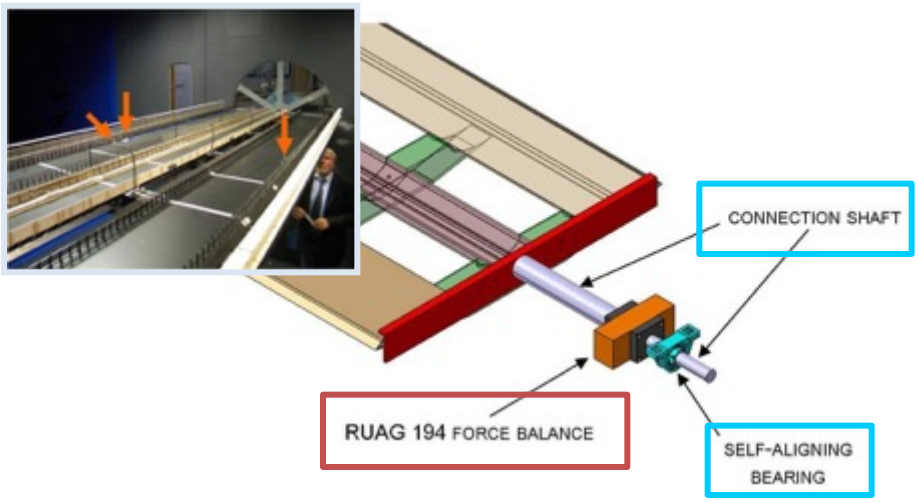

External force balances to measure drag, lift and moment loads

The constrain system permit to change the angle of attack by using a hydraulic actuator

Accelerometers to measure the dynamic behavior of the models

VIV: (almost) rigid model set-up (scale 1:45)

- Pressure taps distribution

Upwind roadway girder

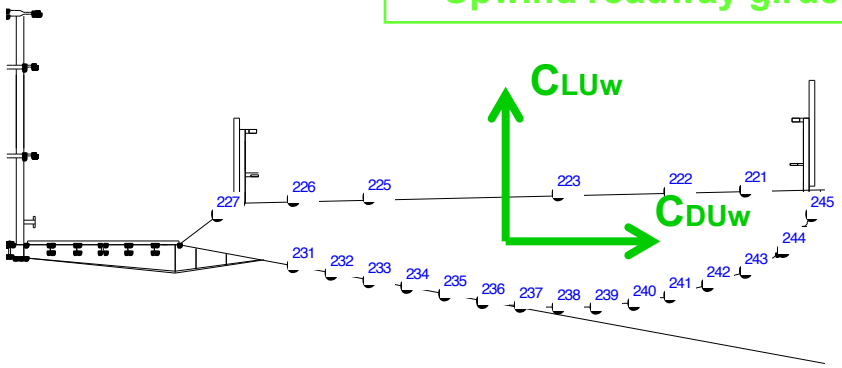

Downwind roadway girder

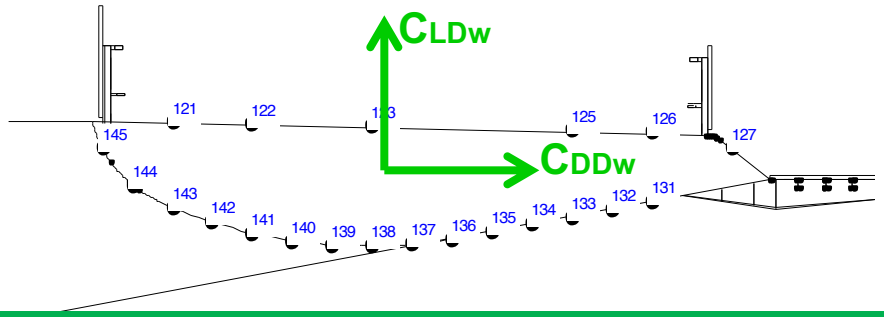

Pressure Taps on Deck

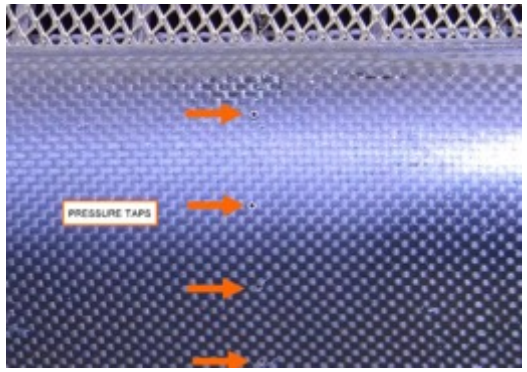

- Measuring points connected to high sample rate pressure scanners

→ Non dimensional pressure coefficients

$$C_p = \frac{P_i - P_s}{q}$$

→ Non dimensional force coefficients for each roadway girder (by the integration of the surface pressures)

$$C_{DUw}, C_{DUw}, C_{DDw}, C_{LDw}$$

VIV: (almost) rigid model set-up (scale 1:45)

Pressure Taps VIV Analysis

Model: MB01

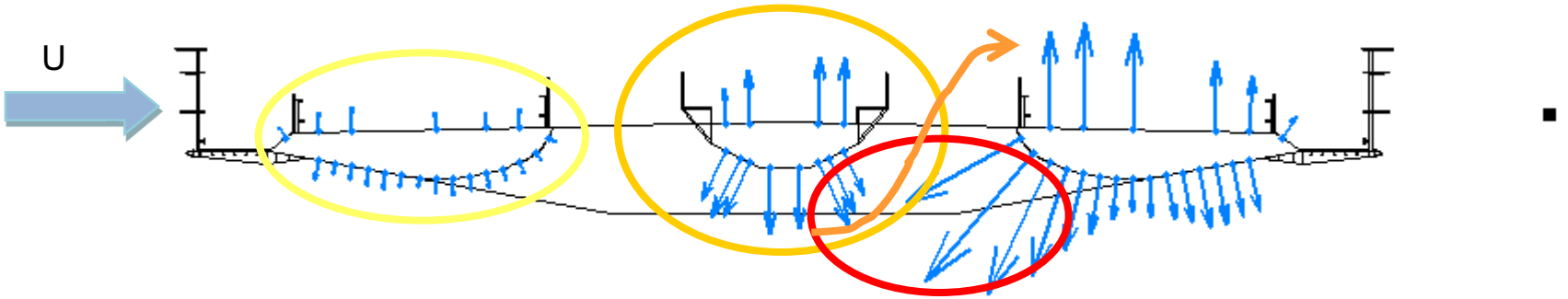

- **Peak spectra** of the pressure coefficients at V=4.64 m/s (excitation of the first flexural frequency of the model)

Small peaks on the Upwind roadway girder

Main role of the railway girder in the vortex street definition

Flow in the gap between railway girder and the Downwind roadway girder influences the vortex way

Strong pressure fluctuations can be observed in the gap

VIV: (almost) rigid model set-up (scale 1:45)

Flow Visualization VIV Analysis

Model: MB01

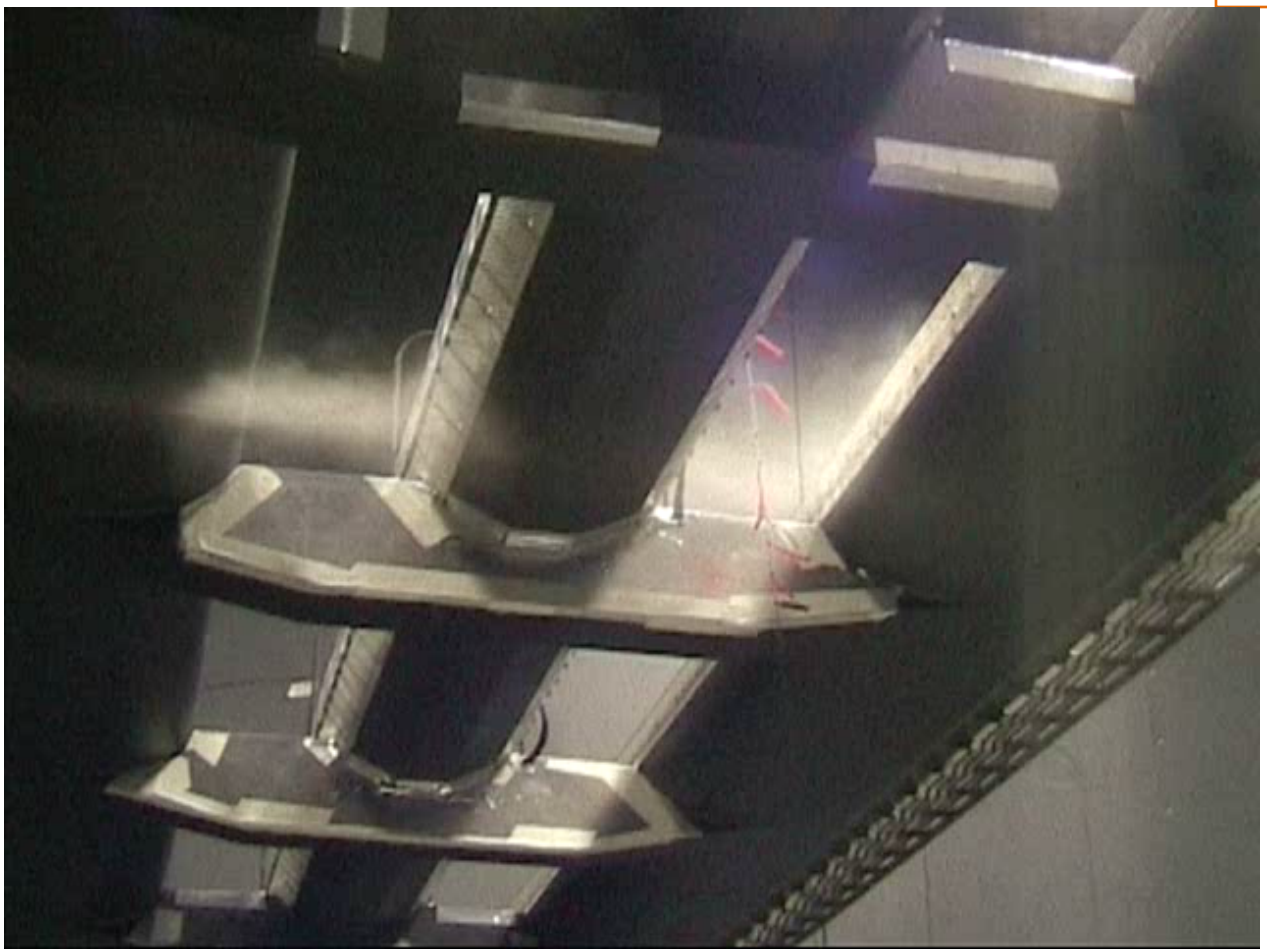

VORTEX SHEDDING ANALYSIS

VIV: (almost) rigid model set-up (scale 1:45)

Pressure Taps VIV Analysis

Pressure Tap 144

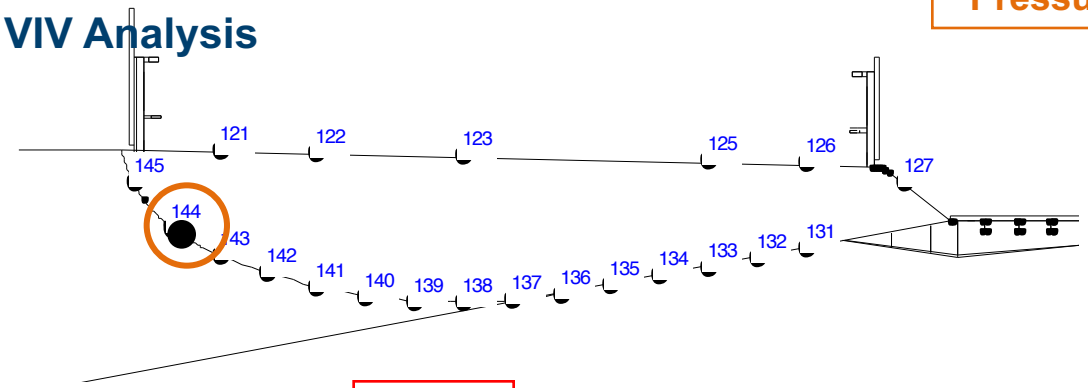

MB01

V=4.64 m/s

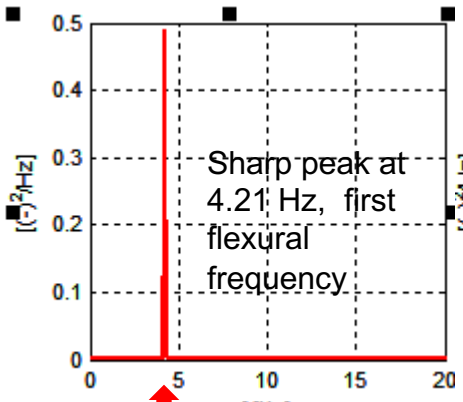

Sharp peak at 4.21 Hz, first flexural frequency

V=6.79 m/s

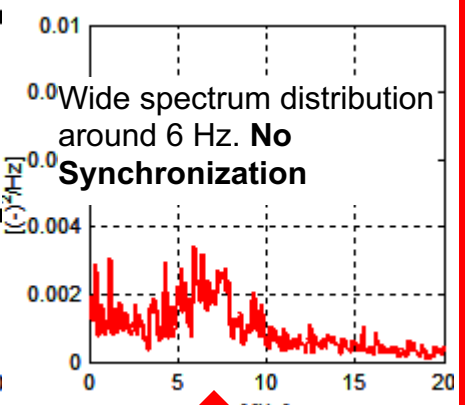

Wide spectrum distribution around 6 Hz. **No Synchronization**

MB02

V=4.64 m/s

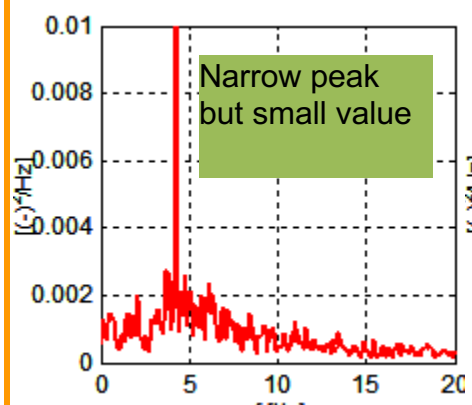

Narrow peak but small value

V=6.79 m/s

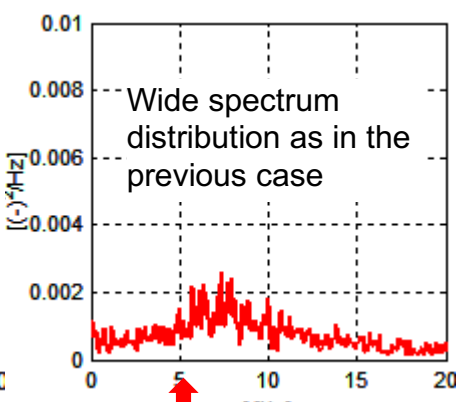

Wide spectrum distribution as in the previous case

Model MB02 seems to experience vortex shedding as model MB01, but with a lower level

The shape of the railway girder has been evaluated fundamental in influencing vortex shedding phenomenon

VIV: Low mass-damping set-up (scale 1:45)

- Elastically suspended rigid model: Low Frequency set-up

Accelerometers to measure the dynamic behavior of the models

Boundary layer test section:

- Maximum velocity: 15 m/s
- Turbulence level: < 2 %

The model was suspended on stays and springs in order to obtain:

- Low damping ratio i.e. low **Scruton Number**
- Natural vertical frequency of the model (**f_N=2.74 Hz**) tuned to have the lock-in region at about **4 m/s**, a wind velocity that permit to have a good excitation by the flow

VIV: Low mass-damping set-up (scale 1:45)

STEADY STATE RESPONSE: z/B

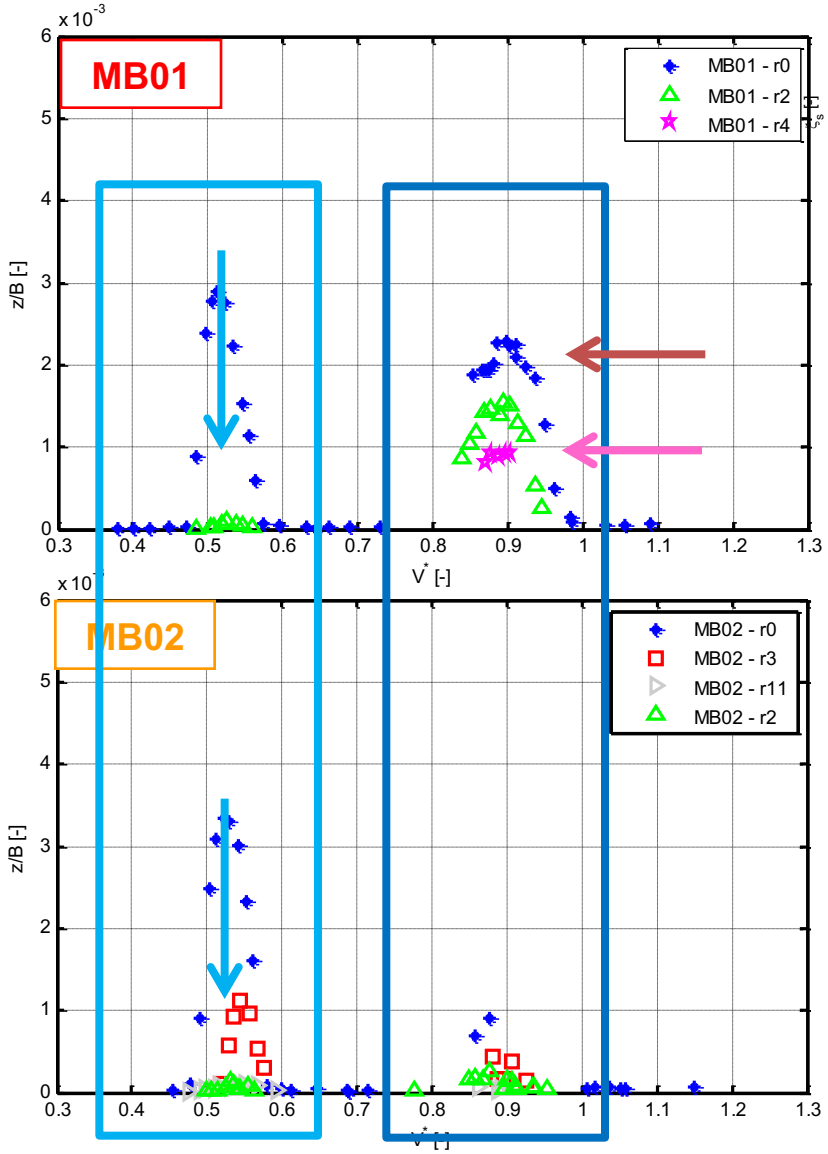

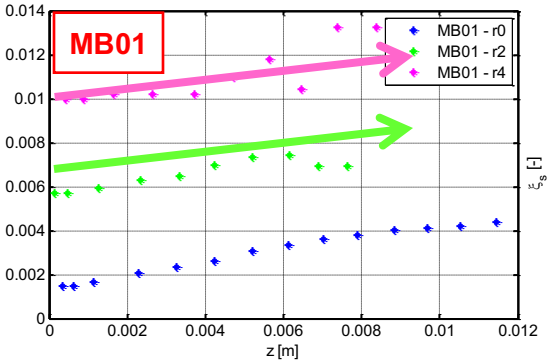

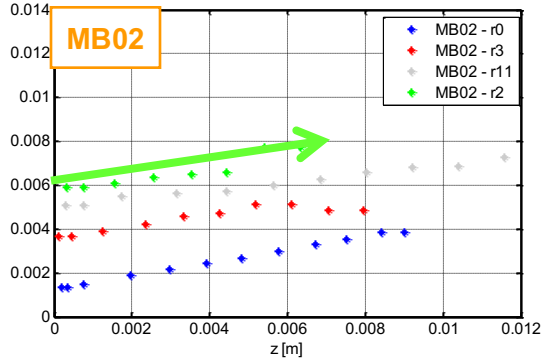

- Different levels of non dimensional damping

Two lock-in regions

- $V^* \approx 0.5$
  - Similar behavior of the two models
  - High sensitivity to damping increase
  - $z/B < 10^{-4}$ with ξ=0.5-0.6 %
- $V^* \approx 0.8$
  - Higher amplitude for model MB01
  - Low sensitivity to damping increase
  - **MB01**: high z/B with ξ=1%
  - **MB02**: low z/B with ξ=0.5%

VIV: Low mass-damping set-up (scale 1:45)

STEADY STATE RESPONSE: C_{LDww}, C_{LUww}

Upwind roadway girder

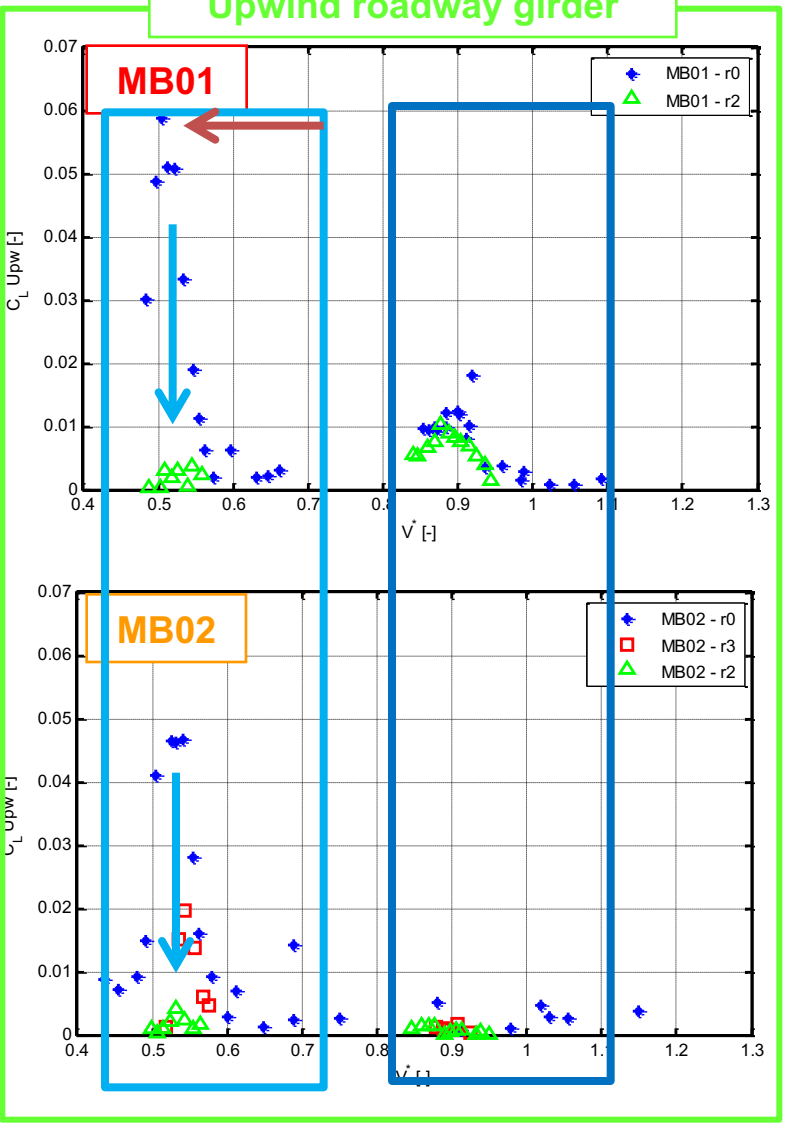

Downwind roadway girder

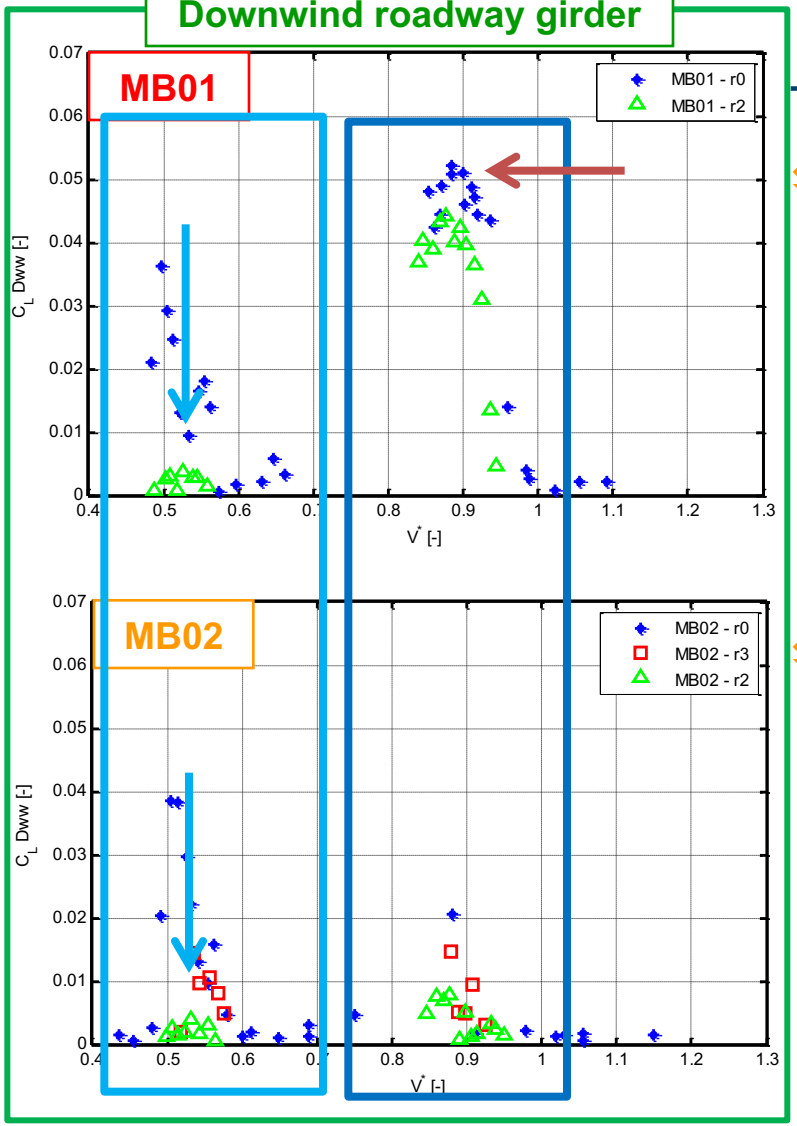

Two lock-in regions

- $V^* \approx 0.5$
  - Similar behavior of the two models
  - High sensitivity to damping increase
  - Higher values on the Upwind girder
- $V^* \approx 0.8$
  - Higher level of Lift coefficient for MB01
  - Higher values on the Downwind girder

VIV: Low mass-damping set-up (scale 1:45)

STEADY STATE RESPONSE: C_p peak spectra

MB01

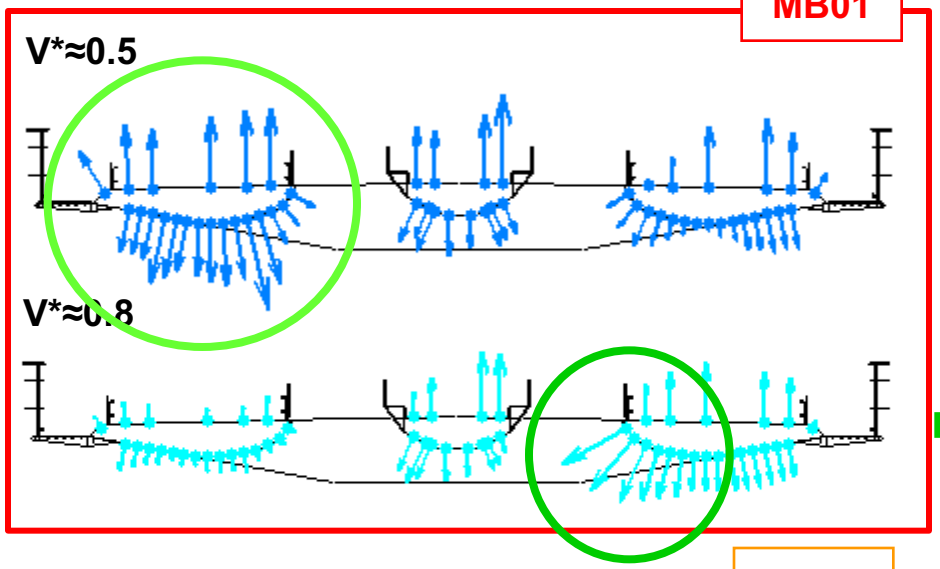

Similar behavior of the two models: higher pressures in the Upwind roadway girder than in the Downwind one

Similar to pressure distribution observed with external balance set-up

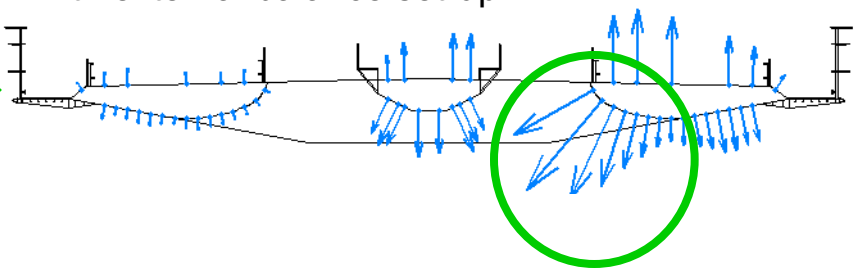

High pressures

MB02

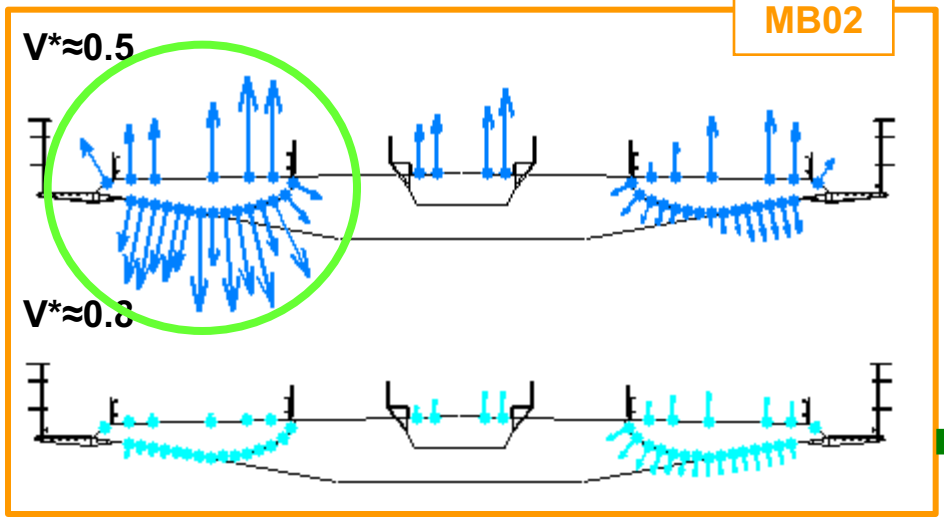

Very low values of surface pressure

Something more “In Deep”

Large displacements / Large Angle of Attack

→ Non Linearities !!!

Aerodynamic force hysteresis loops: non linear effects

Flutter derivatives are measured using small variation of the angle of attack around a mean value:

→ Linear information

→ "Frequency-Domain-Born" approach

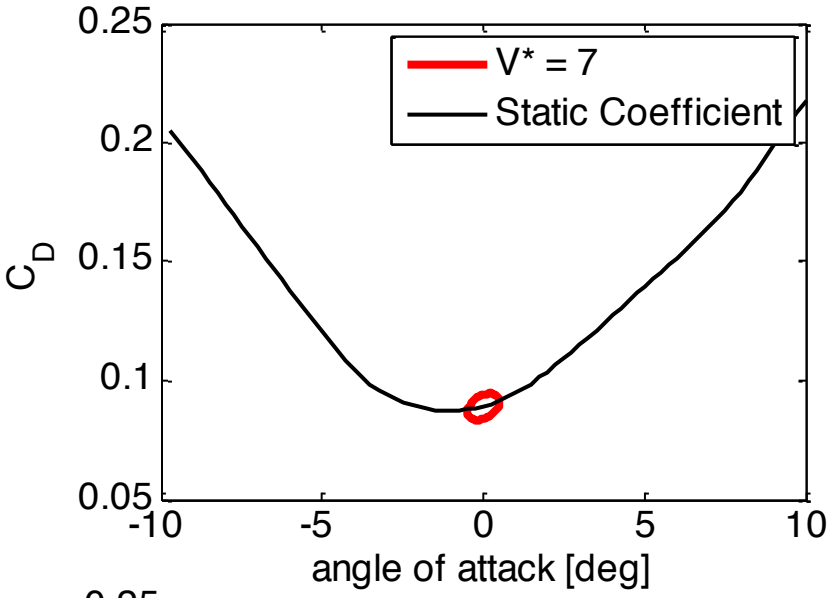

Hysteresis loops are measured using large variation of the angle of attack around a mean value:

→ Non Linear information

→ Typical "Time-Domain-Born" approach

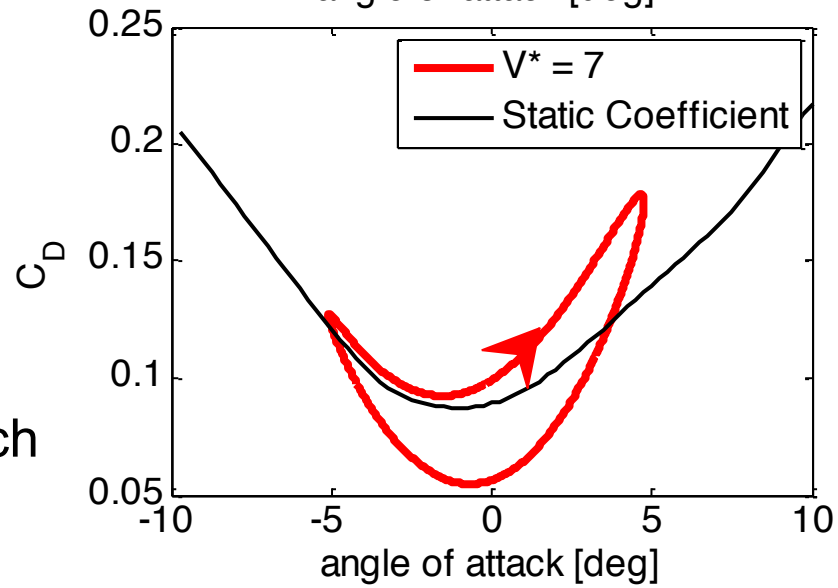

Force hysteresis loops: aeroelastic interpretation

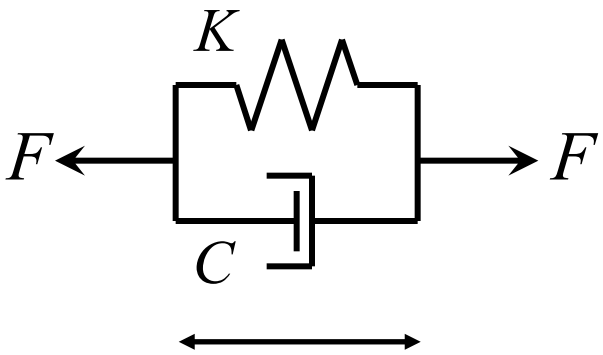

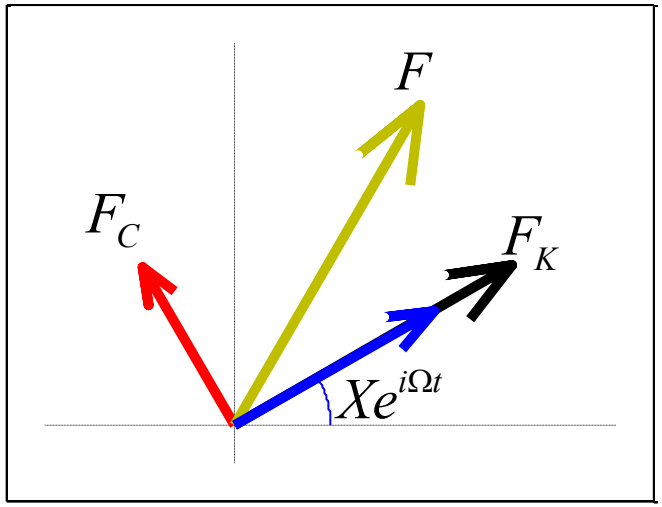

$$\Delta x = Xe^{i\Omega t}$$

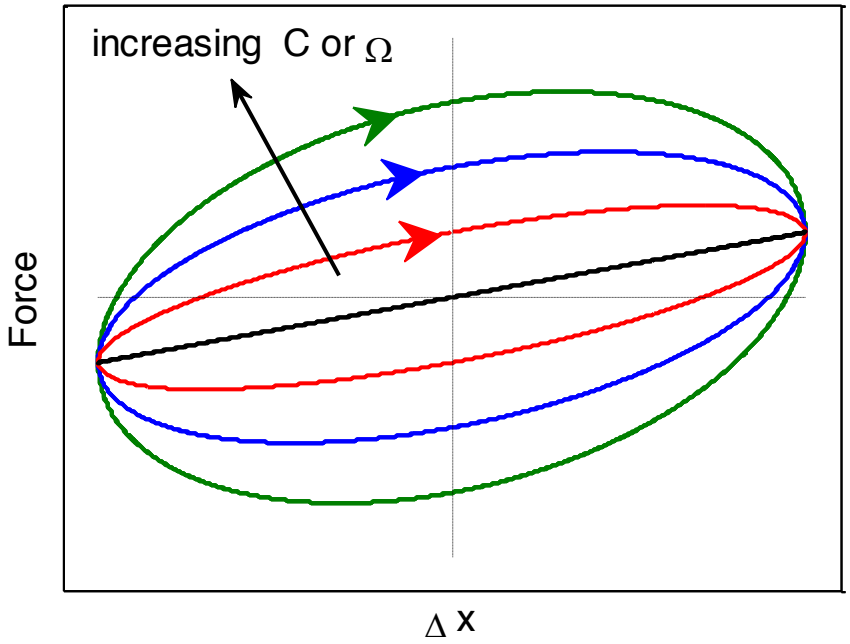

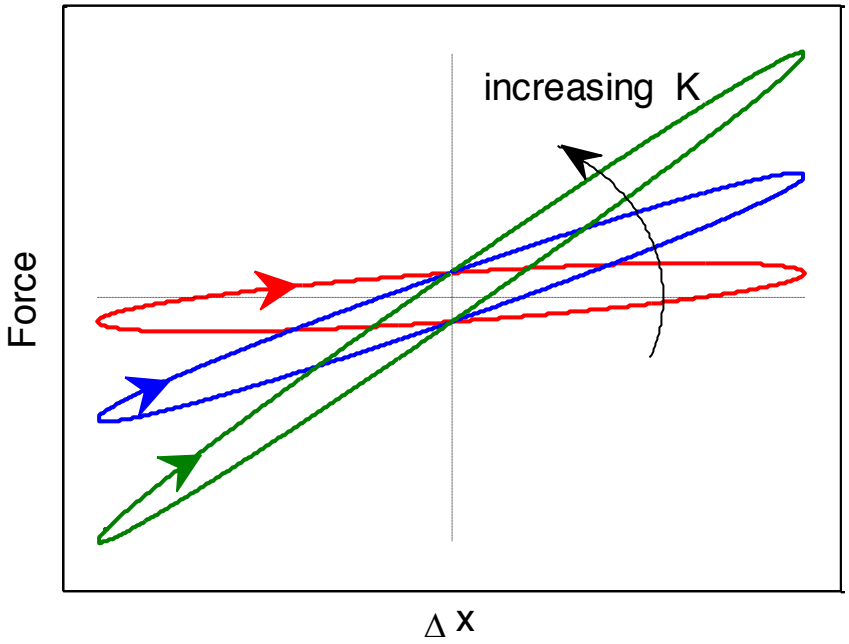

Force hysteresis loops: non linear effects

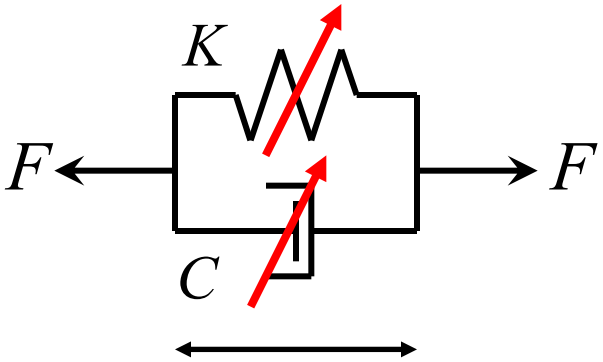

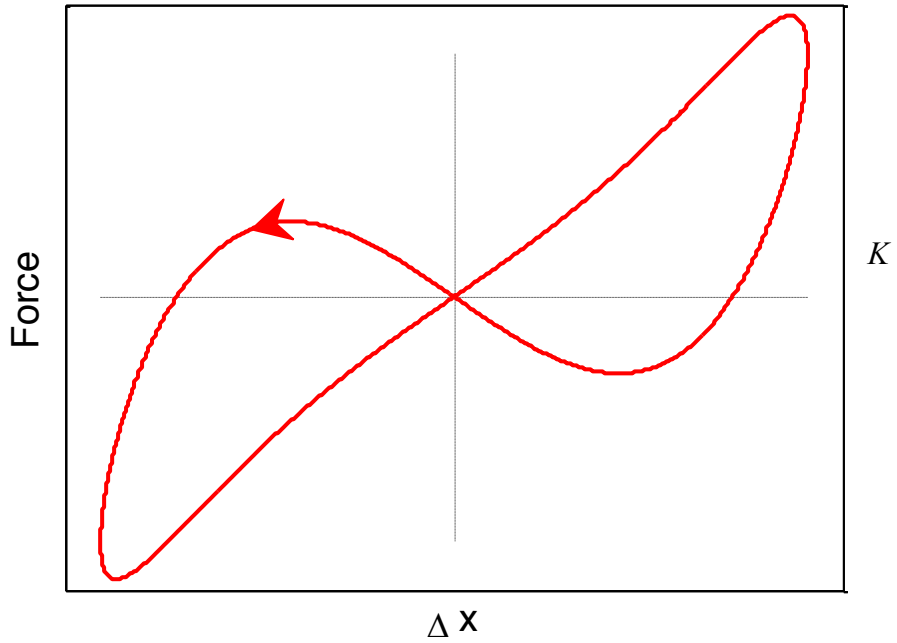

$$\Delta x = Xe^{i\Omega t}$$

The phase shift between force and displacement (clockwise or anti-clockwise path) represents whether energy is lost or gained

The area of the loop represents the work done by the force in each cycle.

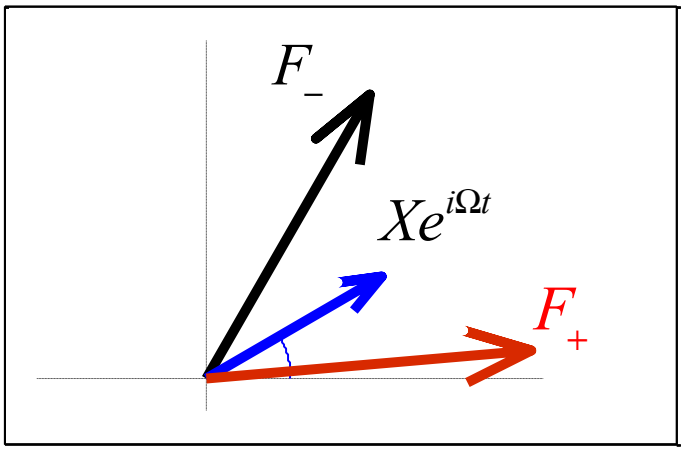

Dynamic angle of attack

Aerodynamic forces are a non linear function of the angle of attack and of the reduced velocity:

$$F_{Aero} = F_{Aero}\left(\psi, V^*\right)$$

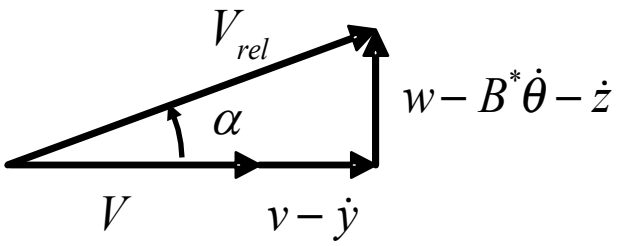

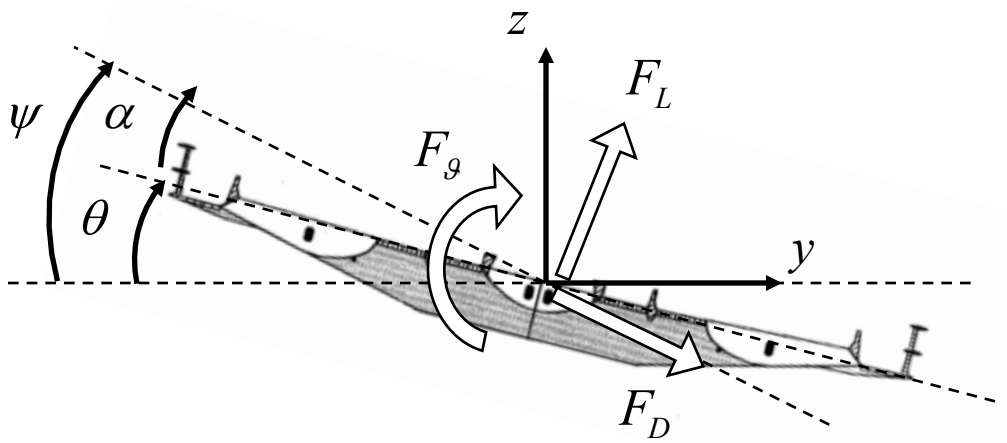

General configuration

$$\psi = \theta + \alpha = \theta + \tan^{-1}\left(\frac{-B^*\dot{\theta} - \dot{z} + w}{V + v - \dot{y}}\right)$$

Forced motion test $\quad \psi_\theta = \theta + \tan^{-1}\left(\frac{-B^*\dot{\theta}}{V}\right)$

Buffeting tests $\quad \psi_w = \theta + \tan^{-1}\left(\frac{w}{V}\right)$

Rheological model approach

Choice of B* - Moment
(V* = 9, θ_m = 0 deg, $\Delta\theta$ = 5 deg)

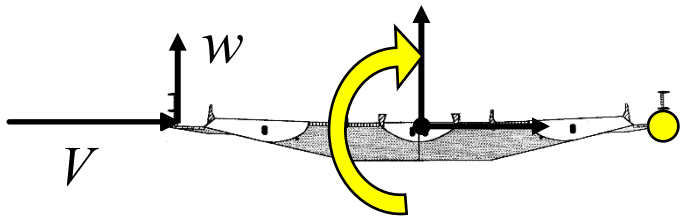

$$B^* = -B/2$$

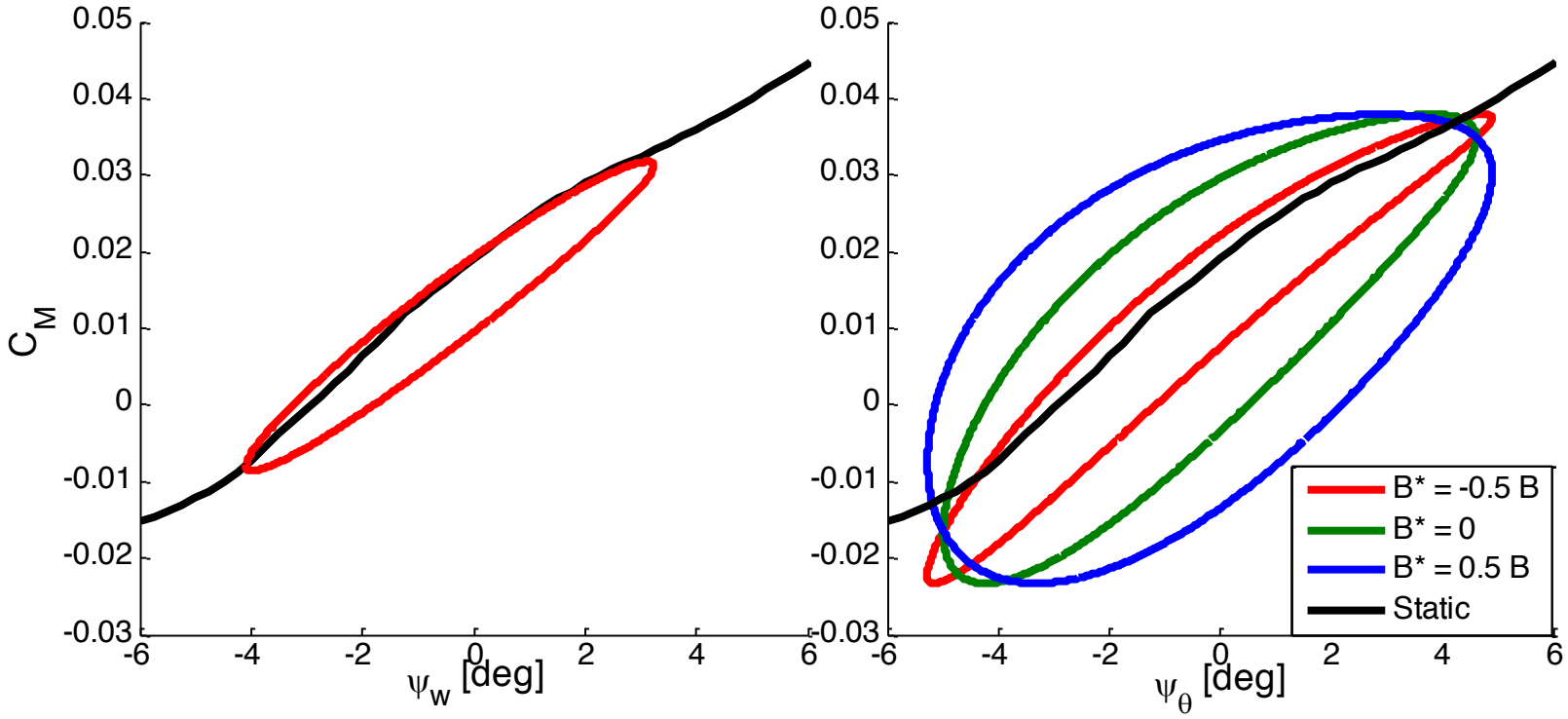

Rheological model approach

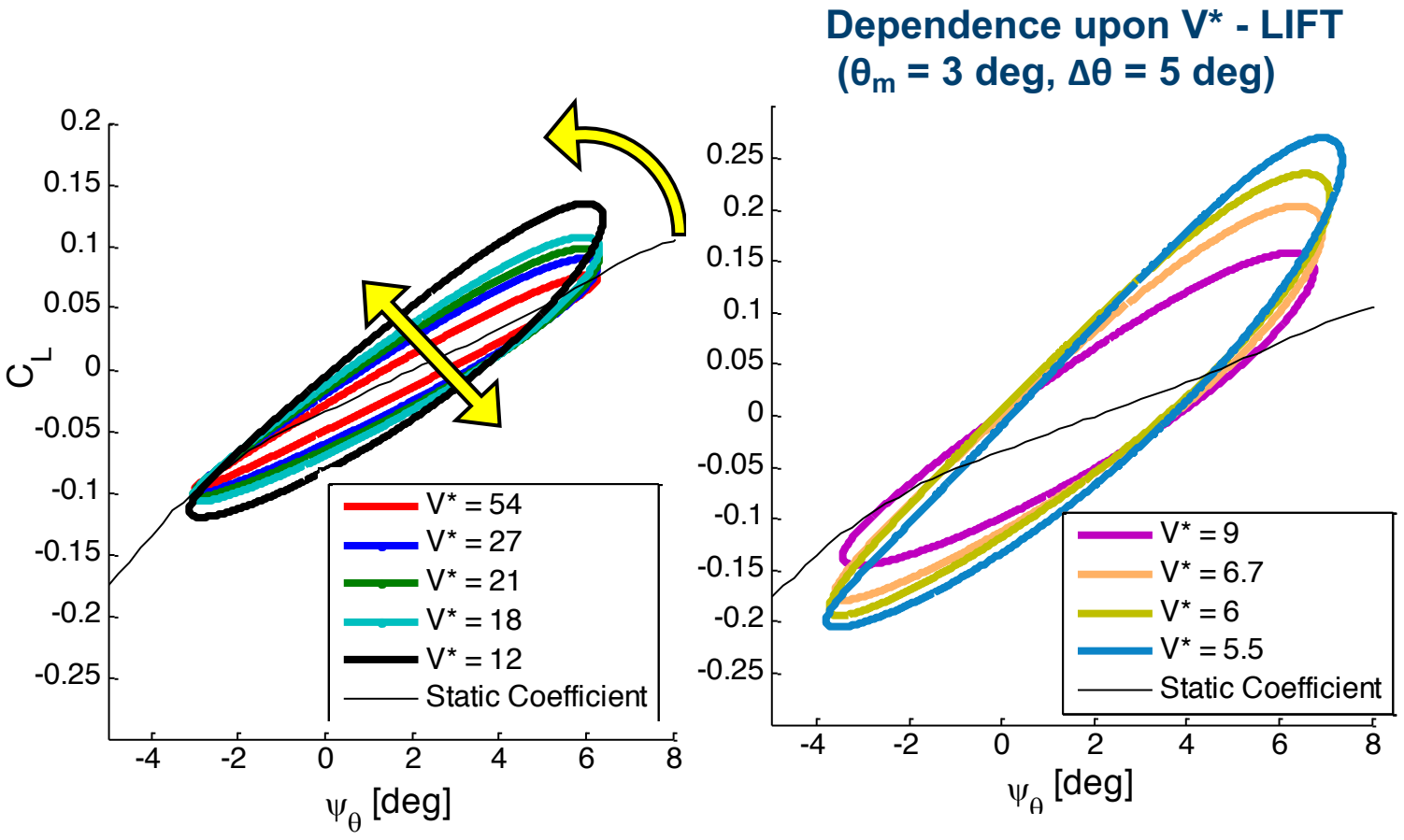

ψ_θ Tests are considered in the model identification since we can analyze more V*

Rheological model approach

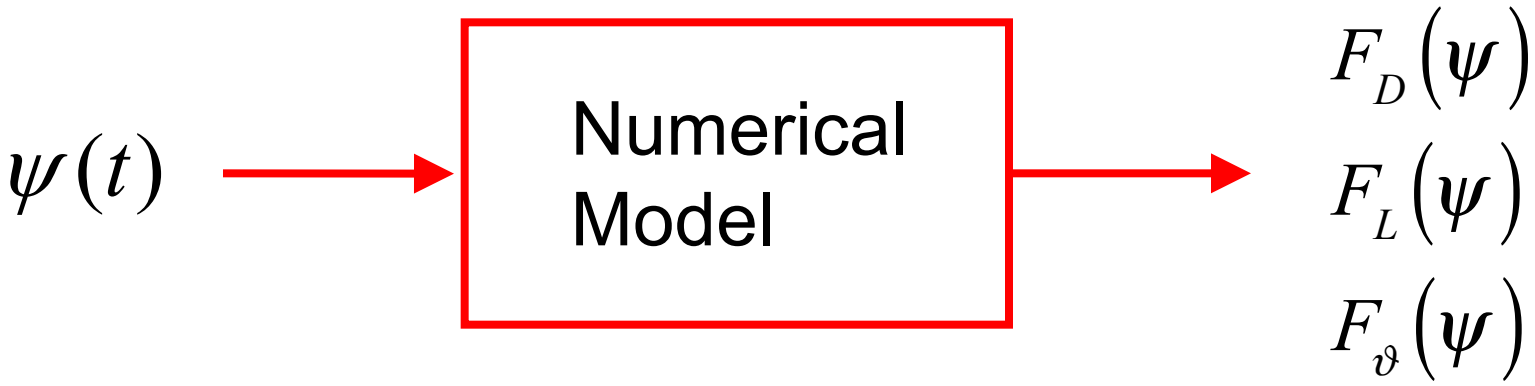

$$F_x = F_x^{ST}(\psi) + \ldots$$

$$\beta_1 \quad + \ldots$$

$$\beta_2 \quad \psi + \beta_3\dot{\psi} + \ldots$$

$$\beta_4 \quad \psi^2 + \beta_5\psi\dot{\psi} + \ldots$$

$$\beta_6 \quad \psi^3 + \beta_7\psi^2\dot{\psi}$$

Rheological model approach

$\psi(t)$ → Numerical Model → $F_D(\psi)$, $F_L(\psi)$, $F_\vartheta(\psi)$

$$F_x = F_x^{ST}(\psi) + \ldots \quad \rightarrow \text{Static Force}$$

$$\beta_1 \quad + \ldots$$

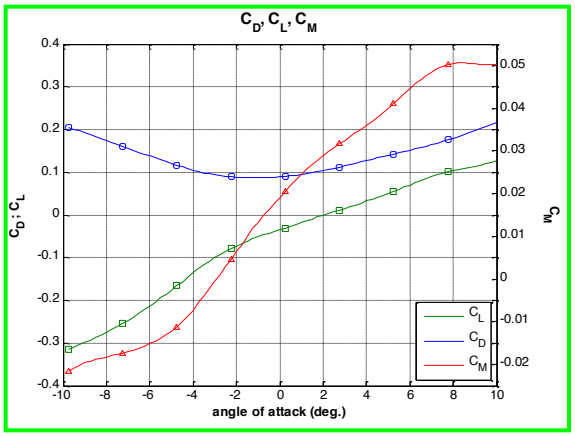

$$\beta_2 \quad \psi + \beta_3\dot{\psi} + \ldots$$

$$\beta_4 \quad \psi^2 + \beta_5\psi\dot{\psi} + \ldots$$

$$\beta_6 \quad \psi^3 + \beta_7\psi^2\dot{\psi}$$

Rheological model approach

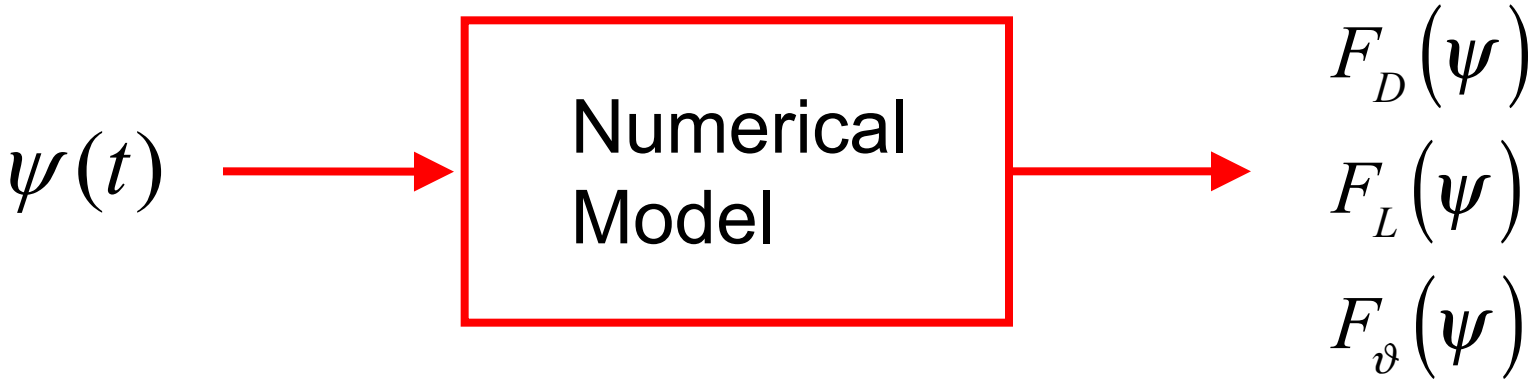

$$F_x = F_x^{ST}(\psi) + \ldots$$

$$\beta_1 + \ldots$$

$$\beta_2 \quad \psi + \beta_3\dot{\psi} + \ldots$$

$$\beta_4 \quad \psi^2 + \beta_5\psi\dot{\psi} + \ldots$$

$$\beta_6 \quad \psi^3 + \beta_7\psi^2\dot{\psi}$$

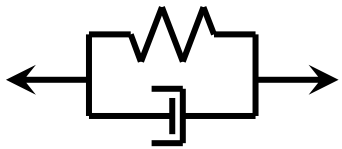

linear

Rheological model approach

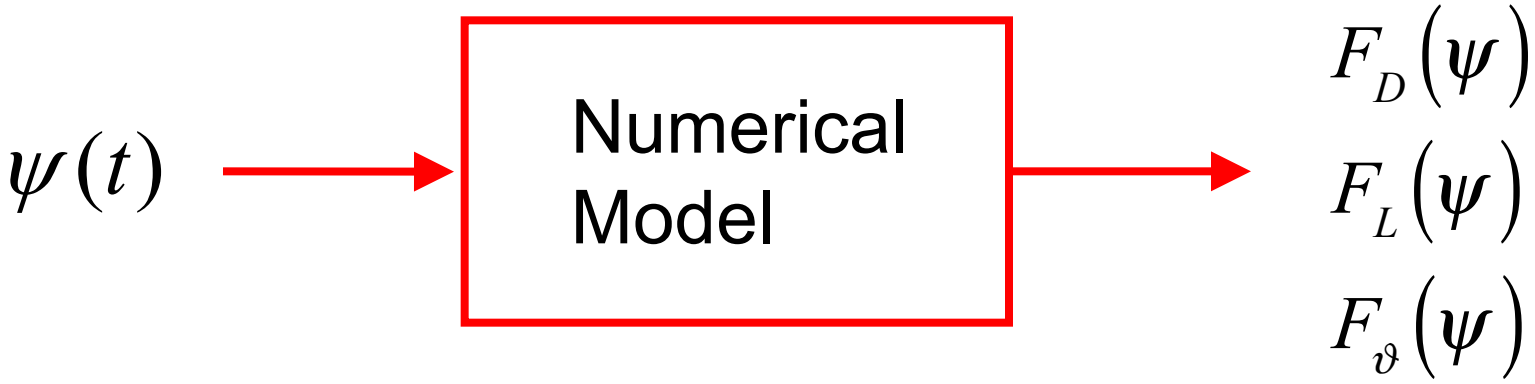

$$F_x = F_x^{ST}(\psi) + \dots$$

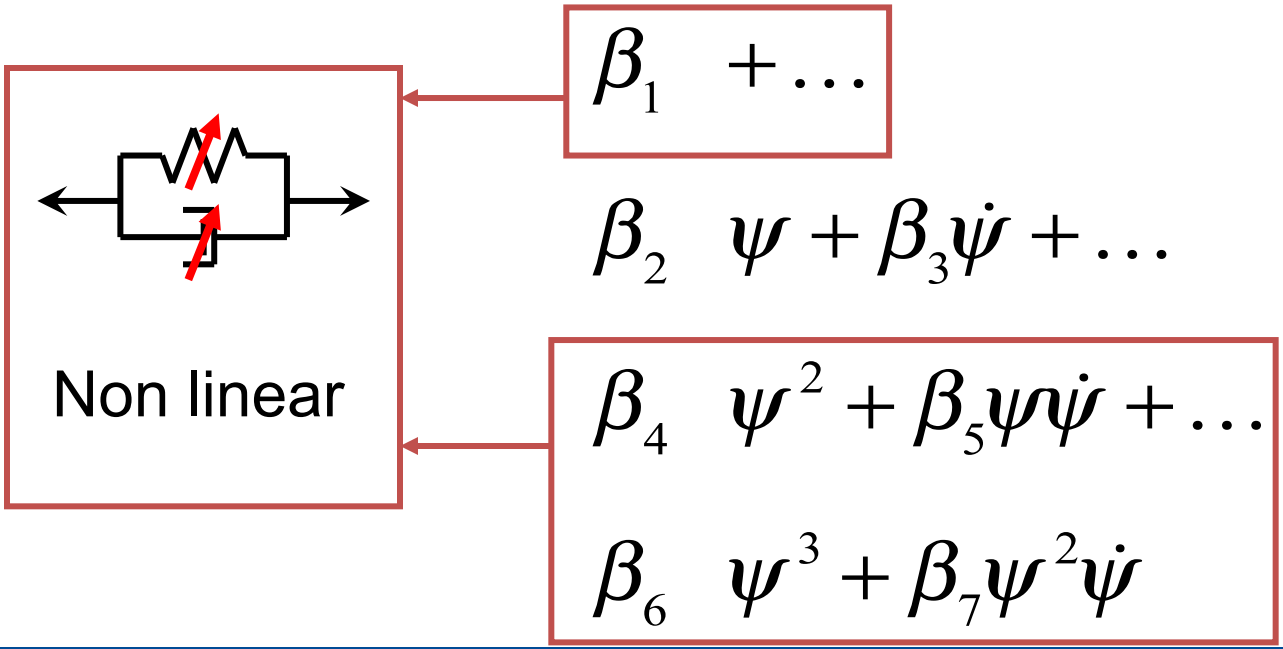

Rheological model approach

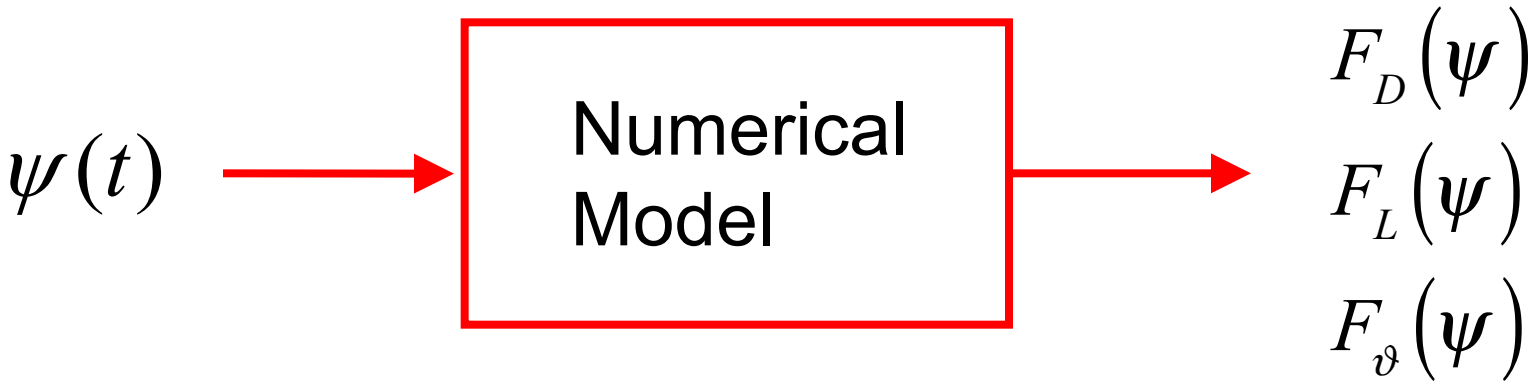

$$F_x = F_x^{ST}(\psi) + \ldots$$

$$\beta_1 + \ldots$$

$$\beta_2 \quad \psi + \beta_3\dot{\psi} + \ldots \quad \Rightarrow \text{Identification of } \beta_i$$

$$\beta_4 \quad \psi^2 + \beta_5\psi\dot{\psi} + \ldots$$

$$\beta_6 \quad \psi^3 + \beta_7\psi^2\dot{\psi}$$

Rheological model approach: Num-Exp-Comp.

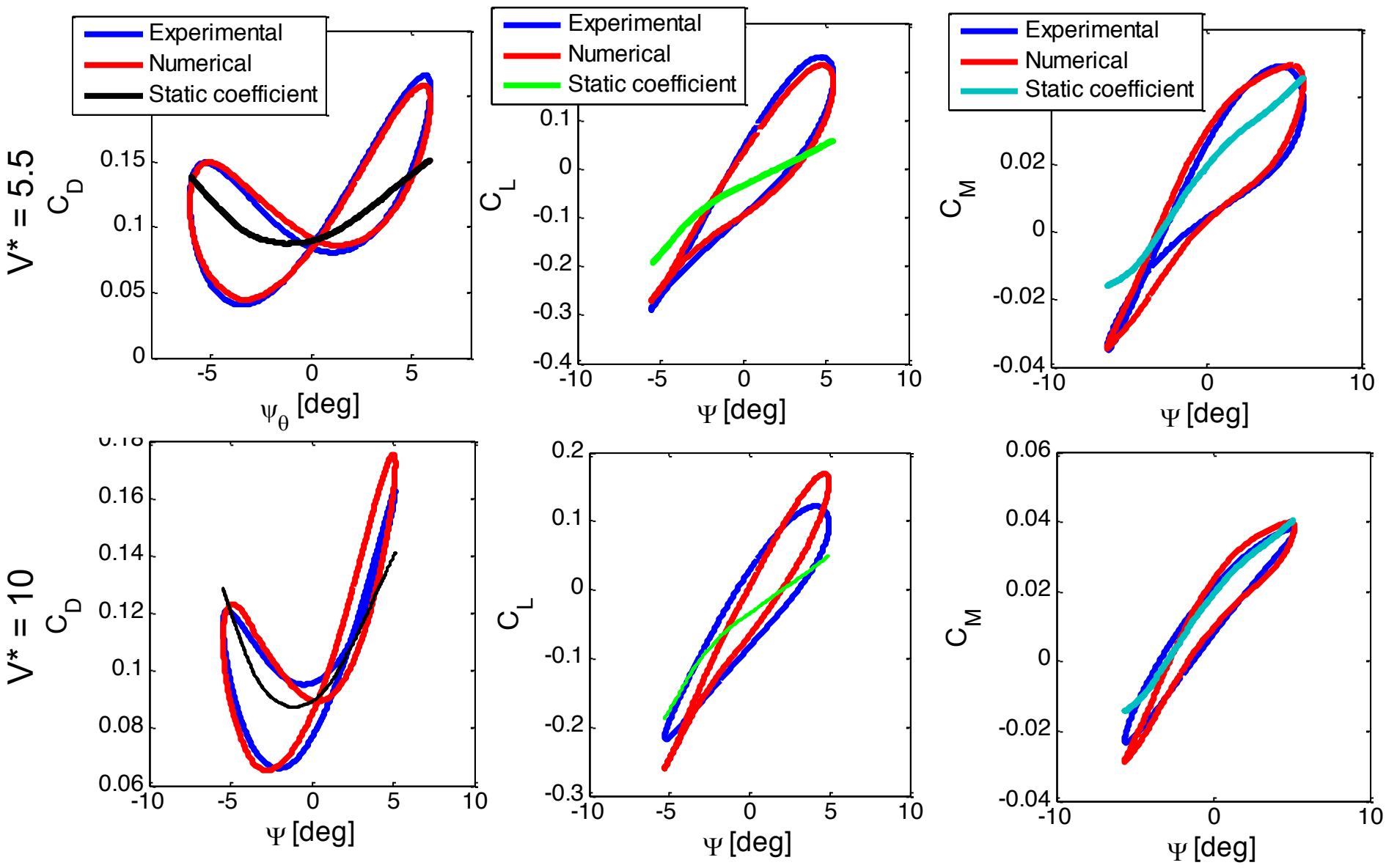

Something more “In Deep”

Explaining the Global Force Effects …

→ Looking down to Local Pressures !!!

Understanding the physics of Flutter Derivatives

- To define steady and unsteady aerodynamic forces, we usually adopt global coefficients:
  - Static $$M = \frac{1}{2}\rho V^2 B^2 C_M$$
  - Self-excited $$M_{se} = \frac{1}{2}\rho V^2 B^2 \left(-a_2^* \frac{i\omega\vartheta B}{V} + a_3^* \vartheta \right)$$
  - Buffeting $$M_b = \frac{1}{2}\rho V^2 B^2 \left(\chi_{Mw}^* \frac{w}{V} \right)$$

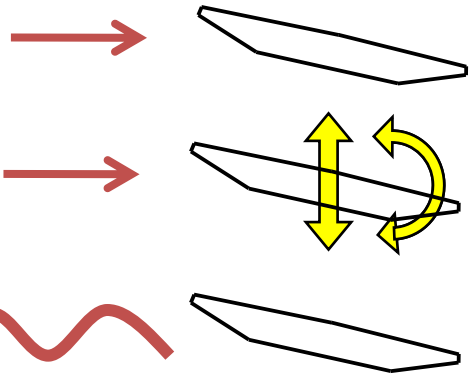

- Global coefficients are a synthetic representation of the integral action of fluid structure interaction

- While global coefficients are an effective tool for numerical/analytical analyses, a distributed representation allows for a more detailed analysis on the physics of the phenomenon

Understanding the physics of Flutter Derivatives

- Static forces can be represented either as static coefficients or as pressure distribution around the deck

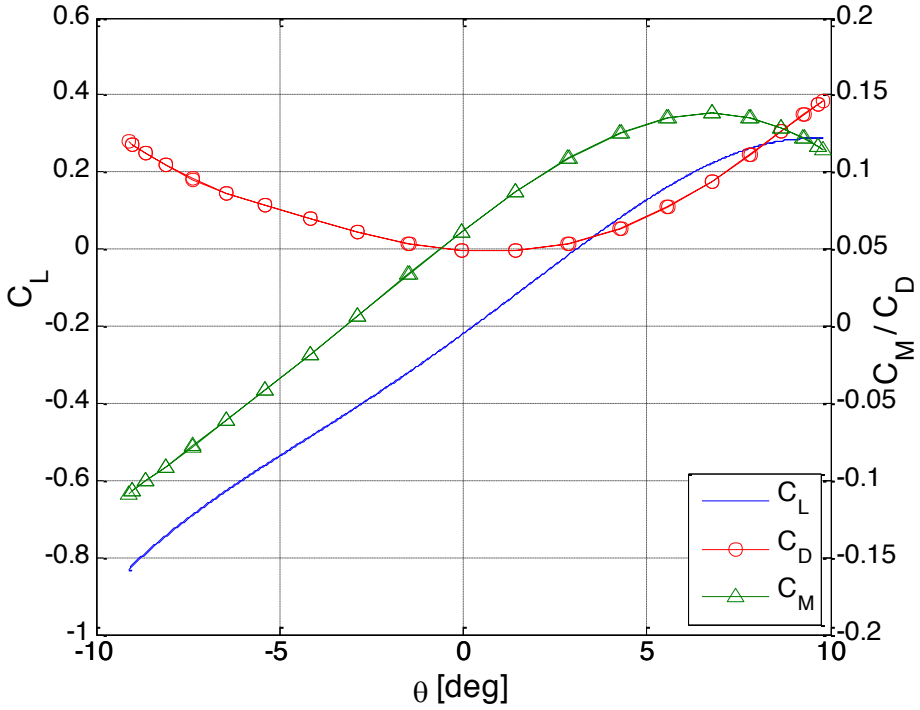

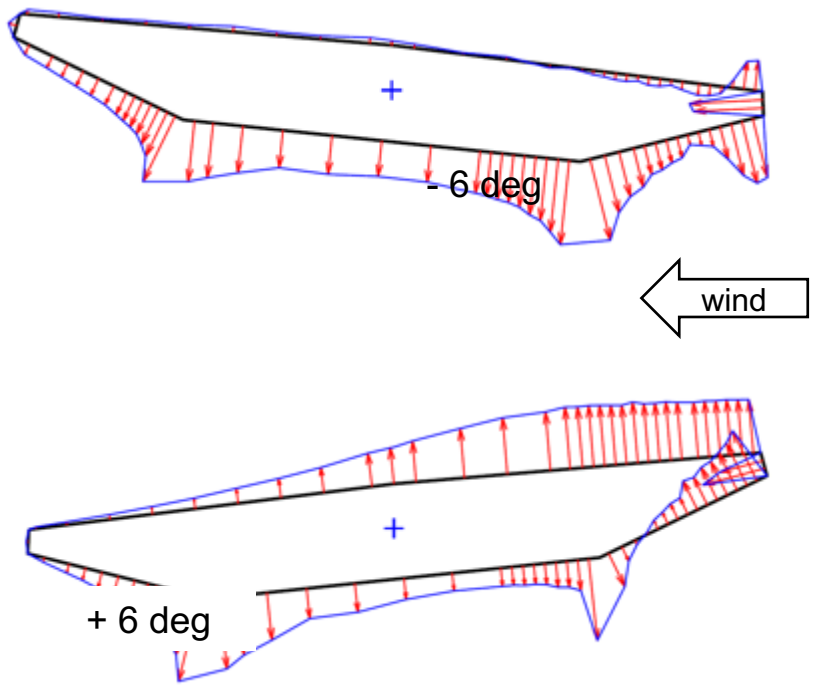

- Flutter derivatives are the global coefficients for unsteady self-excited forces: what is their distributed counterpart and what kind of information can we get from it?

Torsional instability at + 6 deg

$$M_{se} = \frac{1}{2}\rho V^2 B^2 \left(-a_2^* \frac{i\omega B}{V} + a_3^* \right) \theta$$

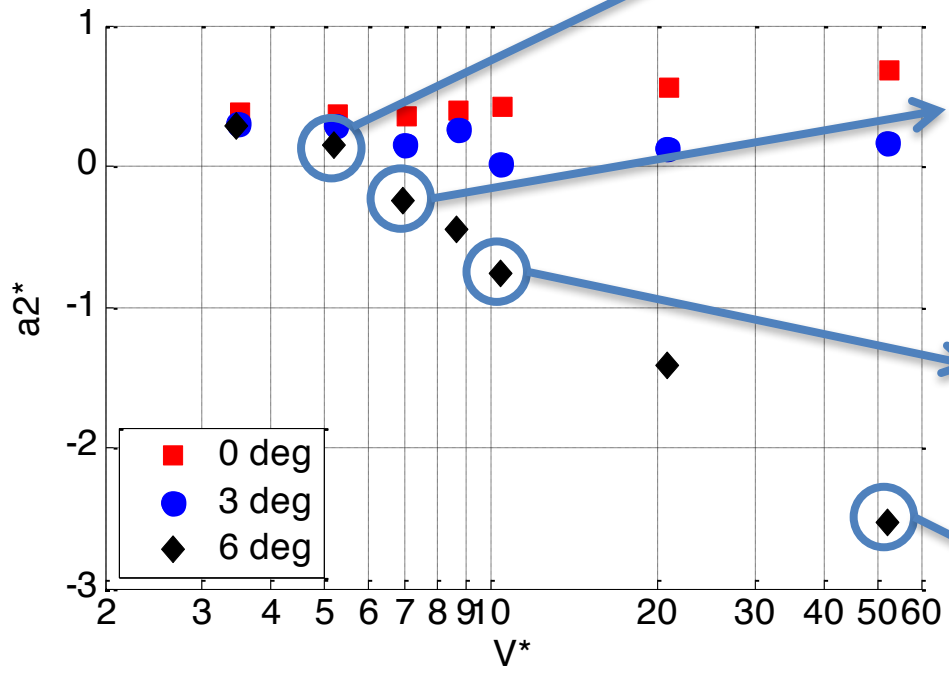

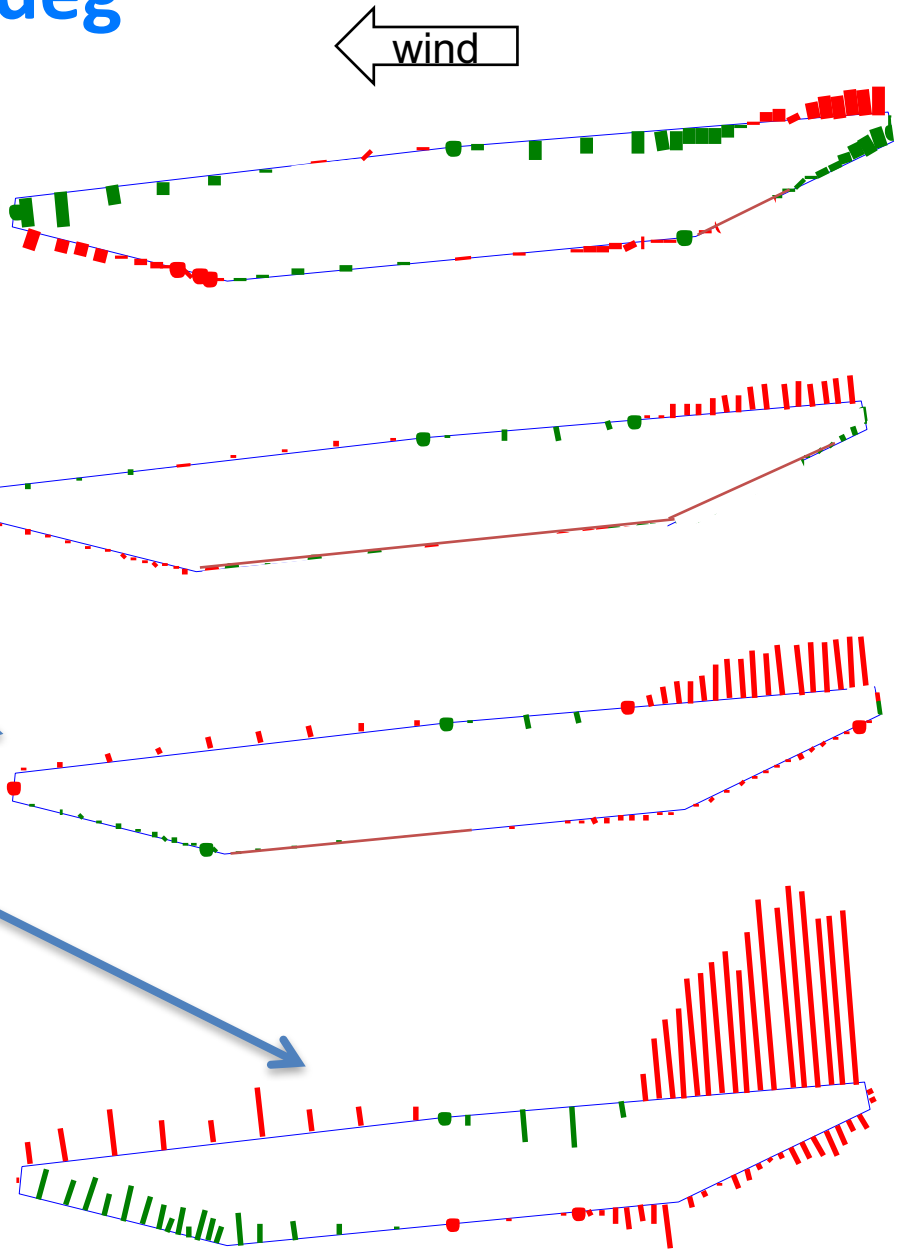

FD from pressure distribution

Verified with dynamometric measurements

«Distributed» Flutter Derivatives

- The idea is to exploit the knowledge of the unsteady pressure field around the contour of the deck to determine the contribution of each part of the deck to global value of the coefficient

Global:

$$M_{se} = \frac{1}{2}\rho V^2 B^2 \left(-a_2^* \frac{i\omega B}{V} + a_3^* \right) \theta$$

Distributed:

$$M_{se} = \sum_{j=1}^{ntaps} M_{se,j} = \frac{1}{2}\rho V^2 B^2 \sum_{j=1}^{ntaps} \left(-a_{2,j}^* \frac{i\omega B}{V} + a_{3,j}^* \right) \theta$$

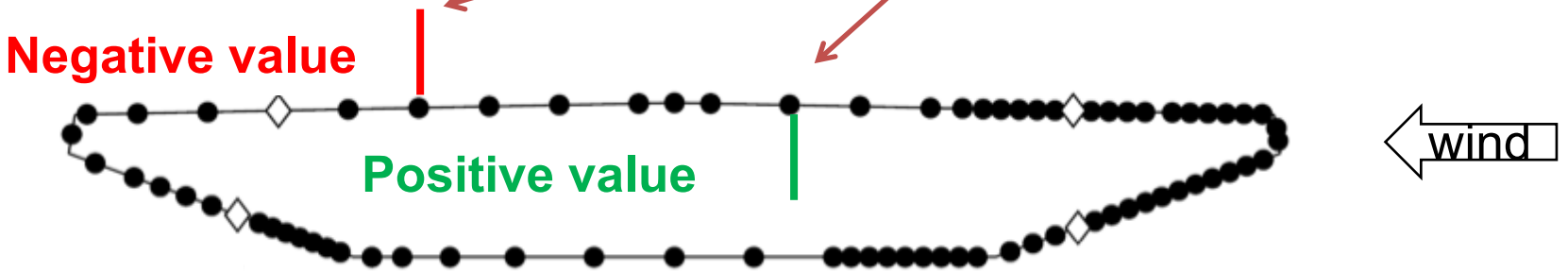

Analysis of V* = 10

$$M_{se} = \frac{1}{2}\rho V^2 B^2 \left(-a_2^* \frac{i\omega B}{V} + a_3^* \right) \theta$$

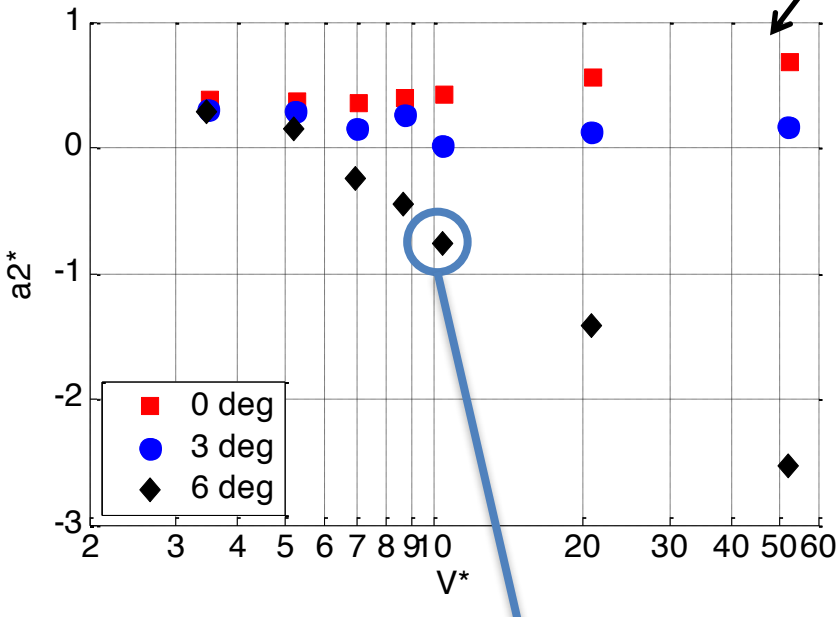

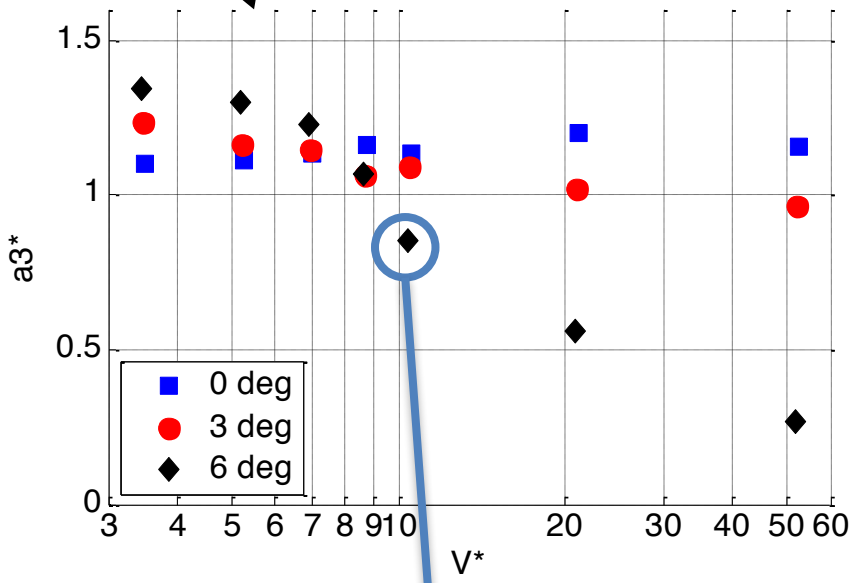

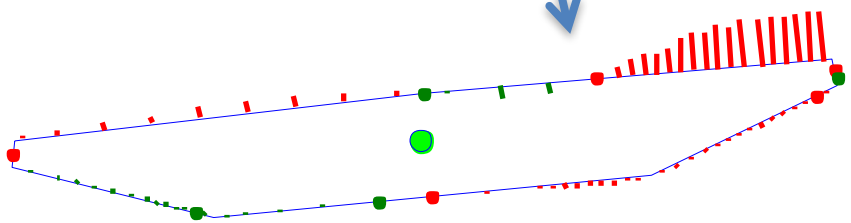

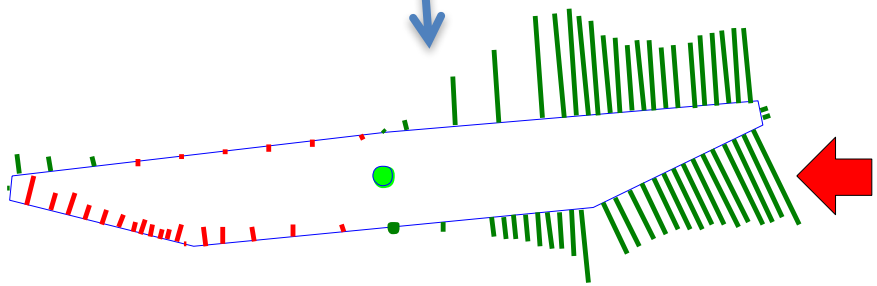

V* = 10, +6 deg: Unsteady pressure during one cycle of motion

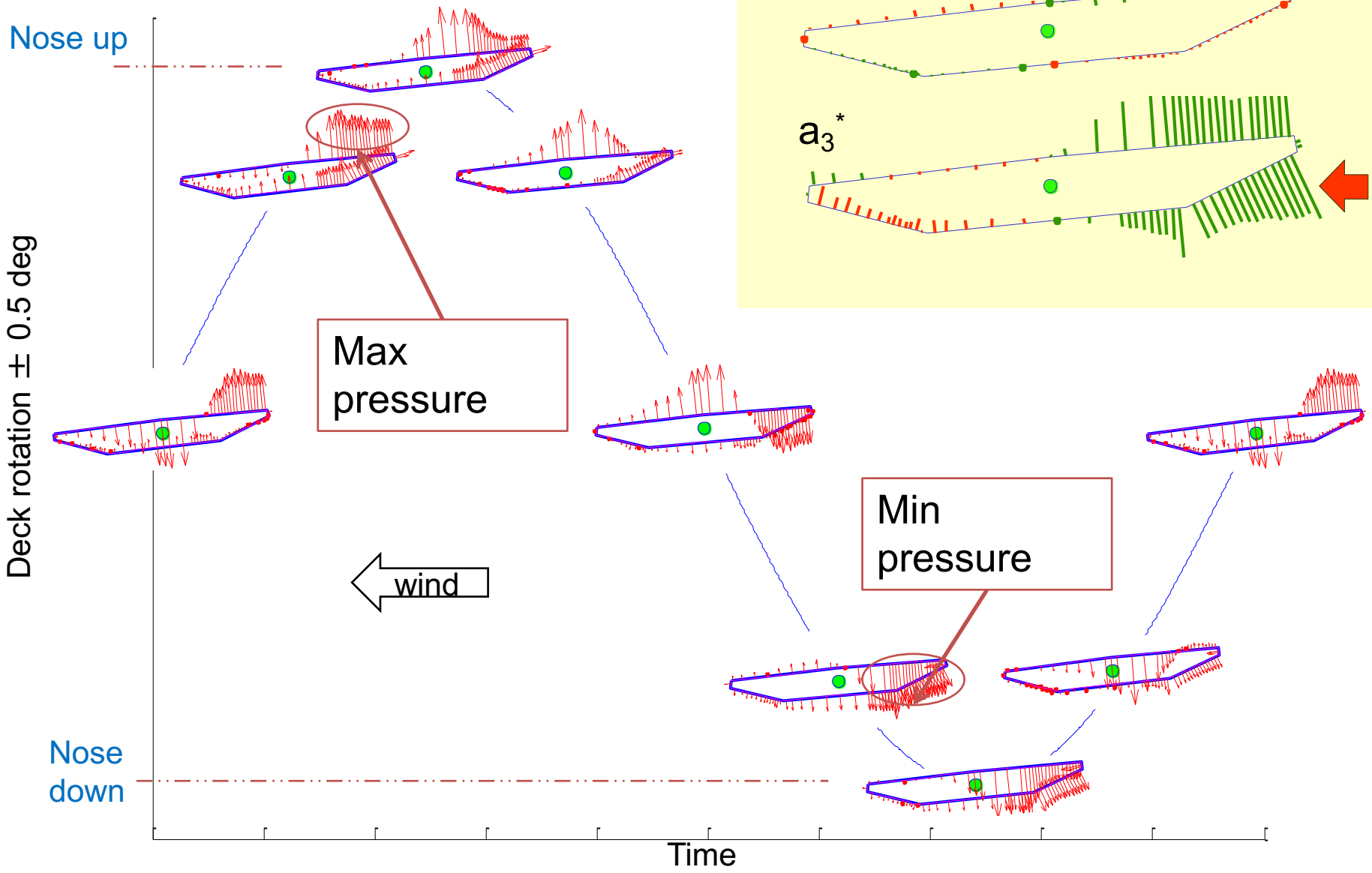

Something very “New”

→ **Just Open Bosphorous Bridge 3rd**

BB3: Third Bosphorous Bridge

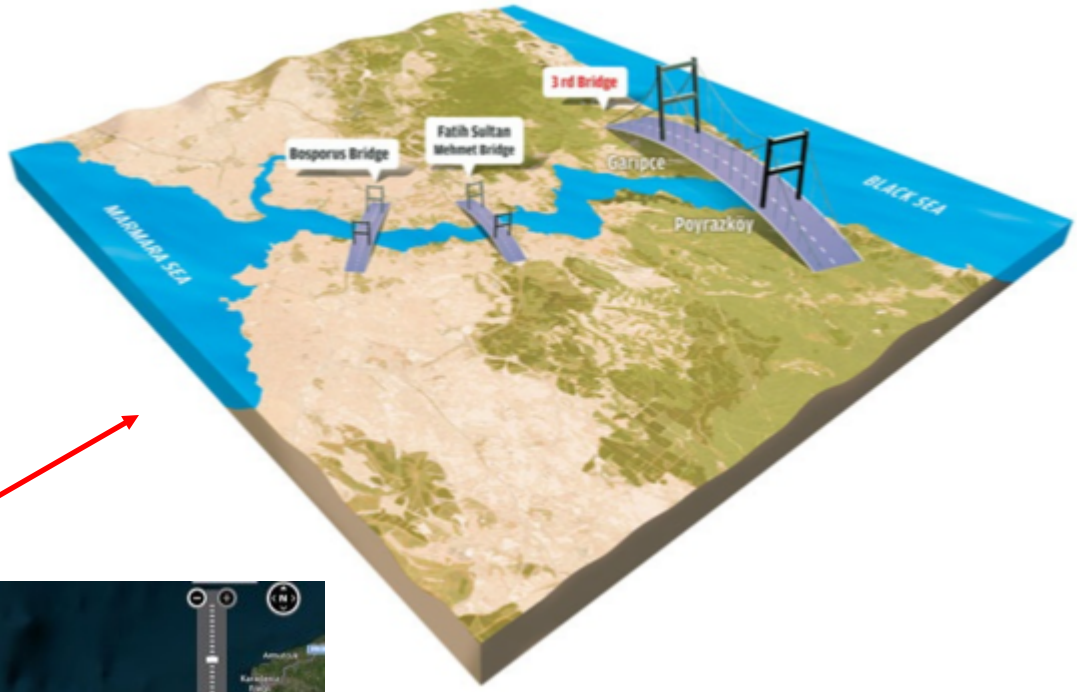

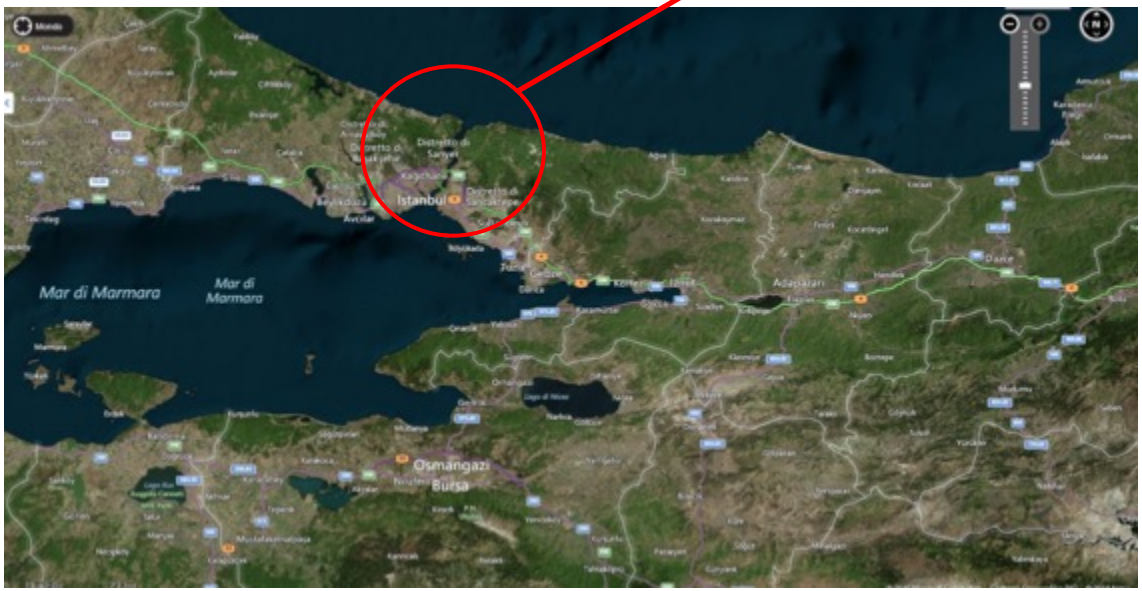

BB3 - Aerodynamic Challenges

- Highest span length on innovative structural solution
- Widest 60m deck → large aerodynamic derivatives expected
- Low-frequency bending and torsional modes in deck and towers
- Frequent strong lateral winds at the bridge site (higher than BB1)

- **Great opportunity from aerodynamic optimization:**

  → Improved structural wind interaction performances

  → Improved safety on vehicles & train runability

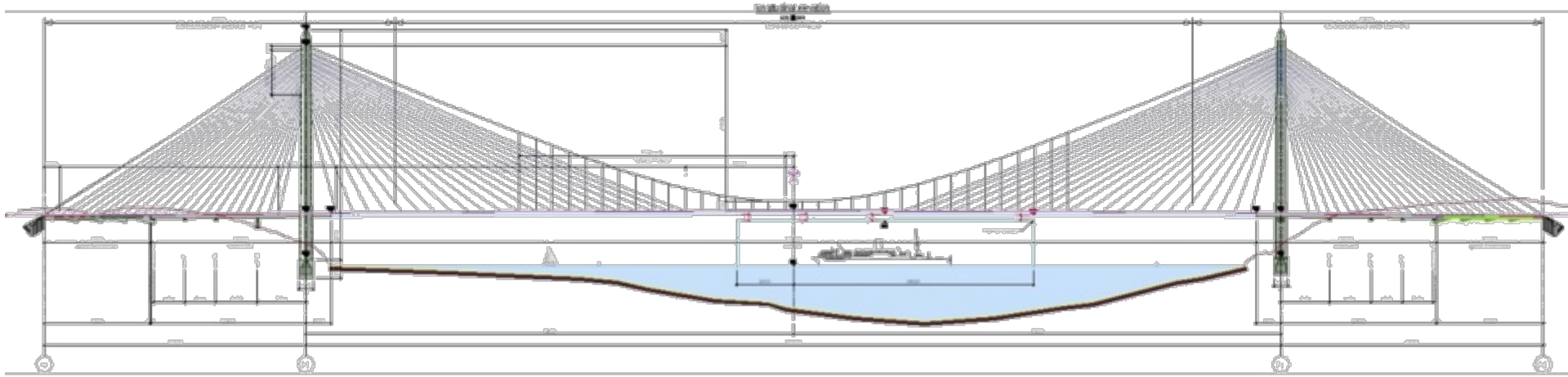

Full Aeroelastic Bridge @POLIMI BB3

- Response to Turbulent Wind → 1:180 scale model
- Combined effects of exposure angle and upwind roughness considered

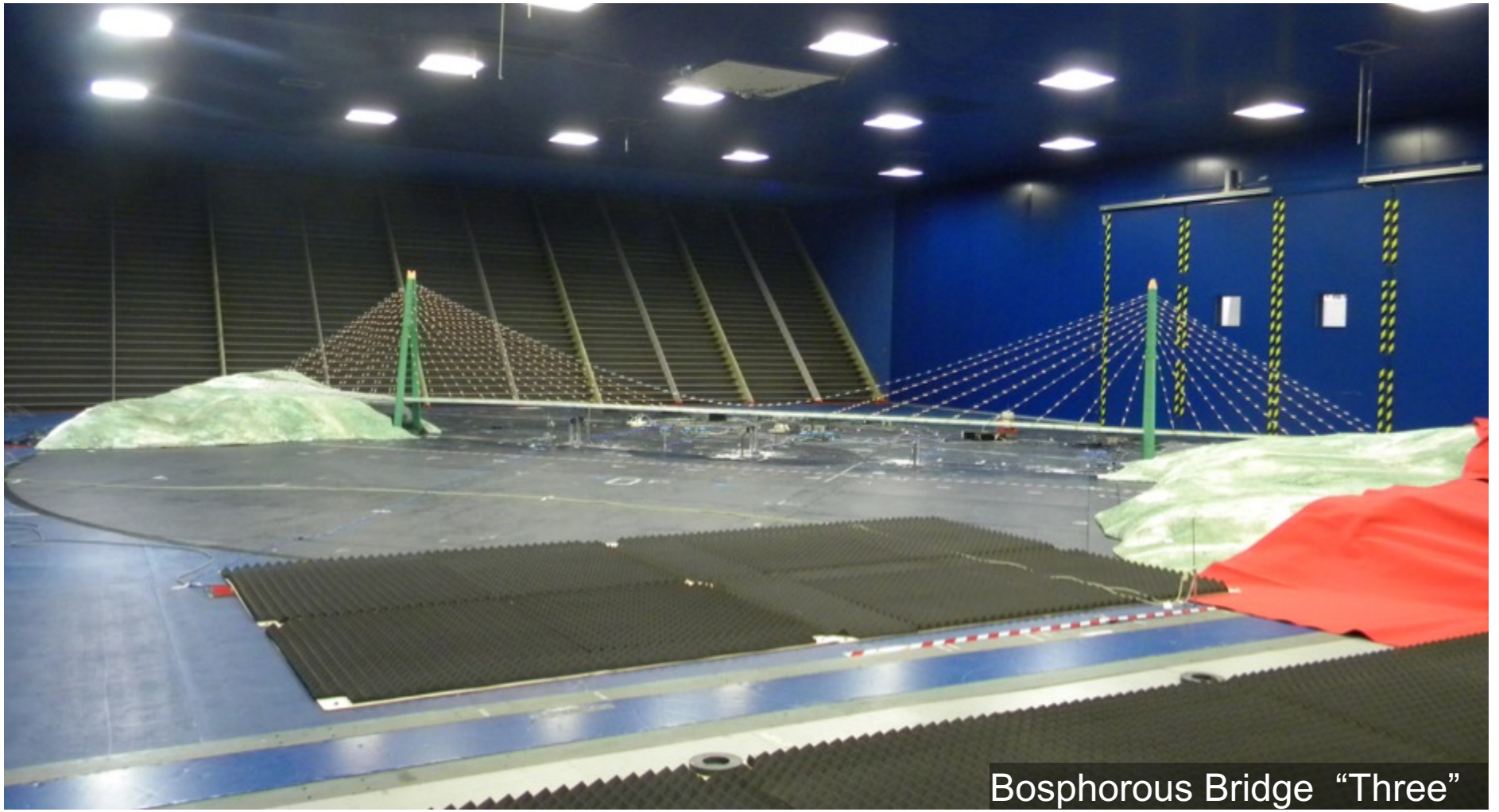

Full Aeroelastic Bridge @POLIMI BB3

- Construction stage Wind Studies

BB3 Deck: High Slenderness Cross Section

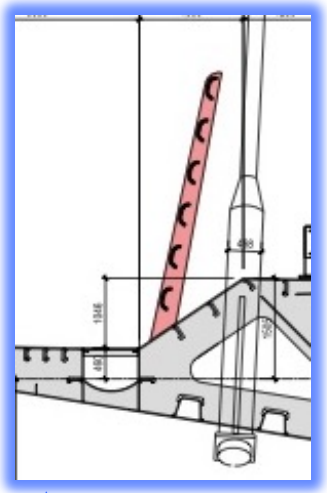

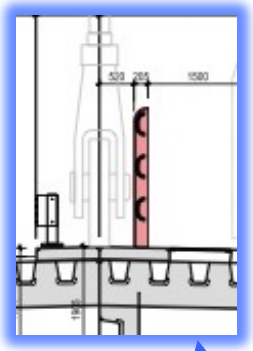

High slenderness steel deck

2 x 4 lanes of traffic

Provision for future 2 rail track

Possible wind screens aerodyn. optimization:

Vehicles wind loads & VIV control

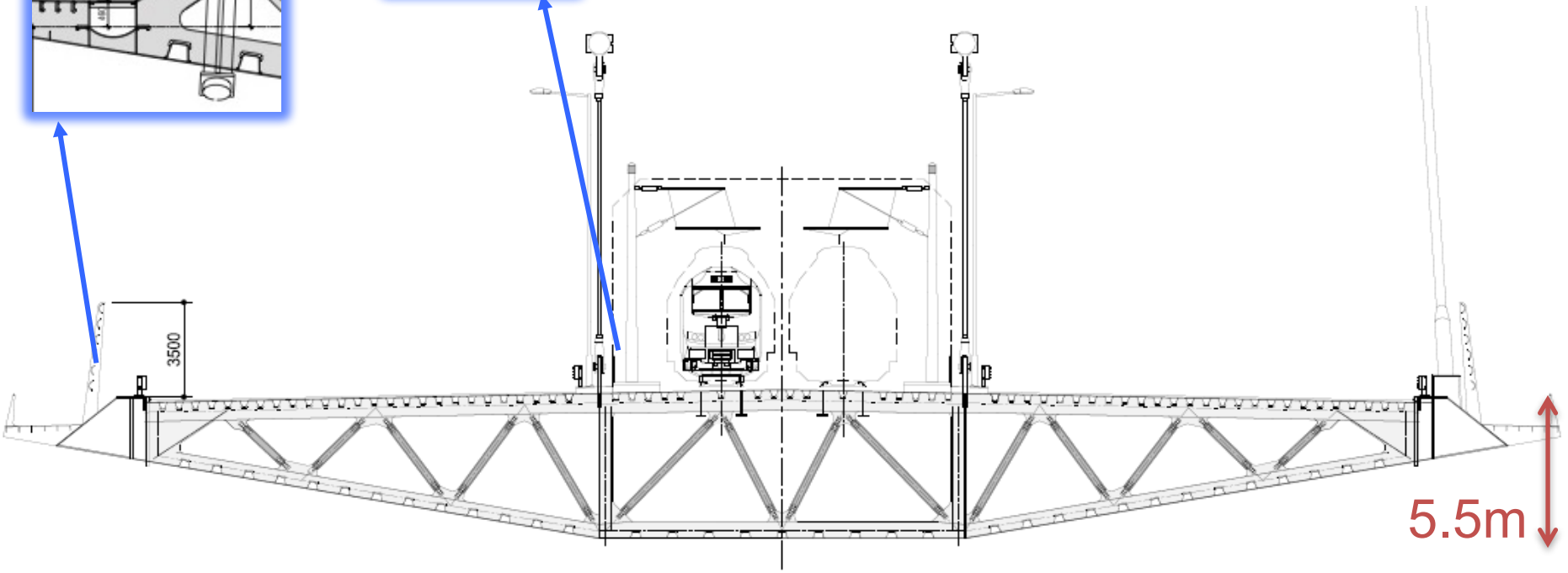

Slenderness = W / h = 11

58m

BB3 Deck: Large Scale Aeroelastic Model

- 1:50 Scale / Aeroelastic deformable / Very low damping → Low Scruton
- Up to 16 m/s → Re=2.0E+6
- Measures: Aeroelastic response
  Unsteady pressure distribution on deck and screens
  Wind Screen aerodynamic characterization
  Wind velocity profiles on road & train lanes

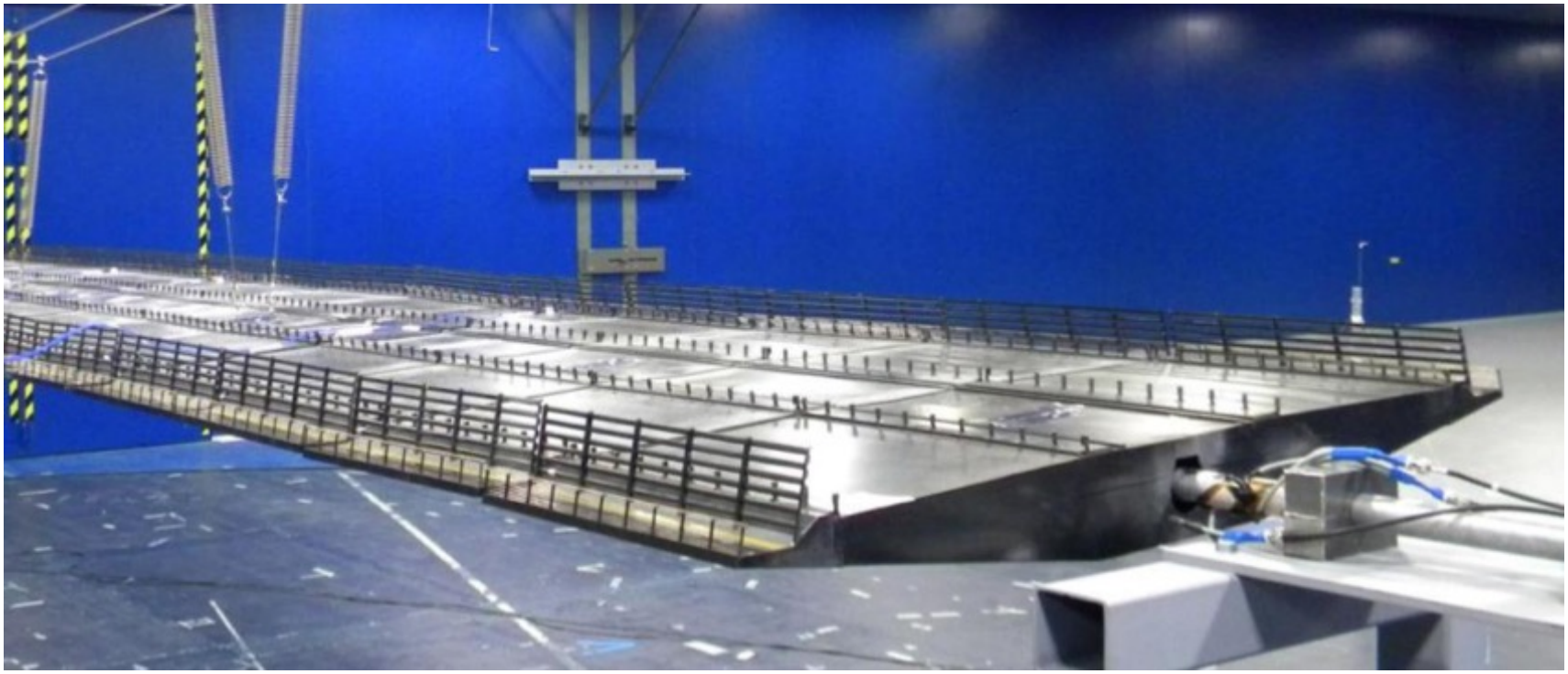

CSTB-POLIMI Cross Check / Re Effects

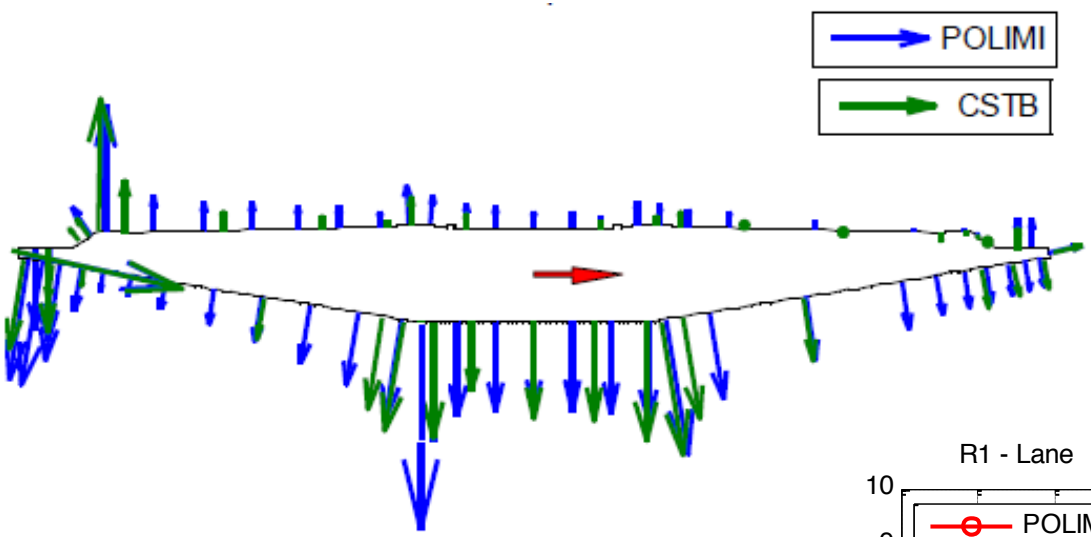

Reynolds Range:

CSTB → Re= 1.3E+7

POLIMI → Re= 2.0E+6

Wind Screens & Deck Aerodynamics:

Optimum cross validation

CSTB – POLIMI results on

Mean pressure distribution

Mean velocity profiles

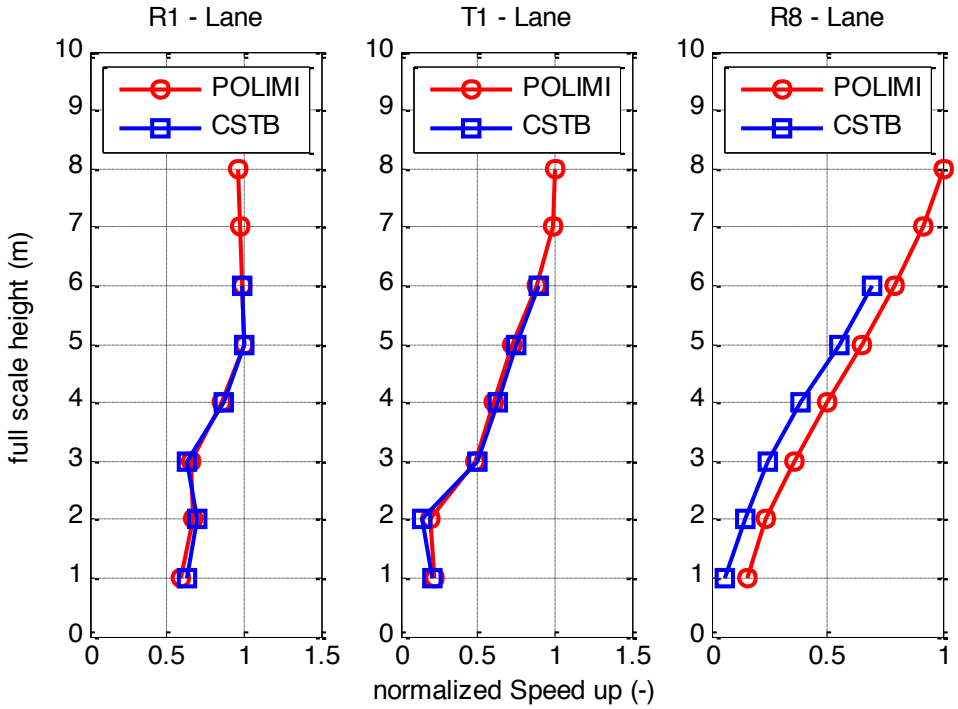

Safety & Performance → Wind Screen Design

- Operating configurations:

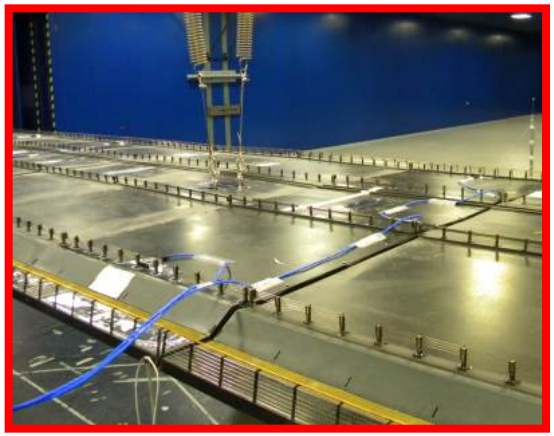

NACKED

The bridge is provided just with guard-rails

2WS (two wind screens)

The wind screens for the road lanes are installed on the bridge

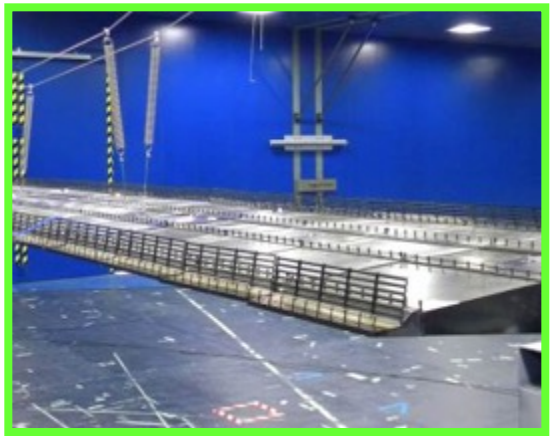

2WS + WING

The wind screens for the road lanes are installed on the bridge together with the wings

Safety & Performance → Wind Screen Design

- Test case:

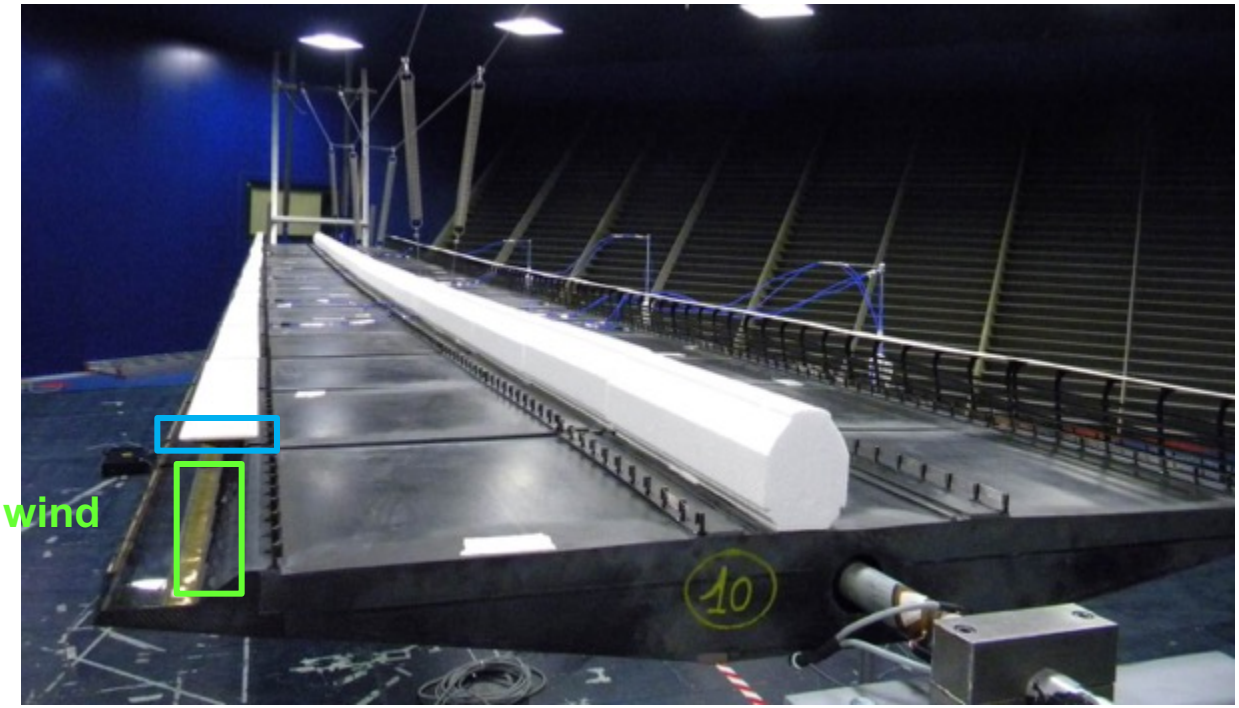

Bridge with a train model in the rail lane. All the operating conditions were investigated

- **NACKED**
- **2WS**
- **2WS + WING**

Wind Screen Design → No Traffic / No Train

- Half-difference contribution of the accelerometers at ¾ span

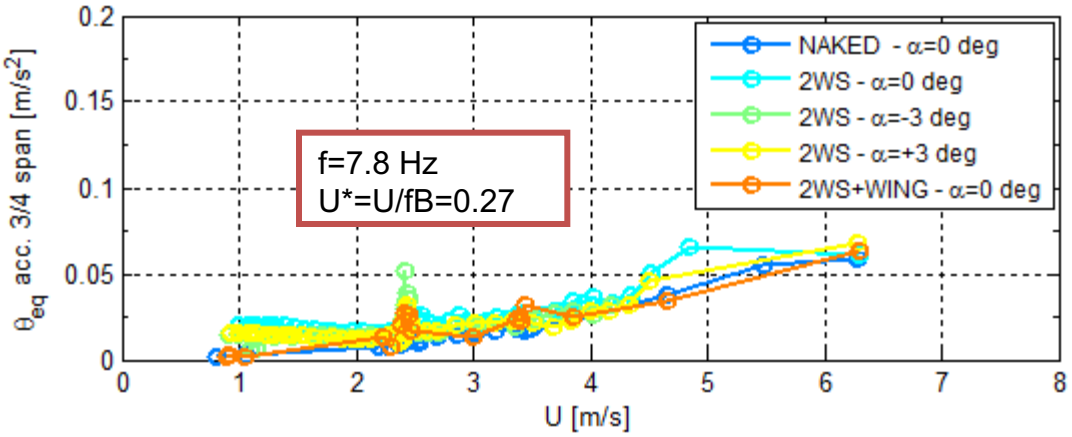

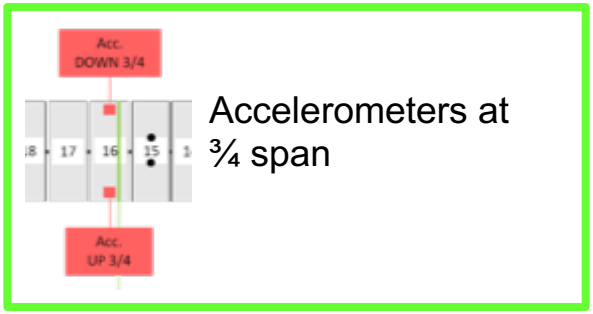

The deck was investigated also changing the angle of attack

- Half-sum contribution of the accelerometers at ¾ span

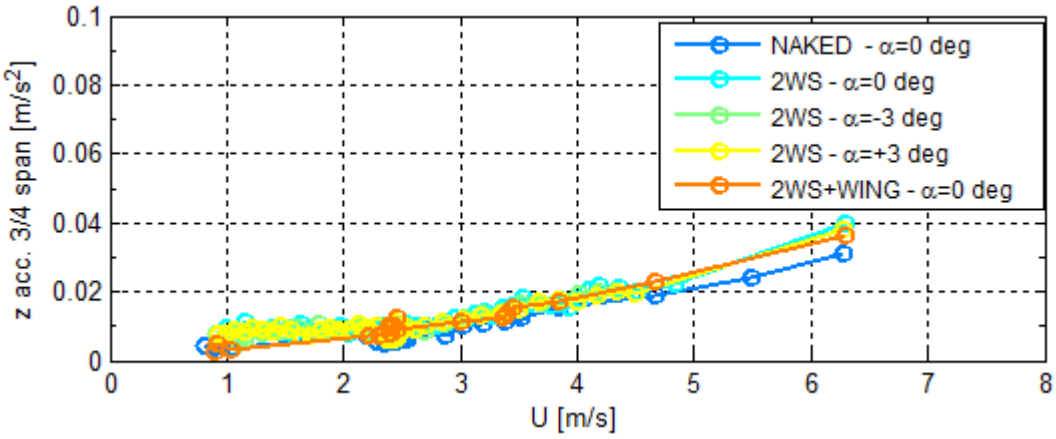

- A very narrow lock-in region is defined around the peak corresponding to an excitation of the **second torsional** mode in particular for the **2WS configuration**.
- The absolute value of the peak in the real scale is about 1 mm

Wind Screen Design → With Train

- Half-difference contribution of the accelerometers at ¾ span

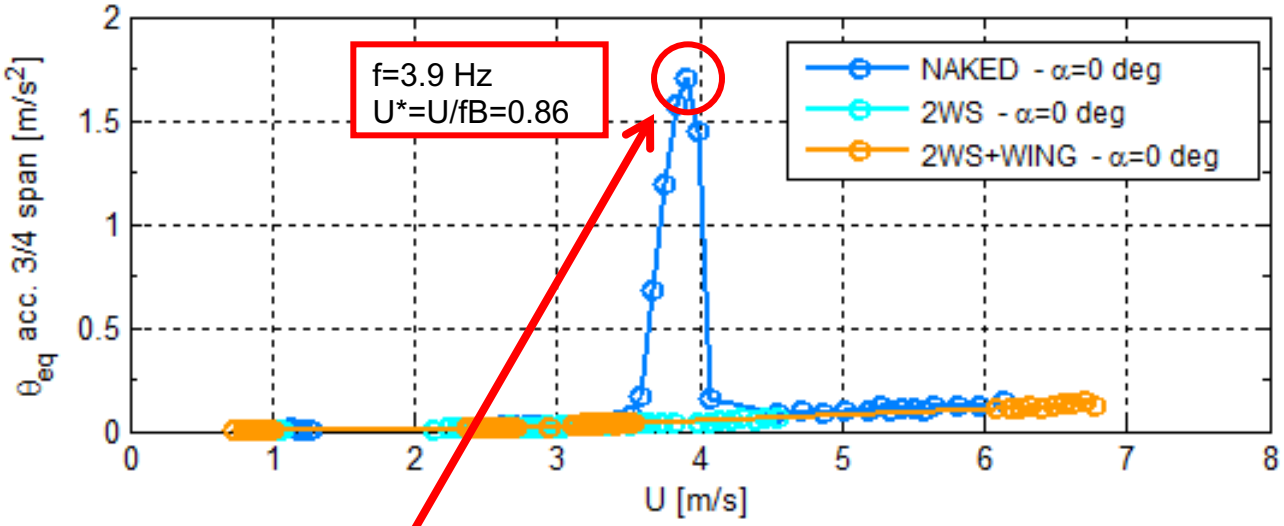

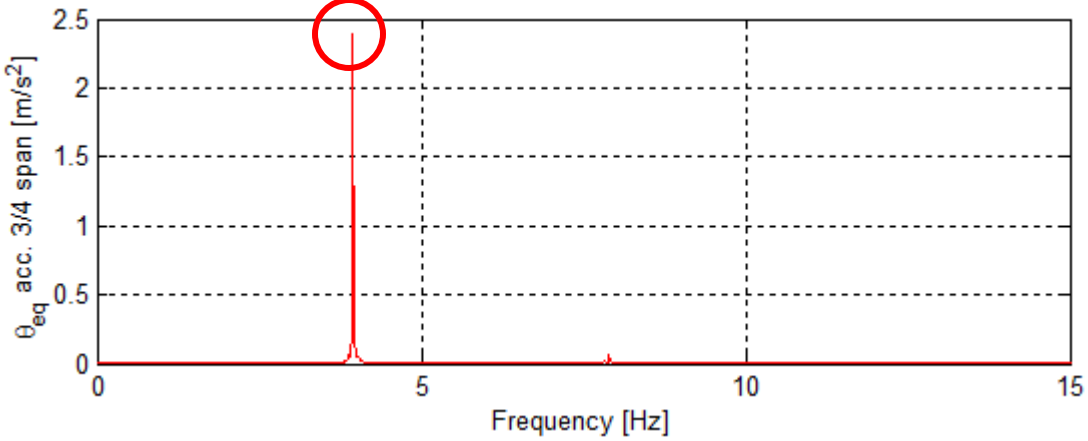

- Significant level of excitation was reached by the **naked configuration**
- **First torsional mode** was excited
- Well defined and narrow peak in the spectrum

Wind Screen Design → With Train

- Half-sum contribution of the accelerometers at ¾ span

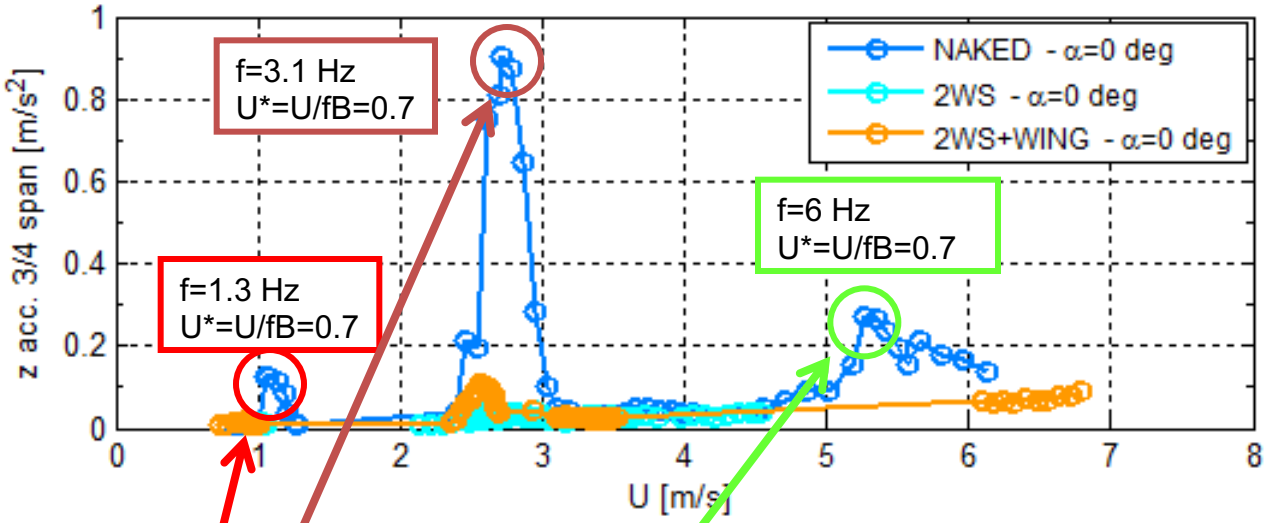

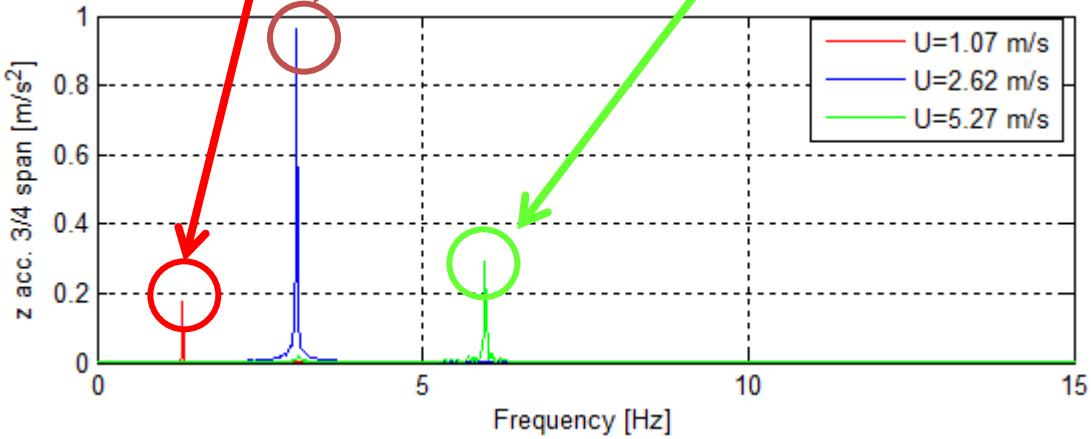

- Significant level of excitation was reached by the **naked configuration**
- **First three flexural modes** were excited
- Well defined and narrow peak in the spectrum
- Same reduced velocity for the three modes

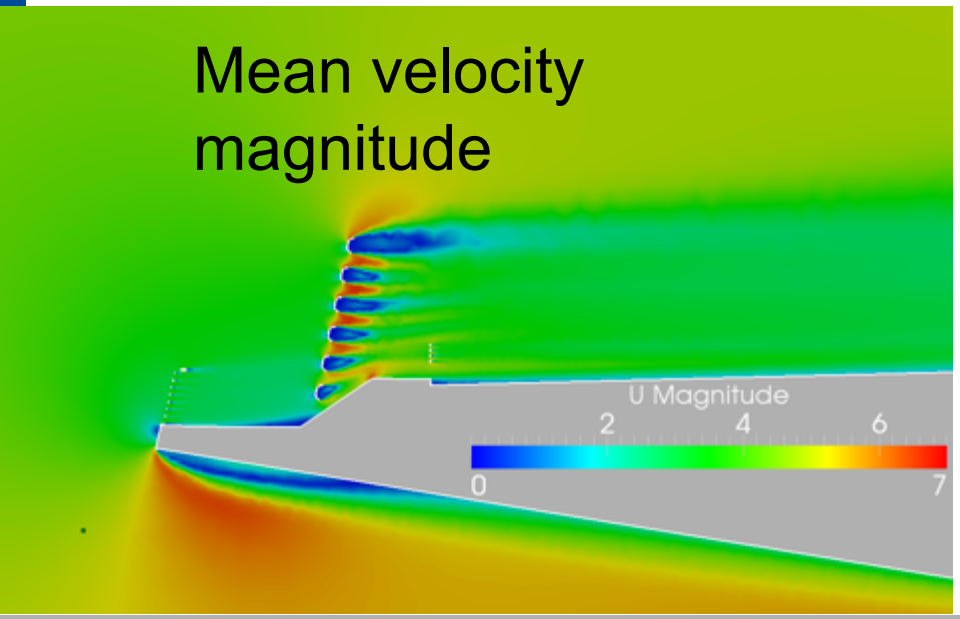
Mean velocity magnitude
U Magnitude
2
4
6
0
7

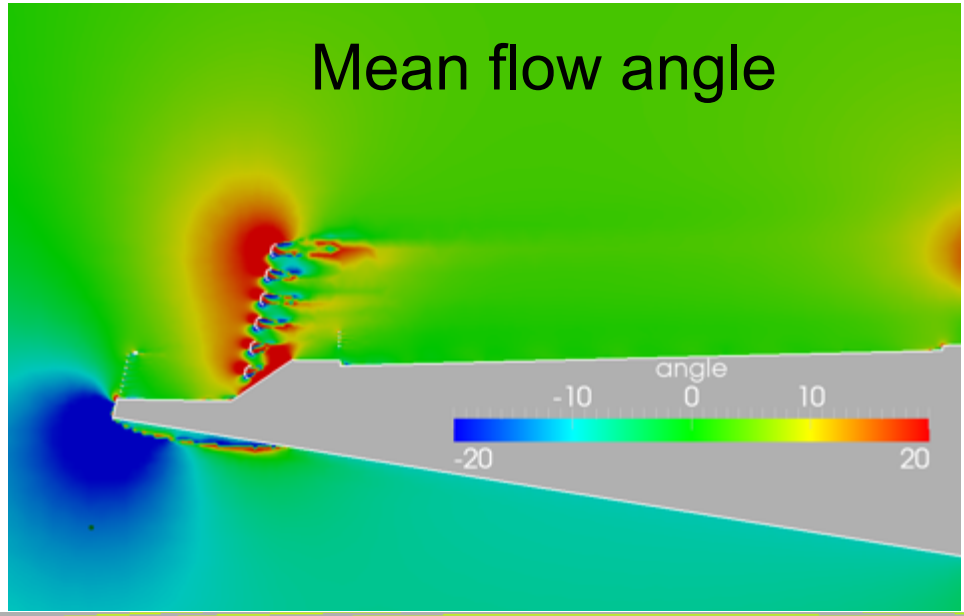
Mean flow angle
angle
-10
0
10
-20
20

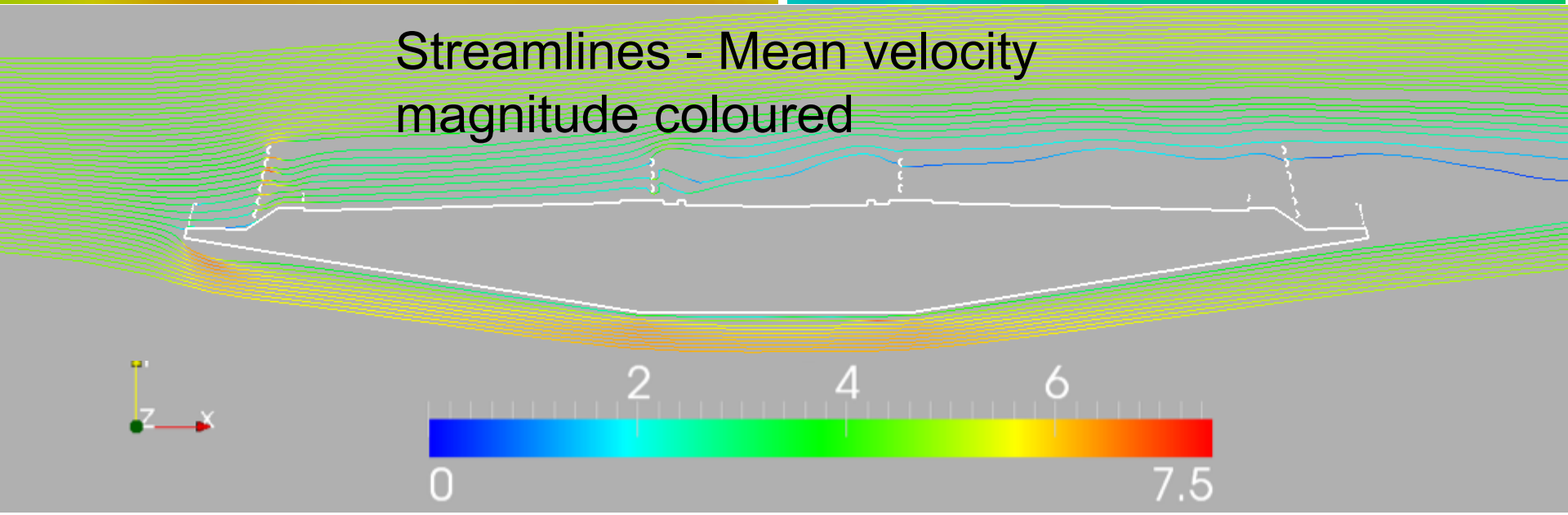
Streamlines - Mean velocity magnitude coloured
2
4
6
0
7.5

POLIMI - CFD / Exp. Cross Validation

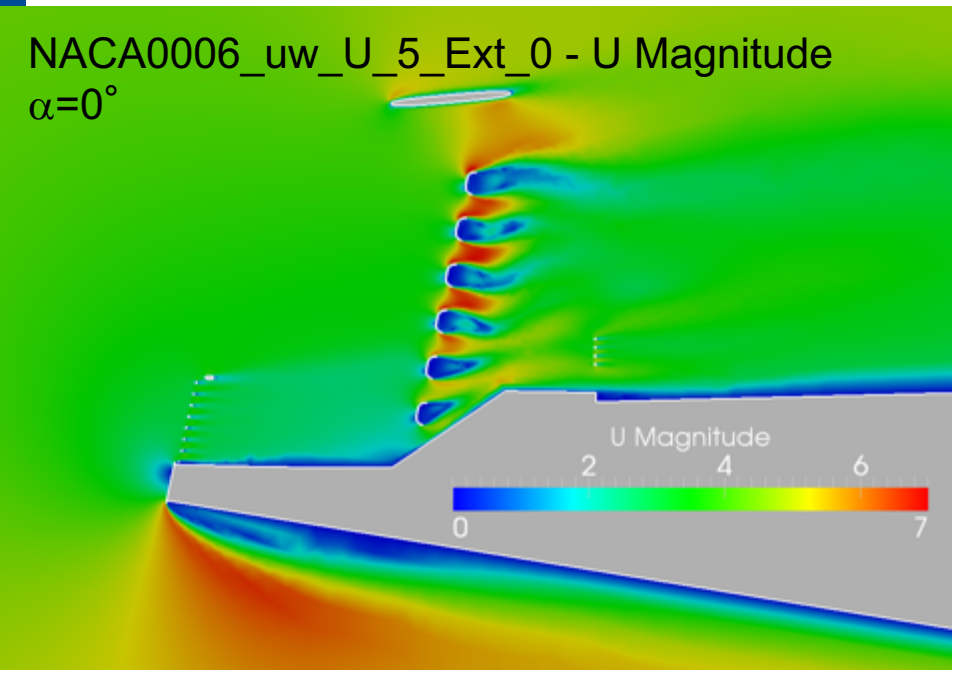

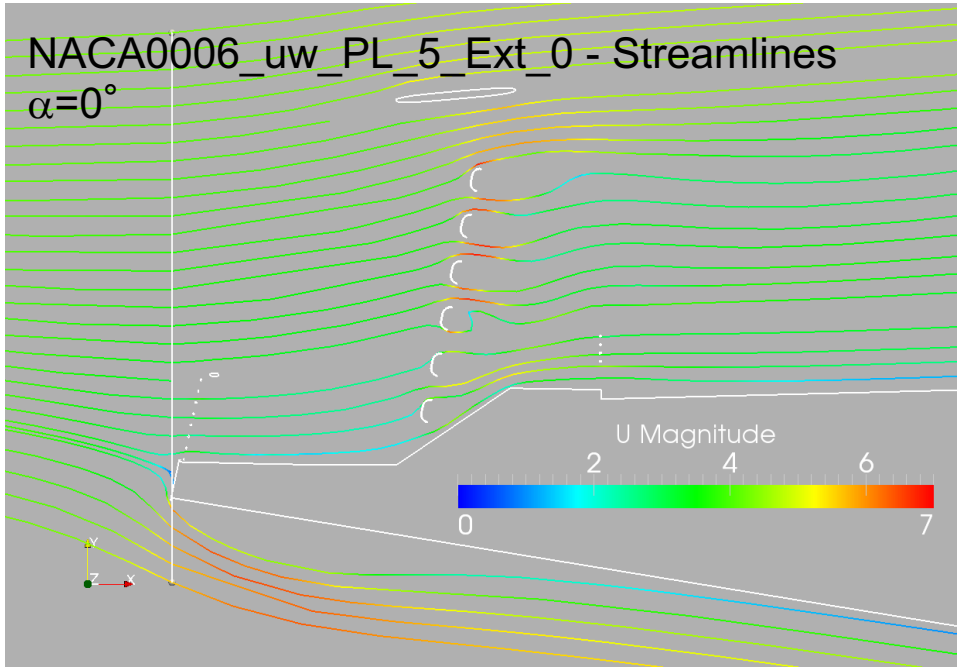

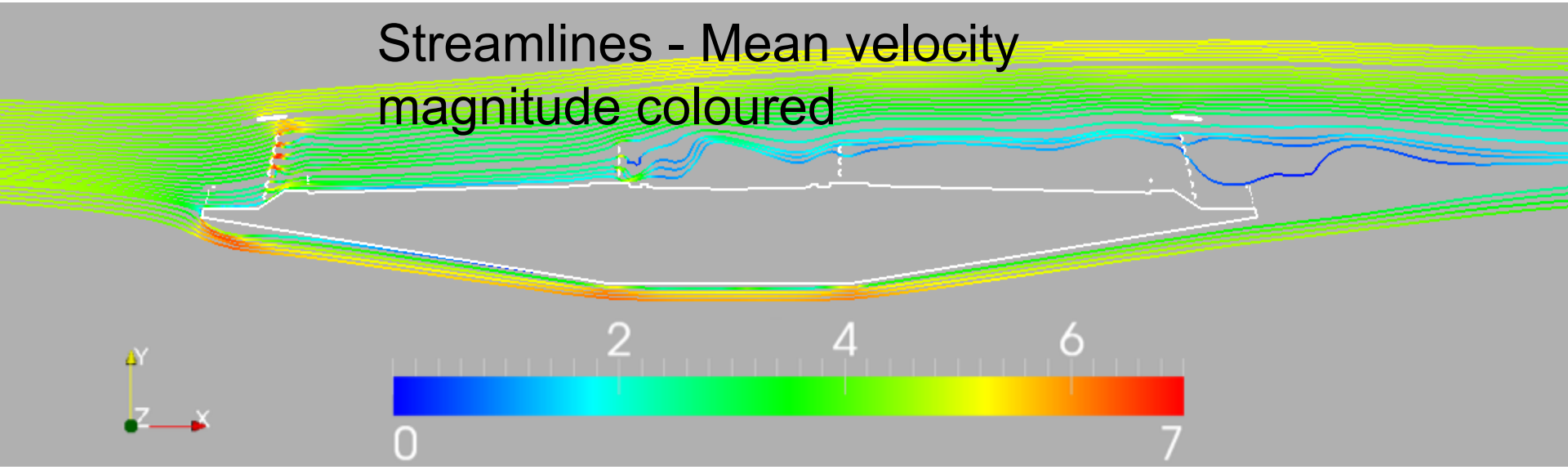

Multi-Span Crossing → Floating Tower Solution

→ **Aero-Hydro-Elastic Co-Simulations**

→ **Experimental Validation Needed !!!**

Coastal Highway Route E39 Project

- Fully Coupled Dynamic Problem → Aero-Hydro-Elastic
- Challenging numerical co-simulation approach
- Experimental validation needed !!!

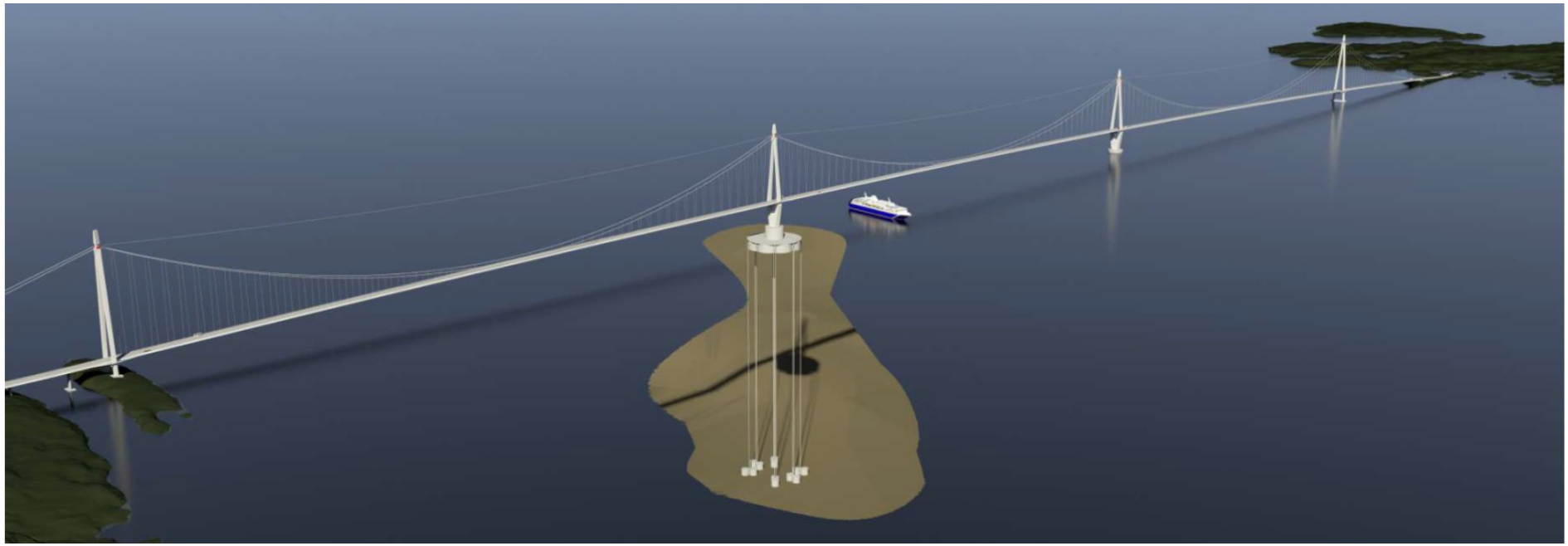

Source: Norwegian Public Roads Administration

Simulation tools: submodules

MOORING SYSTEM

Linear/NonLinear/Fem

MIMOSA (MARINTEK)

MoorDyn (NREL)
FEAmooring (NREL)
MAP++ (NREL)

HYDRO

Frequency Domain 3D Potential Flow (Linear/2° order/ QTF)

WAMIT (MIT)

OpenWarp-Nemoh (NREL/ECNantes)

Wave kinetics and loads

RIFLEX (MARINTEK)

HydroDyn (NREL)

STRUCTURE

Floater

SIMA (MARINTEK)

OpenWarp-Nemoh (NREL/ECNantes)

Bridge

SAP/ANSYS

ADTFem (PoliMi)

AERO

Turbulente Inflow

TurbSim (NREL)
InHouse(PoliMi)

Commercial
OpenSource/InHouse

Integrated analysis:
→ Experimental Validation Needed

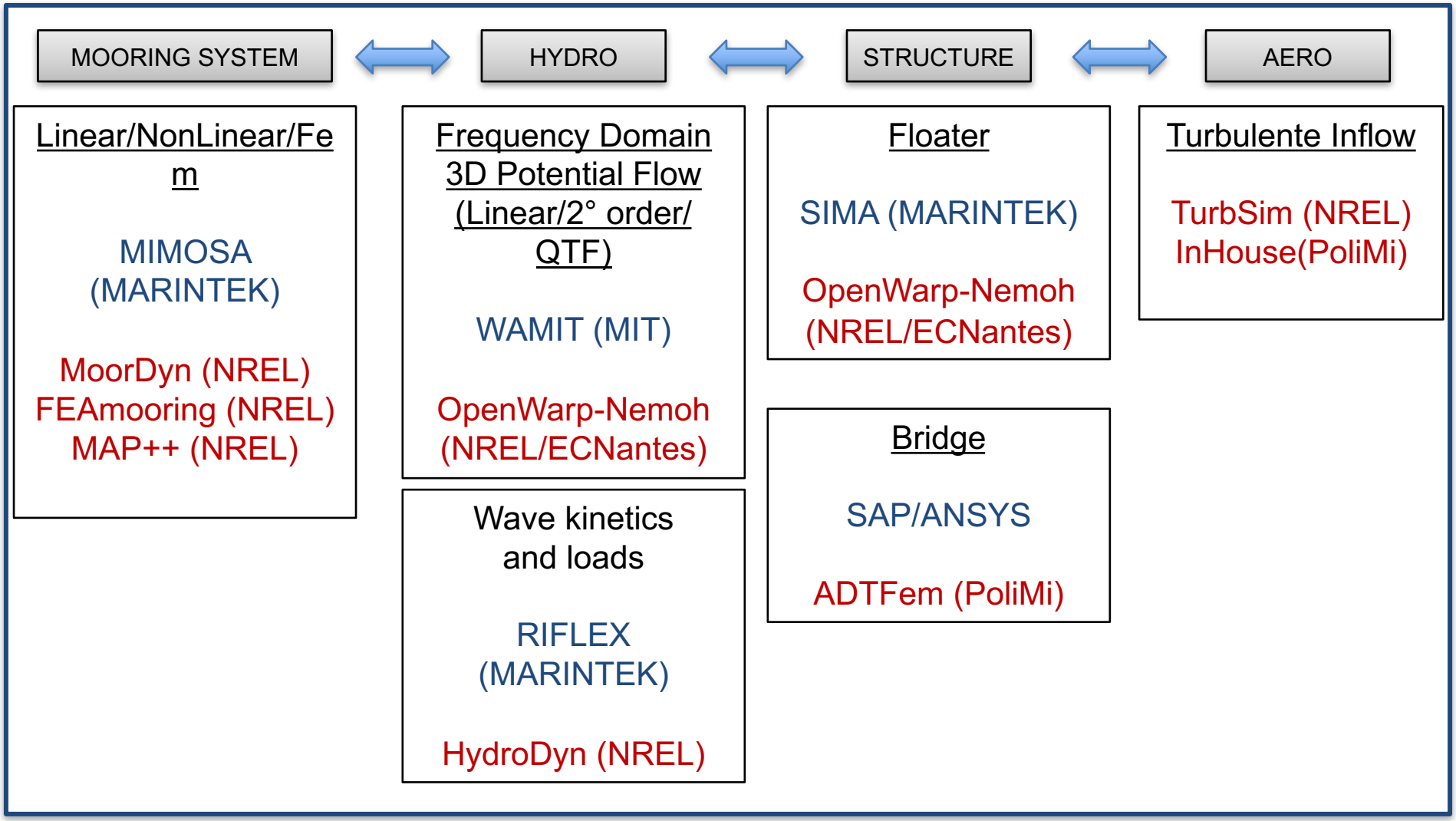

Offshore Wind Energy Example

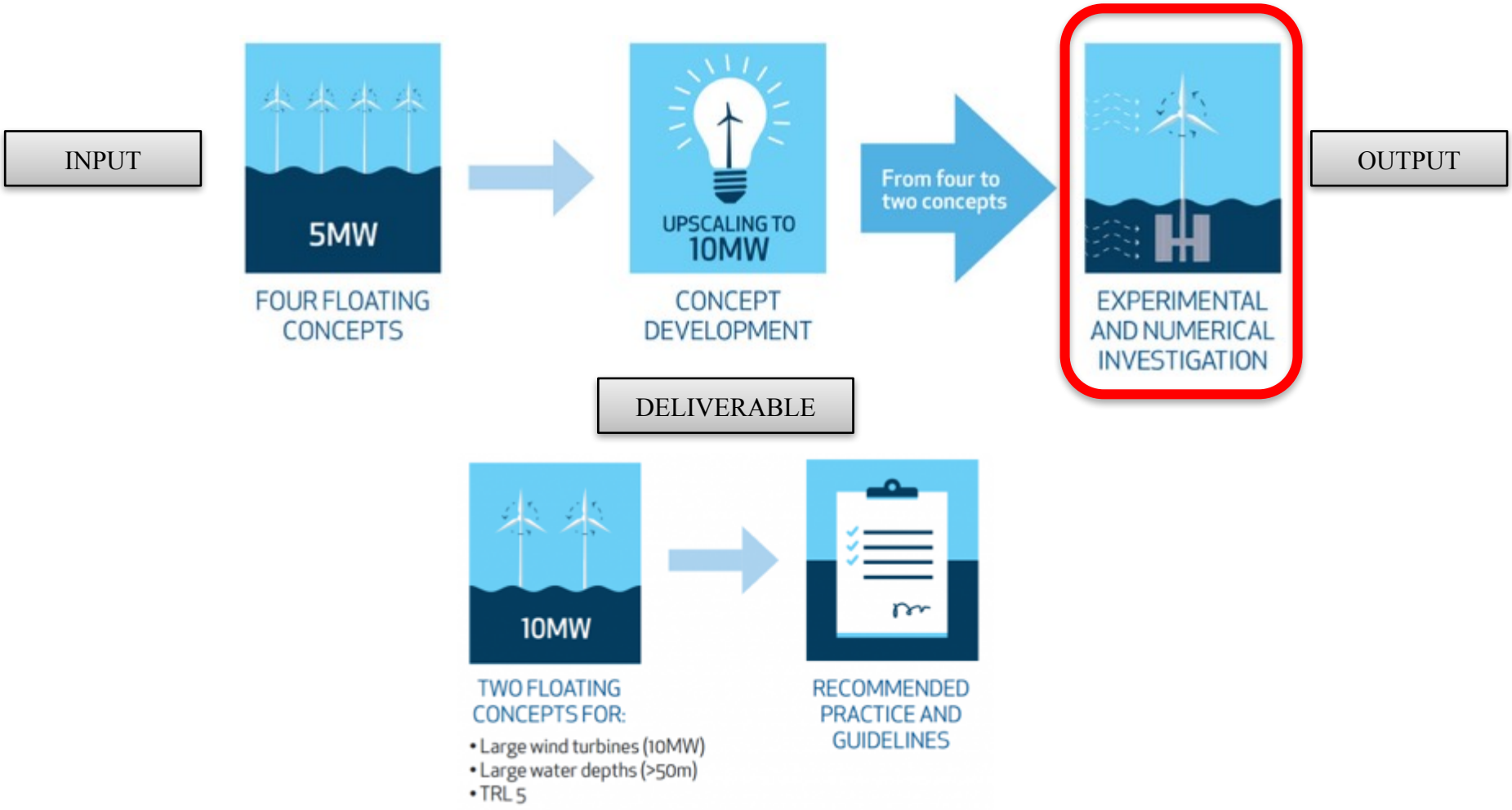

Floating offshore Wind Turbines: Experiments

- Complex physics behind
- Combined Aero -Hydro contribution

$$[M]\ddot{x}+[C]\dot{x}+[K]x = F_{Aero}\left(\rho_{Air},\mu_{Air},C_T,C_P,U_{Wind},\Omega\right)+ F_{Hydro}\left(\rho_{Water},\mu_{Water},g,H,d,T,C_D,V_{Platform}\right)$$

Structure = Aero + Hydro

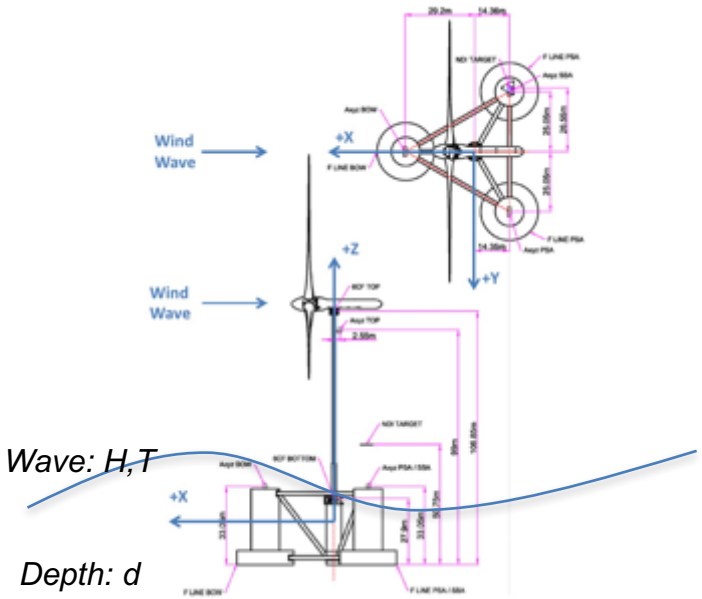

Symbol	Dimensionless Number	Force Ratio	Definition
R_e	Reynolds Number	Inertia/Viscous	$\frac{UL}{\nu}$
F_n	Froude Number	Inertia/Gravity	$\frac{U}{\sqrt{gL}}$
M_n	Mach's Number	Inertia/Elasticity	$\frac{U}{\sqrt{E_V/\rho}}$
W_n	Weber's Number	Inertia/Surface tension	$\frac{U}{\sqrt{\sigma/\rho L}}$
St	Strouhall number	-	$\frac{f_v D}{U}$
KC	Keulegan-Carpenter Number	Drag/Inertia	$\frac{U_A T}{D}$

NTNU, TMR7 Experimental Methods in Marine Hydrodynamics – lecture

Floating offshore Wind Turbines: Experiments

$$[M]\ddot{x}+[C]\dot{x}+[K]x=F_{Aero}\left(\rho_{Air},\mu_{Air},C_T,C_P,U_{Wind},\Omega\right)+$$
$$+F_{Hydro}\left(\rho_{Water},\mu_{Water},g,H,d,T,C_D,V_{Platform}\right)$$

Structure = Aero + Hydro

IT'S IMPOSSIBILE TO HAVE SIMILARITY FOR EACH ADIMENSIONAL PARAMETER

- *Length and velocity scale limited by facility*
- *Froude-Reynolds conflict*
- *Too low speed = high noise/signal*
- *Frequency bandwidth (Control)*

Symbol	Dimensionless Number	Force Ratio	Definition
R_e	Reynolds Number	Inertia/Viscous	$\frac{UL}{\nu}$
F_n	Froude Number	Inertia/Gravity	$\frac{U}{\sqrt{gL}}$
M_n	Mach's Number	Inertia/Elasticity	$\frac{U}{\sqrt{E_v/\rho}}$
W_n	Weber's Number	Inertia/Surface tension	$\frac{U}{\sqrt{\sigma/\rho L}}$
St	Strouhall number	-	$\frac{f_v D}{U}$
KC	Keulegan-Carpenter Number	Drag/Inertia	$\frac{U_A T}{D}$

NTNU, TMR7 Experimental Methods in Marine Hydrodynamics – lecture

LIFES50+

Hybrid Testing
(Hardware-In-the-Loop)

- Overcoming scaling issues
- Exploiting separately Ocean Basin / Wind Tunnel advantages

LIFES50+ : HIL approach

- Overcoming scaling issues
- Exploiting separately Ocean Basin/ Wind Tunnel advantages

6DoF

Wind tunnel test
due date march 2018

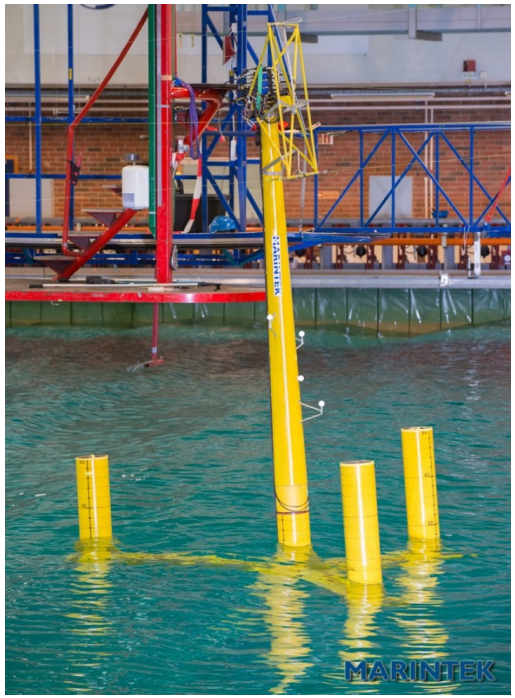

Aero validation

Hydro validation

MARINTEK

POLIMI

Ocean Basin/HIL

- Real time computation of Aero forces
- Force control (rotor)
- Advanced testing: waves/moorings

Wind Tunnel/HIL

- Real time computation of Hydro forces
- Motion control (tower's base)
- Advanced testing wind/turbulence/IPC

Hardware-In-The-Loop Hybrid Tests

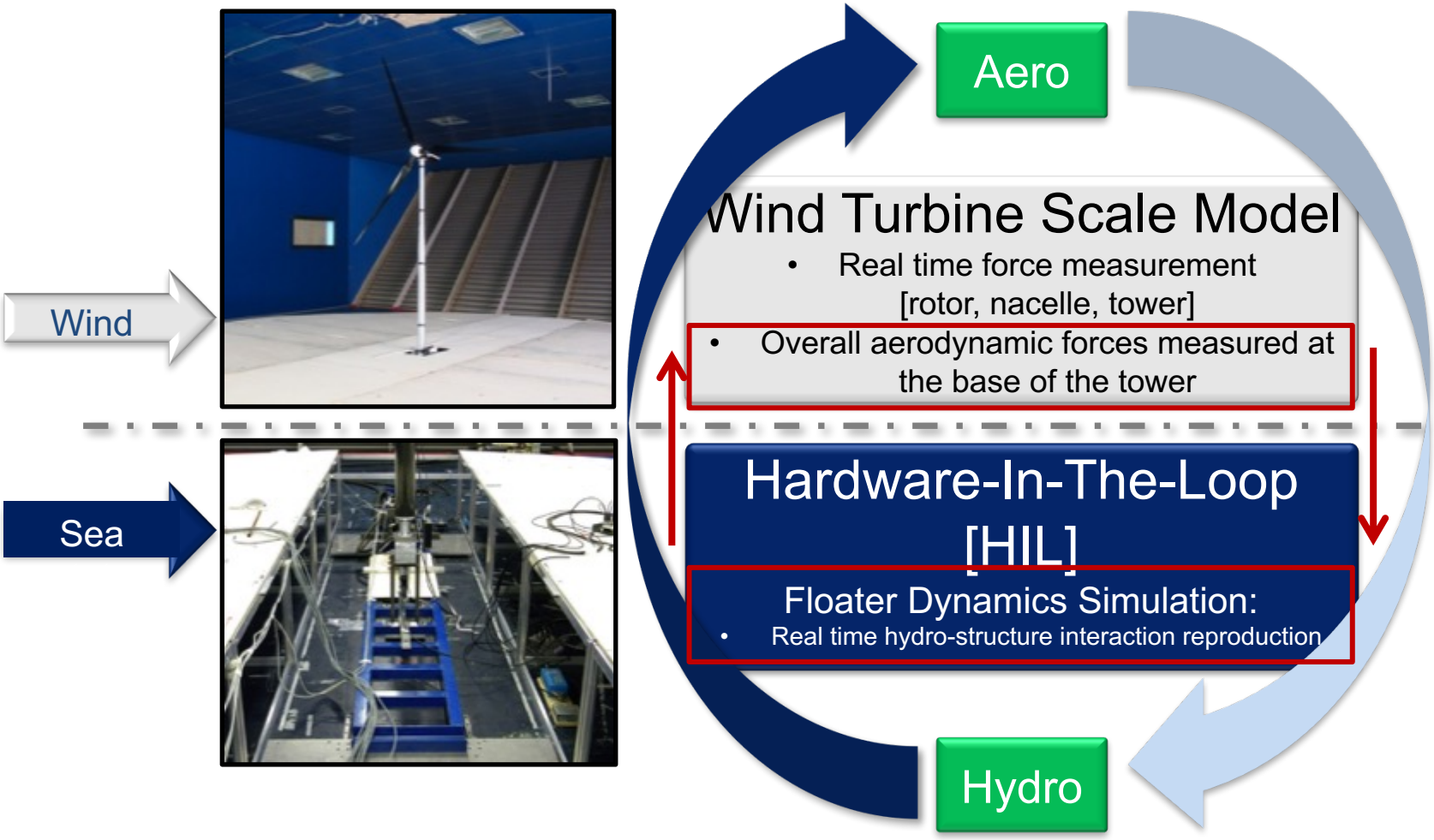

Towards 6 DoF Robot / W.Tunnel HIL Tests

Finalizing the construction of the robot:
due date march 2018

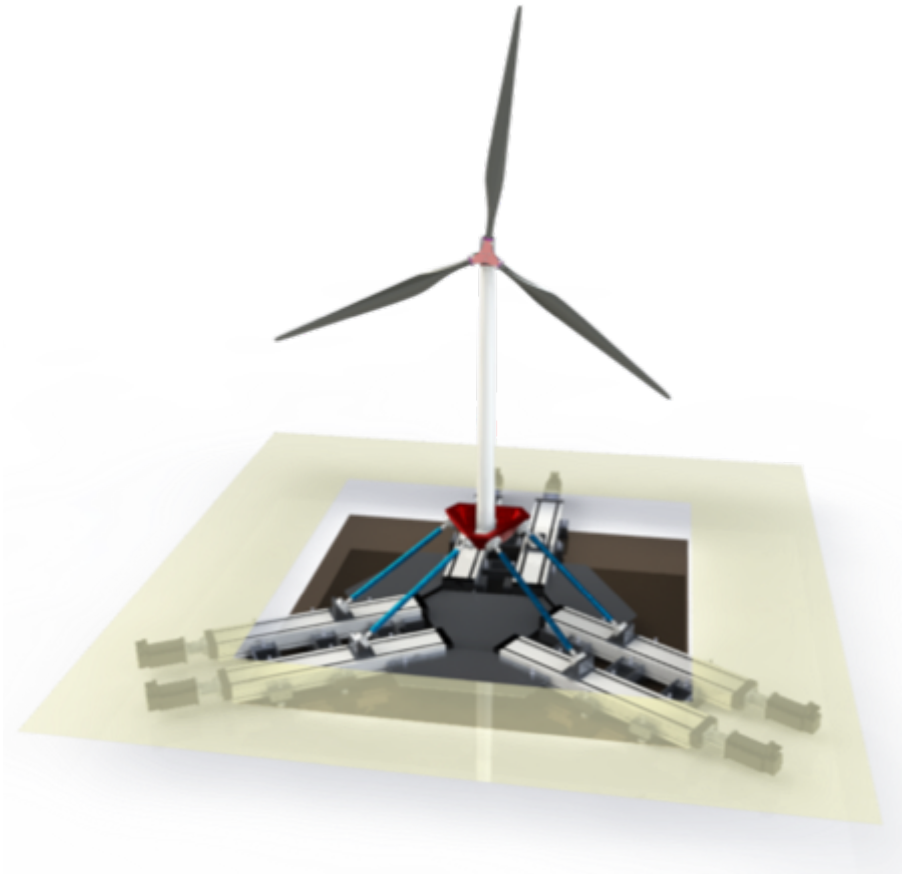

HIL ongoing side activities

- Modelling and implementation of hydro-structure interaction on RT hardware
- Implementation excercise on a small scale prototype of the robot (''desk'')
- Error and sensitivity analysis

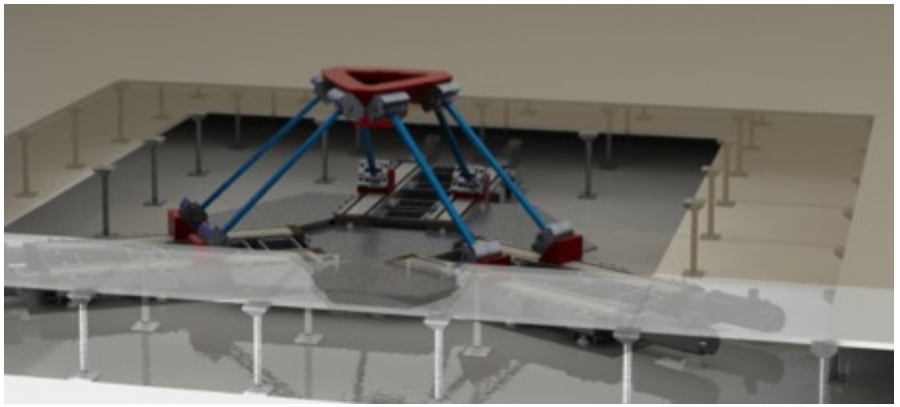

POLIMI DTU 10MW scale model & HIL

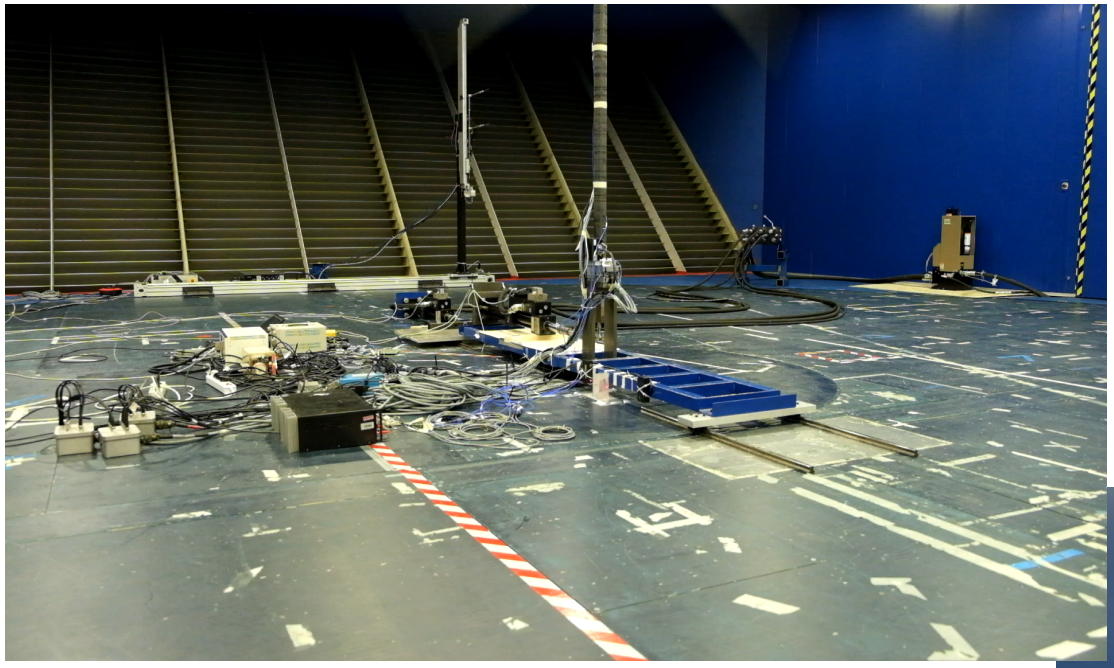

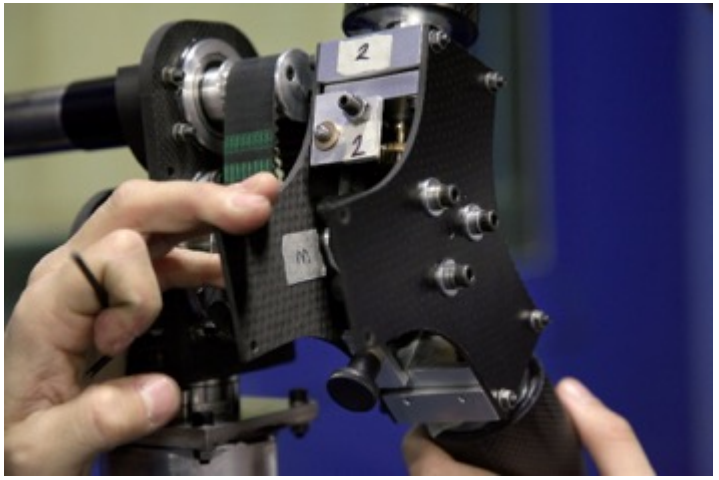

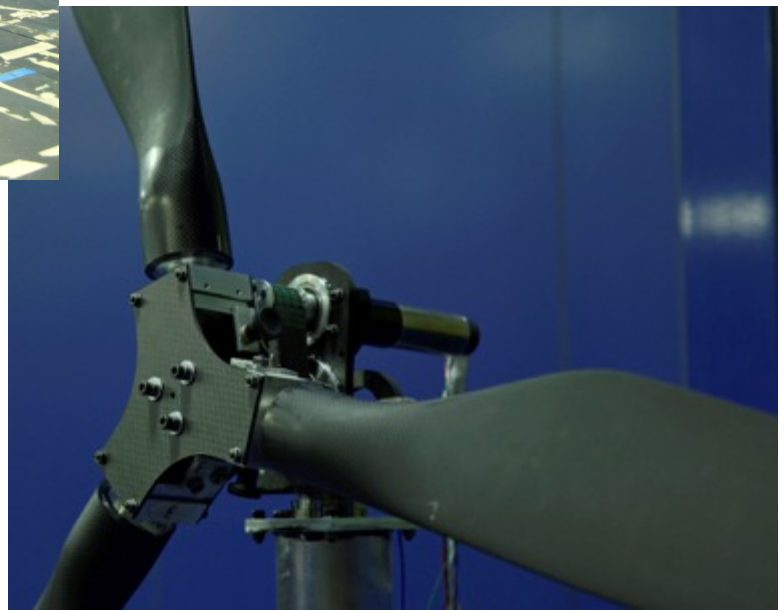

Bayati, Belloli, Bernini, Fiore, Giberti, Zasso, "*On the functional design of the DTU10 MW wind turbine scale model within LIFES50+ project*", Journal of Physics: conference series, 2016 (Torque Conference)

Interaction: key role of Frequency Ranges

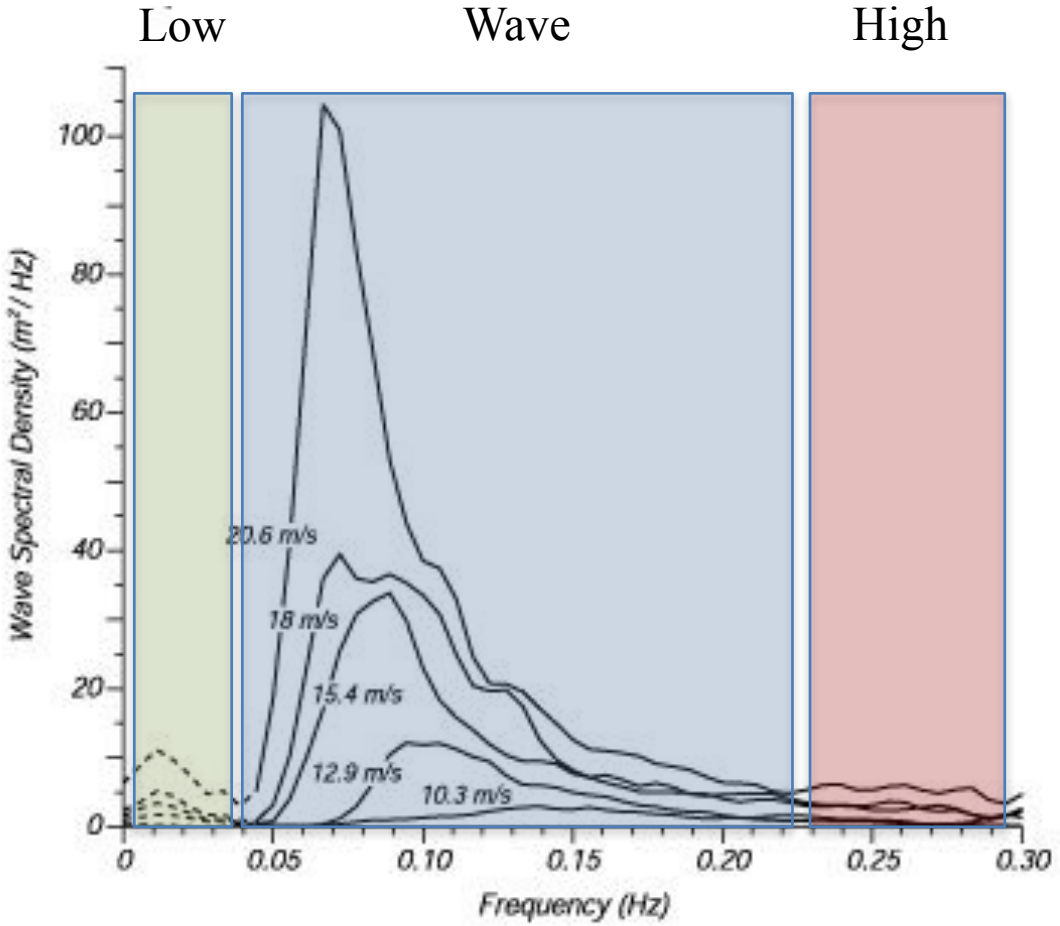

Wave Range

- Low Frequency
- Wave Frequency
- High Frequency

Wave Type

- Second Order Difference
- Linear
- Second Order Sum

Natural Freq. Floating Bridge

- Spar / Barge / TLP
- Bridge / Multispan
- Mutual Interaction

Coastal Highway Route E39 Project

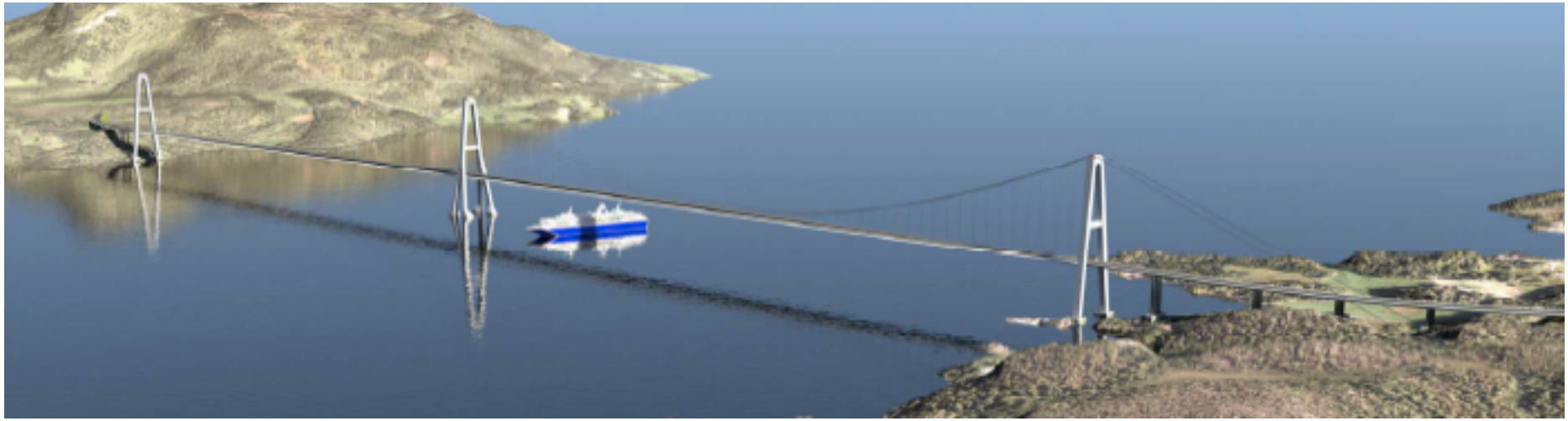

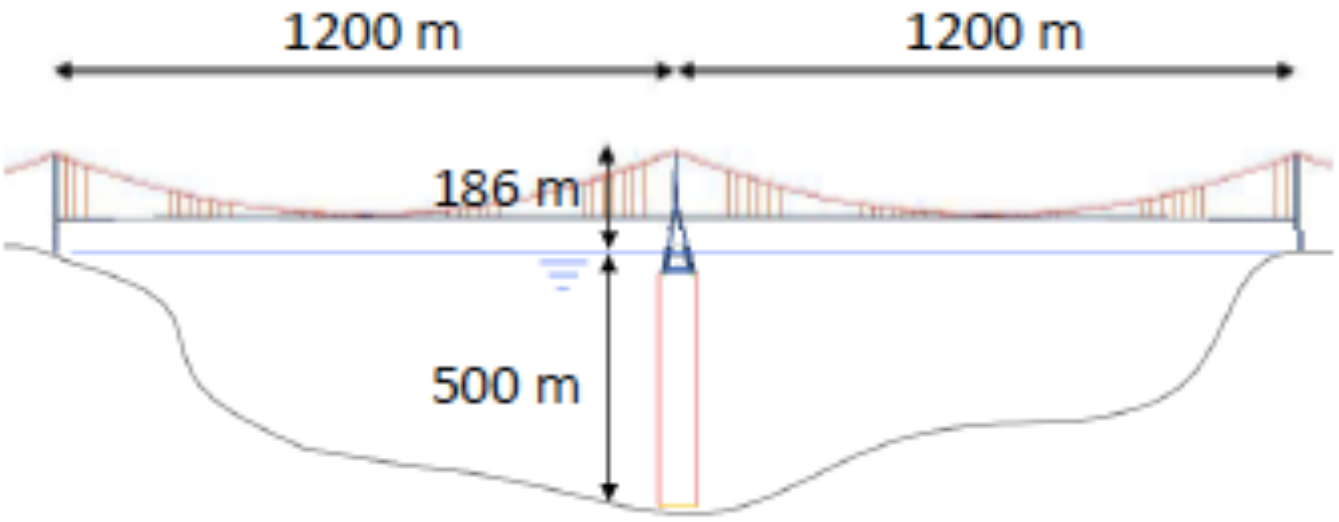

Coastal Highway Route E39 Project